The Role of Class I Histone Deacetylases in Cardiovascular Development and Disease

APPROVED BY SUPERVISORY COMMITTEE

Eric N. Olson, Ph.D.

Michelle D. Tallquist, Ph.D.

Steven A. Kliewer, Ph.D.

Joseph A. Hill, M.D., Ph.D.

To My Wife Ashley

To My Parents

ACKNOWLEDGEMENTS

Throughout my graduate school training, there have been numerous people that have been instrumental in my development as a scientist as well as a person. My deepest appreciation and gratitude goes towards my mentor, Dr. Eric Olson. I am particularly thankful for the opportunity to work in such an exciting and productive laboratory. Eric's continued thirst and enthusiasm for new "hot" data and science transverberates to his people making his laboratory a particularly stimulating environment to pursue research. His encouragement, guidance, and "staying at 35,000 feet" have made me realize self- and scientific-potentials I would have never imagined. Eric is the type of mentor all students and fellows strive to become and will forever remain a role model of mine.

I am also extremely thankful to Dr. Rhonda Bassel-Duby. Her genuine care for the lab and for people has proven to be invaluable to my success and the success of the entire lab. Her support and patience have made my graduate career infinitely smoother and more productive. She has always been available for scientific discussions as well as times of venting and for this I am grateful.

I would like to thank my committee members, Drs. Michelle Tallquist, Joseph Hill, and Steven Kliewer for their time, support, and advice through my training.

I would also like to thank Dr. James Richardson, John Shelton, and the entire histology core for their work on histological sections. I would like to thank Jenny Hsieh for the fruitful collaboration with the brain studies. I also would like to thank Sasha Qi for her amazing work with gene targeting in ES cells. Without her, none of this work would be possible. Special thanks to John McAnally for his transgenic work, Cheryl Nolan for all

her time and help with the mouse studies, Alisha Tizenor for her help with figures and graphics, Jennifer Brown for all her help with manuscripts and travel, and the entire Molecular Biology departmental staff for all their help.

Additionally, there have been a number of people within the lab, past and present, that have contributed immensely to my success over the years. I owe much of where I am to Chris Davis, whose teaching, support, and encouragement have been extremely influential to my career. I would also like to thank Matthew Potthoff, Rick Vega, Mike Haberland, Jens Fielitz, Ana Barbosa, Andrew Williams, Eva van Rooij, Nik Munshi, Johannes Backs, Yuri Kim, Kunhua Song, Koichiro Kuwahara, Mei Xin, Bryan Young, Shusheng Wang, Viviana Moresi, Mayssa Mokalled, Shurong Chang, Teg Pipes, Ning Liu, Drazen Sosic, Eric Small, Lillian Sutherland, Svetlana Bezprozvannaya, and Mi-Sung Kim. Their support, sharing of scientific ideas and reagents, and friendships have made the Olson lab an immeasurable environment to learn and pursue research.

Finally, I would like to thank my wife Ashley and my entire family for their love, support, and patience through the years.

The Role of Class I Histone Deacetylases in Cardiovascular Development and Disease

by

RUSTY L. MONTGOMERY

DISSERTATION

Presented to the Faculty of the Graduate School of Biomedical Sciences

The University of Texas Southwestern Medical Center at Dallas

In Partial Fulfillment of the Requirements

For the Degree of

DOCTOR OF PHILOSOPHY

The University of Texas Southwestern Medical Center at Dallas

Dallas, Texas

March, 2008

THE ROLE OF CLASS I HISTONE DEACETYLASES IN CARDIOVASCULAR DEVELOPMENT AND DISEASE

Rusty L. Montgomery, Ph.D.

The University of Texas Southwestern Medical Center at Dallas, 2008

Supervising Professor: **Eric N. Olson, Ph.D.**

Histone acetylation/deacetylation is a dynamic process that coordinates proper gene expression through the opposing actions of histone acetyltransferases (HATs) and histone deacetylases (HDACs). HDAC inhibitors continue to show promise in a multitude of pathological settings such as cancer and heart disease, however the role of individual HDACs remains largely unexplored. Genetic studies have shown class II HDACs regulate developmental and physiological processes through the interaction with and repression of myocyte enhancer factor 2, MEF2, however the biological functions of class I HDACs have not been determined. To potentially understand the role of individual class I HDACs in development and disease, we generated conditional knockout alleles for HDAC1, HDAC2, and HDAC3. Through global and tissue specific analyses, we hope to identify specific roles of these enzymes in developmental, physiological, and pathological settings.

Here I show that HDAC1 and HDAC2 act redundantly in controlling cardiac growth, morphogenesis, and contractility. Mice with cardiac-specific deletion of either HDAC1 or HDAC2 are viable and lack obvious phenotypes, however cardiac-specific deletion of both HDAC1 and HDAC2 results in lethality by two weeks of age. These mice show cardiac arrhythmias, dilated

cardiomyopathy, and increased expression of calcium channels and skeletal muscle-specific contractile proteins.

HDAC3 is closely related to HDAC1 and HDAC2, however results from genetic deletion show HDAC3 is an independent regulator of cardiac development. Global deletion of HDAC3 results in embryonic lethality, whereas cardiac-specific deletion of HDAC3 results in massive cardiac hypertrophy by 3 months of age and lethality by 16 weeks. These mice show metabolic abnormalities including up-regulation of genes involved in fatty acid uptake and oxidation, down-regulation of the glucose utilization pathway, and ligand induced myocardial lipid accumulation. Additionally, these hearts show mitochondrial dysfunction and decreased cardiac efficiency. These studies have identified HDAC3 as a central regulator of myocardial energy metabolism.

In addition to cardiac studies, tissue-specific deletions in multiple cell-types have led to the discovery that functional redundancy of HDAC1 and HDAC2 is not restricted to postnatal cardiomyocytes, but extends to early cardiomyocytes, endothelial cells, smooth muscle cells, chondrocytes, and neurons. Deletion of HDAC1 or HDAC2 individually in these cell types does not evoke a phenotype, however deletion of both HDAC1 and HDAC2 results in embryonic lethality or neonatal lethality. Taken together, these studies identify HDAC1 and HDAC2 as redundant regulators of multiple cell types during development.

Collectively, these studies have identified distinct and specific roles for HDAC1, HDAC2, and HDAC3 during development and disease. Furthermore, these genetic studies have provided mechanistic insight into the pathways regulated by each enzyme. Additional analyses on these mice will prove instrumental to the development of more specific inhibitors for the treatment of a wide array of pathological conditions.

TABLE OF CONTENTS

Page

LIST OF PUBLICATIONS

1. **Montgomery, R.L.**, Barbosa, A.C., Richardson, J.A., Hsieh, J. and Olson, E.N. Control of hippocampus and cerebellum development by histone deacetylases 1 and 2. *Manuscript in preparation.*

2. **Montgomery, R.L.**, Potthoff M.J., Sadek, H.A., Richardson, J.A., and Olson E.N. Control of cardiac energy metabolism by histone deacetylase 3. *Manuscript in preparation.*

3. Montgomery, R.L., Davis, C.A., Potthoff, M.J., Haberland, M., Fielitz, J., Qi, X., Hill, J.A., Richardson, J.A., and Olson, E.N. Histone deacetylases 1 and 2 redundantly regulate cardiac morphogenesis, growth, and contractility. *Genes and Dev*. 2007. 21: 1790-1802.

LIST OF FIGURES

LIST OF TABLES

LIST OF ABBREVIATIONS

ANF	atrial natriuretic factor
APL	acute promyelocytic leukemia
AR	androgen receptor
BNP	brain natriuretic peptide
BrdU	5-bromo-2-deoxyuridine
CaMK	calcium/calmodulin-dependent protein kinase
cDNA	complementary DNA
ChIP	chromatin immunoprecipitation
CoREST	Co-repressor to RE1 silencing transcription factor
CTCL	cutaneous T-cell lymphoma
dBKO	double brain-specific knockout
dCKO	double cardiac-specific knockout
DMEM	Dulbecco's Modified Eagle's Medium
DNA	deoxyribonucleic acid
ECG	electrocardiography
EDTA	ethylenediaminetetraacetic acid
ER	estrogen receptor
FDA	Food and Drug Administration
GAPDH	glyceraldehyde-3-phosphate dehydrogenase
GFAP	glial fibrillary acidic protein
HAT	histone acetyltransferases
HDAC	histone deacetylase
IP	immunoprecipitation
MEF2	myocyte enhancer factor 2
MHC	myosin heavy chain
N-CoR	nuclear receptor co-repressor
NFAT	nuclear factor of activated T cells
NLS	nuclear localization signal
NRSF	neuron-restrictive silencing factor
NuRD	nucleosome remodeling and deacetylating
PCR	polymerase chain reaction
PML	promyelocytic leukemia
PPAR	peroxisome-proliferator-activated receptor
RAR	retinoic acid receptor
RNA	ribonucleic acid
RT-PCR	reverse transcriptase-polymerase chain reaction
RXR	retinoid X receptor
SAHA	Suberoylanilide Hydroxamic Acid
SMRT	silencing mediator for retinoic acid and thyroid hormone receptors
TAC	thoracic aortic constriction
TSA	trichostatin acid
VPA	valproic acid
WT	wild-type
YY1	yin yang 1

Chapter I

Histone Deacetylases in Development and Disease

Introduction

Almost all cellular processes including proliferation, differentiation, and metabolism depend upon the coordinated regulation of gene expression. The precise transcriptional activation and repression of specific genes in response to both external and internal signals is necessary for proper cell maintenance, function, and viability. A key regulator of eukaryotic gene expression is the posttranslational modification of nucleosomal histones including acetylation, phosphorylation, methylation, ubiquitination, sumoylation, and ADP ribosylation (Jenuwein and Allis 2001). The nucleosome is the basic core of chromatin, consisting of 146 base pairs of DNA wrapped around histone octamers composed of 2 copies of the core histone proteins H2A, H2B, H3, and H4. Nucleosomes are able to bind one another and form a "beads on a string" appearance as seen by electron microscopy (Kornberg and Lorch 1999). Histone proteins are highly conserved and contain an internal globular domain as well as an amino-terminal tail that structural studies have shown to protrude from the nucleosomal core (Luger et al. 1997). It is the posttranslational modifications of these N-terminal extensions that determine if the chromatin is in a transcriptionally active "open" or transcriptionally inert "closed" state. Furthermore, these modifications have become increasingly attractive therapeutic targets for a variety of disease states because of their influence on a multitude of cellular processes in addition to transcription, such as replication, DNA repair, and cell cycle progression (Kouzarides 2007).

Covalent histone modifications

The compact architecture of chromatin physically restricts access of DNA to regulatory proteins such as transcription factors. One mechanism by which the cell is able to perform

distinct nuclear and cellular functions in light of dense chromatin is through the "histone code" (Strahl and Allis 2000). The histone code reflects the cell's ability to posttranslationally modify histones individually or in concert with other modifications to direct specific cellular functions (Figure 1.1). These modifications are then "read" to perform the specific cellular process such as transcription, replication, and DNA repair.

Histone phosphorylation Phosphorylation of histone tails has been primarily linked to chromosomal condensation during mitosis and meiosis (Koshland and Strunnikov 1996), however it has also been implicated in transcriptional activation, including that of the immediate-early genes *c-fos* and *c-jun* (Mahadevan et al. 1991). Phosphorylation of serine 10 on histone H3 was the first phosphorylation modification to be associated with chromosomal condensation during mitosis. Serine 28 and threonine 11 of histone H3 have since been shown to be cell-division specific modifications. During mitosis, phosphorylation of serine 10 is regulated by Aurora kinases, however multiple kinases have been shown to phosphorylate serine 10 *in vitro* and during gene activation (Nowak and Corces 2004). In addition to histone H3, N-terminal extensions from other histones are phosphorylated during cellular processes. Histone H2A is phosphorylated upon activation of the DNA-damage signaling pathway and histone H2B is phosphorylated during apoptosis and meiosis (Ajiro 2000; Downs et al. 2000). Histone H4 phosphorylation is necessary for proper germ cell development (Krishnamoorthy et al. 2006; Wendt and Shilatifard 2006).

Histone ubiquitination Far less is known about histone ubiquitination compared to the other covalent histone modifications. It has been shown that histones H2A, H2B, and H3 can be mono- or polyubiquitinated at multiple lysine residues, however the importance of these modifications is still unclear (Zhang 2003). Lysine 119 on histone H2A was the first residue

to be identified as ubiquitinated, however this appears to be restricted to higher eukaryotes as H2A ubiquitination is not seen in *Saccharomyces cerevisiae* (Robzyk et al. 2000). Ubiquitination of histone H2B at human lysine 120 is restricted to monoubiquitination and is seen in all eukaryotic organisms (Thorne et al. 1987). Recently, the identification of the enzymes involved in histone ubiquitination and deubiquitination has provided insight into the possible mechanisms by which this modification may contribute to chromatin dynamics. While it is plausible that histone ubiquitination plays a proteasome-dependent role through the clearance of transcription factors, recent evidence supports ubiquitination as positively correlative to transcription through "histone crosstalk", or affecting nearby lysine methylation that is consistent with active transcription (Dover et al. 2002; Sun and Allis 2002).

Histone methylation Methylation of histone tails can occur on both lysine and arginine residues of histone H3 and H4. Lysines have been identified as mono-, di-, or trimethylated on lysines 4, 9, 27, 36, and 79 of histone H3 and lysine 20 of histone H4, while arginines have only been identified as mono- or dimethylated on histone H3 and H4 (Bhaumik et al. 2007). Histone methyltransferases are characterized by their SET domain and show relatively high specificity toward their substrates compared to other histone modifiers. CARM1 (coactivator arginine methyltransferase) and PRMT1 (protein arginine methyltransferase) methylate arginine residues on histone H3 and H4 whereas multiple lysine methyltransferases are responsible for catalyzing histone H3 and H4 lysine methylation (Shilatifard 2006). The cellular process associated with histone tail methylation is very dependent upon the specific lysine or arginine residue that is modified. Generally, methylation of lysine 4, 36, and 79 of histone H3 is associated with active transcription while

histone H3 lysine 9 methylation is linked to heterochromatin assembly. Similarly, methylation of lysine 27 of histone H3 and lysine 20 of histone H4 are hallmarks of heterochromatin gene silencing (Zhang and Reinberg 2001).

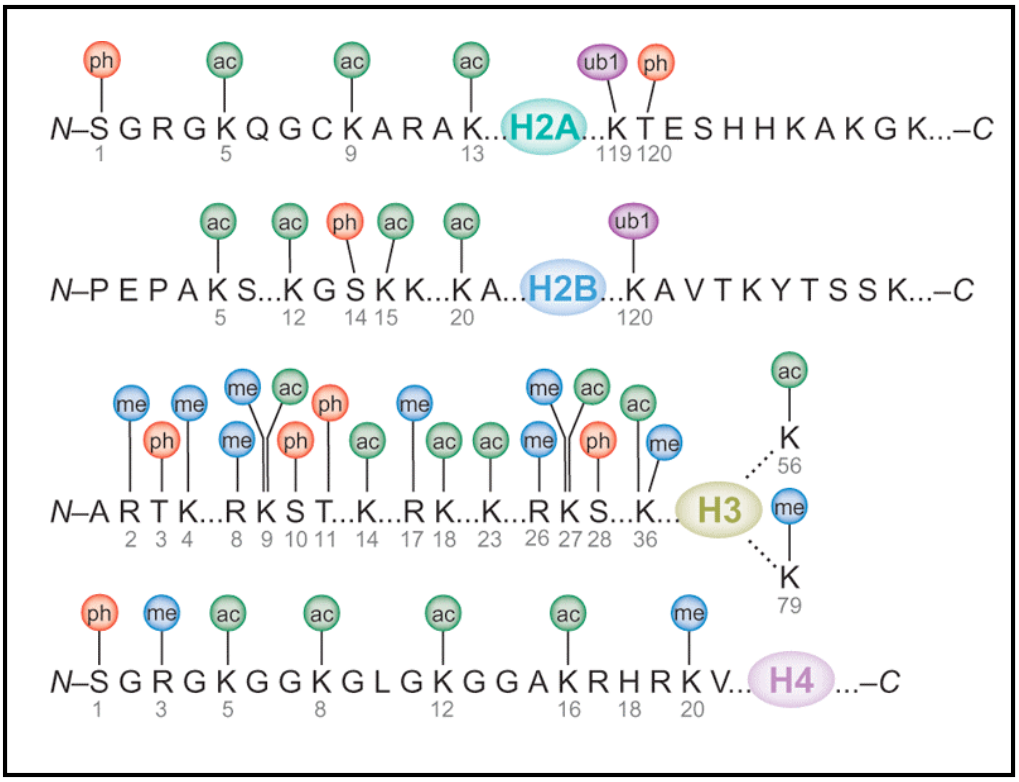

Figure 1.1. Covalent modifications of histone tails. Numerous modifications have been identified on the N-terminal extensions of histones. These include acetylation (ac), methylation (me), phosphorylation (ph), and ubiquitination (ub1). Globular domains are represented as color ovals. (Adapted from Bhaumik et al. 2007)

Until recently, methylation of histone tails was considered an irreversible process; however the identification of histone demethylases has led to an additional level of complexity in chromatin biology. Currently there are two main families of histone lysine demethylases, the lysine specific demethylase 1 (LSD1) and the Jumonji C (JmjC) domain containing family of proteins (Shi 2007). While little is known about the biological functions of these histone demethylases, there does appear to be site specificity for methylated histone

tails. Given the relationship between cancer and aberrant histone methylation, the identified histone demethylases as well as the ones yet to be identified may serve as attractive therapeutic targets.

Histone acetylation Of all the recognized modifications of histone tails, acetylation has been the most intensely studied over the years. Histone acetylation occurs on multiple lysines on all four histones and results in a loss of positive charge effectively relaxing the chromatin architecture (Bhaumik et al. 2007). This "opened" chromatin allows for the binding of transcription factors and coactivators and is the basis for why acetylation is often associated with active transcription. Histone lysine acetylation is catalyzed by histone acetyltransferases (HATs) within protein complexes such as Gcn5/PCAF and CBP/p300 that transfer the acetyl group from acetyl-Coenzyme A to the ε-amine of lysine residues on the histone tails (Marmorstein and Roth 2001; Shahbazian and Grunstein 2007). Histone deacetylases (HDACs) oppose the activity of HATs by catalyzing the removal of acetyl groups from histone tails, resulting in chromatin condensation and a net reduction in transcriptional activity (de Ruijter et al. 2003). Acetyl moieties on histone tails turnover very rapidly as the equilibrium between HATs and HDACs changes within the cell. This turnover allows for the rapid change in gene expression in response to extrinsic or intrinsic signals. Because of this, histone acetylation has become an appealing therapeutic target for a variety of pathological states including cancer, which has just recently seen the HDAC inhibitor Vorinostat be approved by the FDA for cutaneous T-cell lymphoma (CTCL) (Marks and Breslow 2007).

Histone deacetylases as transcriptional regulators

Histone deacetylases There are 4 classes of HDACs that make up an ancient family of enzymes dating back to bacteria (Figure 1.2) (Gregoretti et al. 2004). Class I HDACs (HDAC1, 2, 3, and 8) are highly homologous to the yeast histone deacetylase RPD3 and are ubiquitously expressed (Yang et al. 1997), while class II HDACs can be subdivided into class IIa (HDAC4, 5, 7, and 9) and class IIb (HDAC6 and 10) HDACs, are highly homologous to the yeast protein HDA1, and act as signal responsive transcriptional repressors in eukaryotes (Grozinger et al. 1999; Verdin et al. 2003). Class III HDACs or sirtuins require NAD for deacetylation and are related to the yeast repressor Sir2 (Grozinger and Schreiber 2002) and Class IV HDACs are a recently identified family of deacetylases that share homology to human HDAC11 (Gao et al. 2002). The class I, II, and IV enzymes contain a conserved "deacetylase" domain of about 390 amino acids whereas the class III sirtuins possess an unrelated conserved 275 amino acid catalytic domain. The class IIb HDACs are different in that they contain two tandem deacetylase domains. While class I, II, and IV HDACs contain a conserved HDAC domain, only class I HDACs possess deacetylase activity, however class II HDACs recruit class I HDACs to deacetylate substrates (Fischle et al. 2002). Deacetylase activity occurs through a hydrophobic catalytic pocket within the HDAC domain that contains a zinc binding site and two aspartic acid/histidine charge relay systems (Finnin et al. 1999). The zinc ion is necessary for deacetylase activity and HDAC inhibitors block deacetylase action through the displacement of the zinc ion within the tubular pocket (Finnin et al. 1999).

While the name "histone deacetylase" implies histones are the primary substrate, many HDACs have been shown to deacetylate non-histones, such as the cytoskeletal protein tubulin, the heat shock/chaperone HSP90, nuclear hormone receptors AR and ER, and many

transcription factors including p53, E2F1, c-Jun, YY1, Mad/Max, and NF-κB (Marks et al. 2001a; Hubbert et al. 2002; Yu et al. 2002). The further identification of non-histone targets has broadened the scope of acetylation from transcription to more widespread cellular processes including protein stability, DNA binding, and proteosomal degradation.

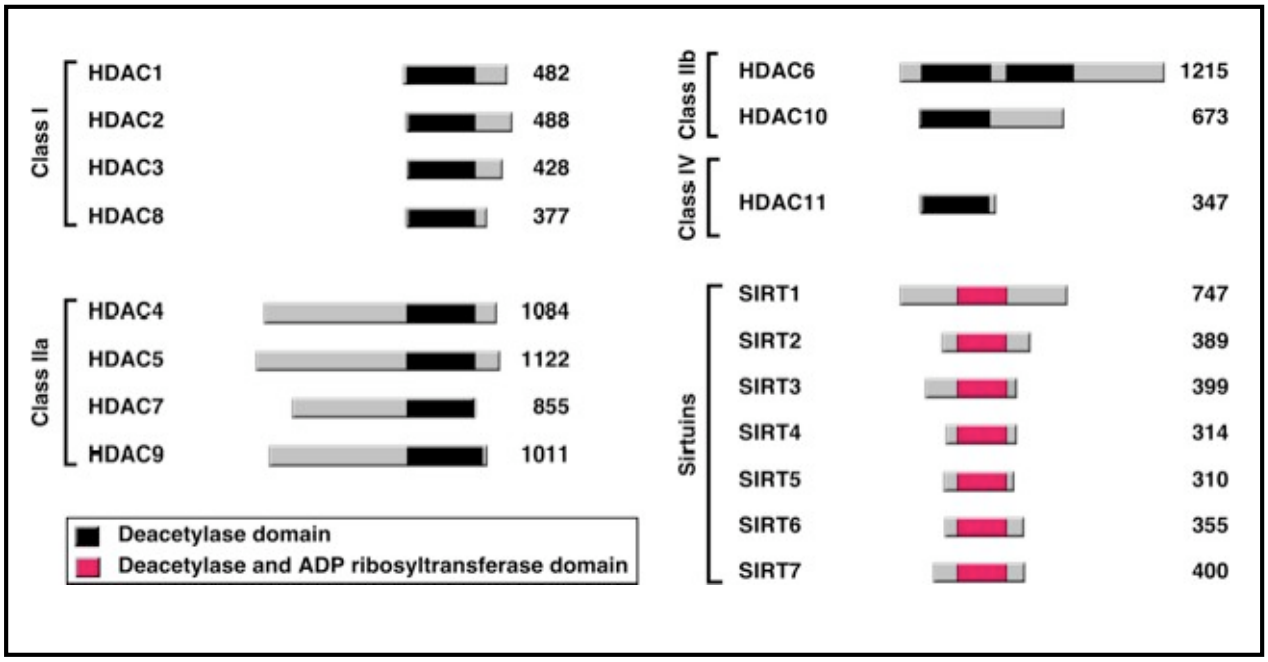

Figure 1.2. Schematic diagram of the family of histone deacetylases. Class I HDACs are smaller than Class II HDACs and comprised almost entirely of their deacetylase domain. The N-terminal extension of class IIa HDACs mediates transcription factor binding. The class III HDACs are also called Sirtuins and require NAD for deacetylation.

HDAC1 was the first histone deacetylase to be identified through the use of a trapoxin affinity matrix (Taunton et al. 1996). Trapoxin was known to inhibit histone deacetylation as well as induce cell cycle arrest; and sequence alignments of HDAC1 showed it to be the mammalian homolog of yeast Rpd3. HDAC2 was identified through a yeast two-hybrid screen using the YY1 transcription factor (Yang et al. 1996). HDAC1 and HDAC2 are the best characterized of all the HDAC proteins and share 85% identity in their amino

acid sequence. HDAC3 shares 53% and 52% amino acid identity with HDAC1 and HDAC2, respectively (Cress and Seto 2000). Mammalian HDAC1 and HDAC2 resulted from a recent evolutionary gene duplication (*Drosophila* has the single RPD3 protein) so it is not surprising HDAC1 and HDAC2 are found in almost all transcriptional repressive complexes together (Gregoretti et al. 2004). The three most characterized repressive complexes that contain HDAC1 and HDAC2 are the Sin3 complex, the NuRD (nucleosomal remodeling and deacetylation) complex, and the CoREST (Co-repressor to RE1 silencing transcription factor/neural restrictive silencing factor) complex (Cress and Seto 2000; Grozinger and Schreiber 2002). Conversely, HDAC3 is predominantly found in a repressive complex with SMRT (silencing mediator for retinoic acid and thyroid hormone receptors) and NCoR (nuclear receptor co-repressor) to repress nuclear receptors as well as other transcription factors (Guenther et al. 2001). As stated earlier, class IIa HDACs recruit HDAC3 as part of their repressive complex to mediate repression of gene expression.

Regulation of HDACs HDACs are able to modulate gene expression by directly binding to transcription factors (e.g. YY1) or may bind indirectly through the recruitment of repressive complexes (e.g. nuclear receptor recruitment of the Sin3 complex). In addition to this mode of regulation, there are multiple mechanisms by which HDAC activity itself may be regulated. HDAC1 and HDAC2 are both phosphorylated to promote complex formation and deacetylase activity (Cai et al. 2001; Tsai and Seto 2002). Two sites on HDAC1 have been mapped to serine 421 and serine 423 (Pflum et al. 2001). Mutations of these sites result in reduced enzymatic activity and complex formation. Additionally, HDAC3 activity is regulated by both phosphorylation and dephosphorylation. HDAC3 is primarily phosphorylated at serine 424 by protein kinase CK2 resulting in up-regulation of deacetylase

activity. This process is negatively regulated by the protein phosphatase PP4 and HDAC3 activity is tightly regulated by the availability of PP4 within the cell (Zhang et al. 2005). Furthermore, HDAC3 is inactive by itself but forms an active complex with the co-repressor SMRT, which is mediated by a chaperone complex (Guenther et al. 2002).

Regulation of class IIa HDACs by post-translational modifications has been extensively studied. HDAC1 and HDAC2 are primarily nuclear, HDAC3 has been shown to be both nuclear and cytoplasmic, and the class IIa HDACs show a phosphorylation-dependent nucleocytoplasmic shuttling as an additional means of regulation (McKinsey et al. 2000a). This is through the phosphorylation of 2 serine-containing motifs in the amino terminus of HDAC4, HDAC5, HDAC7, and HDAC9 (McKinsey et al. 2001). There has been intense focus on identifying HDAC kinases, as these serve as potential therapeutic targets in connecting external stimuli with the genome. CaMKII can phosphorylate HDAC4 specifically while PKD is able to directly phosphorylate HDAC5 (Vega et al. 2004a; Backs et al. 2006). Following phosphorylation, the phosphoserines serve as a docking site for the 14-3-3 chaperone protein, revealing the nuclear export sequence and promoting subsequent nuclear export by CRM-1 (Grozinger and Schreiber 2000; McKinsey et al. 2000b). Further elucidation of this mechanism of sequestration will reveal potential therapeutic targets for multiple disease states as discussed later.

Histone deacetylases and cancer

Histone deacetylases contribute to cancer through multiple mechanisms including increased HDAC expression and activity, recruitment of HDACs to tumor suppressor genes, and fusion proteins from chromosomal translocations aberrantly recruiting HDACs to genes involved in

differentiation (Cress and Seto 2000). HDAC1 is increased in gastric cancer (Choi et al. 2001), whereas HDAC2 and HDAC3 are increased in colon cancer (Wilson et al. 2006). Histone deacetylases are also strongly implicated in the regulation of the cyclin-dependent kinase inhibitor $p21^{WAF1/CIP1}$. p21 inhibits cyclin/CDK complexes, controlling cell cycle progression at the G_1/S transition, and is commonly down-regulated in multiple tumors. Repressive complexes containing HDAC1 and HDAC2 have been shown to regulate *CDKN1A* (gene encoding p21) through recruitment to the Sp1 site within the promoter (Gui et al. 2004). Increased HDAC expression and activity further decreases the expression of p21 resulting in rampant cell proliferation.

Perhaps the most direct evidence for HDACs in cancer is seen through oncogenic chromosomal translocations in certain types of leukemias. Acute promyelocytic leukemia (APL) is often the result of the chromosomal translocation t(15;17), which generates a chimeric protein containing most of the retinoic acid receptor α (RARα) fused to PML (promyelocytic leukemia) or the translocation t(11;17) in which the same region of RARα is fused to PLZF (promyelocytic leukemia zinc finger) (Lin et al. 2001). RARα normally heterodimerizes with RXRα to control promyelocytic differentiation and hematopoiesis. Retinoic acid binds the heterodimer, displaces the repressive complex, and activates myeloid cell differentiation; however, the oncogenic translocations generate a fusion protein that is unresponsive to ligands, resulting in the constitutive recruitment of HDACs by RXRα/RARα, blockade of differentiation, and rampant proliferation. Similar mechanisms are seen in acute myeloid leukemia (AML) in which the chromosomal translocations t(8;21), t(12;21), or t(16;21) generate fusion proteins between AML1 and ETO, AML1 and TEL, or AML and MTG16, respectively (Cress and Seto 2000). AML1 usually acts as a

transcriptional activator in myeloid differentiation, however the fusion proteins block AML1-dependent gene activation through the recruitment of HDAC-containing complexes. These examples in which HDACs are aberrantly recruited to the promoters of genes involved in differentiation support HDACs as a nodal point in the progression of tumors and indicate that even minor alterations in the steady state levels of acetylation might have profound effects on the cellular processes.

HDAC inhibitors

Aberrant expression, activity, and recruitment of HDACs in tumorogenesis have led to the rationale that treatment with HDAC inhibitors might restore normal function in these cell types. Most of the current HDAC inhibitors in clinical trials were not identified for their potent deacetylase inhibition activity, but rather through screens looking for compounds that alter the behavior of transformed cells, either by blocking proliferation or inducing differentiation (Marks et al. 2001a). HDAC inhibitors can indeed reverse aberrant transcriptional repression of genes involved in proliferation and differentiation (as in restoring retinoic acid sensitivity to PML cells). Surprisingly, inhibition of HDACs leads to only a small fraction of genes induced (2% of genes) including many common anti-tumor genes, such as $p21^{WAF1/CIP1}$ (Van Lint et al. 1996). Furthermore, HDAC inhibitors have shown efficacy in *in vivo* tumor models so it is not surprising much research has been focused on identifying new compounds that block deacetylase activity. In doing so, scientists have uncovered a structural array of inhibitors that block deacetylase activity and are showing therapeutic potential in clinical trials.

HDAC inhibitor chemistry There are four main groups of HDAC inhibitors that vary greatly in structure (Figure 1.3). These are: hydroxamic acids (e.g. TSA, SAHA, and scriptaid), short chain fatty acids (e.g. valproic acid and 4-phenylbutyrate), cyclic tetrapeptides (e.g. depsipeptide, apicidin, and trapoxin), and benzamides (e.g. MS-275). Of these, hydroxamic acids are the most commonly studied. TSA was initially an anti-fungal agent, however it's potency in HDAC research has made it the basis by which many new inhibitors are being designed (Yoshida et al. 1990). SAHA (also called Vorinostat) was the first HDAC inhibitor approved by the Food and Drug Administration (FDA). These hydroxamic acids inhibit HDACs and affect cellular proliferation at the nanomolar level (Marks et al. 2001b). Compared to most HDAC inhibitors, the short chain fatty acids are relatively weak inhibitors with activity in the millimolar range. Valproic acid (VPA) has been a commonly prescribed anti-convulsant and only recently identified as an HDAC inhibitor (Phiel et al. 2001). Cyclic tetrapeptides, such as apicidin and depsipeptide, are all active at nanomolar concentrations and are relatively complex in their structure (Nakajima et al. 1998). MS-275, a member of the benzamide class of HDAC inhibitors, is a much weaker inhibitor, acting in the micromolar range, however it shows more selectivity than other HDAC inhibitors (Saito et al. 1999).

Clinical trials of HDAC inhibitors The broad anti-tumor activity of HDAC inhibitors has resulted in more than 100 clinical trials for HDAC inhibitors as either monotherapy or combinatorial therapy for a multitude of hematologic and solid tumors (Dokmanovic et al. 2007). To date, these clinical trials show HDAC inhibitors have potential in both hematologic and solid tumors at concentrations with minimal side effects. As mentioned, Vorinostat was the first HDAC inhibitor approved by the FDA for treatment of cutaneous T-

cell lymphoma (CTCL). Vorinostat is currently in trials with multiple other anti-oncogenic agents for a variety of more advanced cancers. LBH-589 and ITF2357, both hydroxamic acid HDAC inhibitors similar to Vorinostat, are in clinical trials for CTCL and refractory multiple myeloma, respectively. Depsipeptide is currently in phase II trials for both cutaneous T-cell lymphoma and peripheral T-cell lymphoma. It is also in additional combinatorial therapy clinical trials for multiple tumor-types.

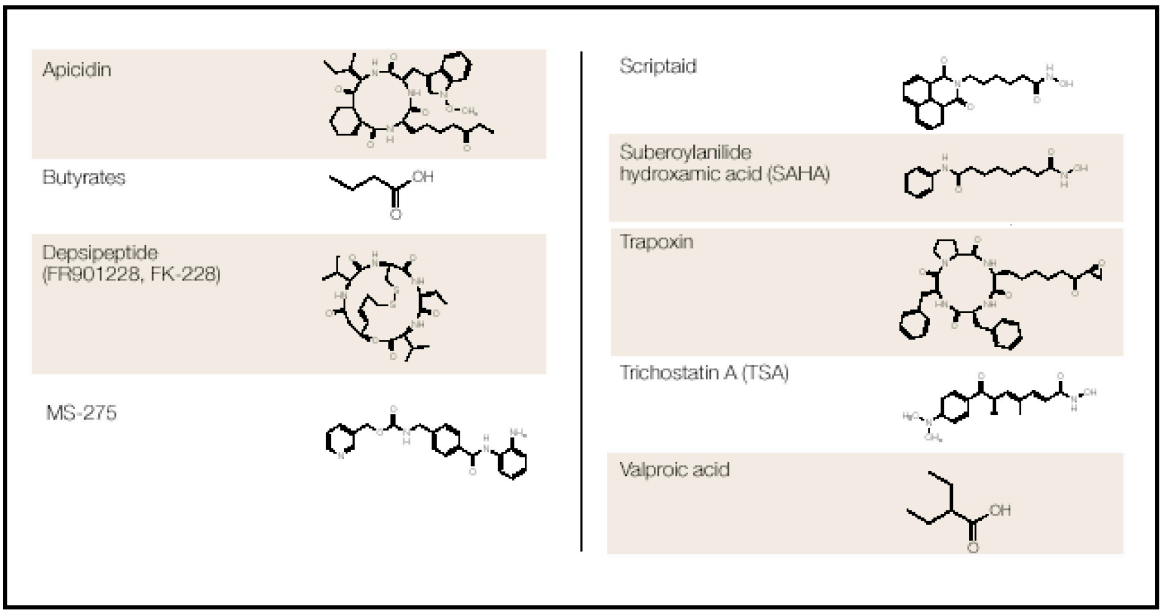

Figure 1.3. Structures of HDAC inhibitors. The chemical structures for the main HDAC inhibitors are shown. These chemicals show strong heterogeneity in structure. (Modified from Marks et al. 2001)

Specificity While these HDAC inhibitors continue to show promise as anti-tumor agents, increasing focus is on the specificity of each inhibitor. The hydroxamic acids are considered pan-inhibitors of both class I and class II HDACs, however given the lack of activity of class II HDACs, there is still debate upon what function these are inhibiting. The short chain fatty acids, VPA in particular, appear to inhibit class I HDACs preferentially and VPA has been

shown to selectively induce degradation of HDAC2 (Kramer et al. 2003). MS-275 selectively inhibits HDAC1 over HDAC3, and shows no activity towards HDAC8 (Hu et al. 2003). Two recently developed synthetic hybrid inhibitors, SK-7041 and SK-7068, show potent selectivity against HDAC1 and HDAC2 specifically (Park et al. 2004). These hybrids have replaced the cap structure of TSA with a pyridyl ring. Tubacin, a small-molecule inhibitor of tubulin deacetylation, is specific for HDAC6 as it has no affect on histone acetylation or gene expression (Haggarty et al. 2003). It is still under debate whether increased specificity will result in better anti-tumor agents, however in the context of other disease states, it may very well be advantageous, as discussed later.

HDAC biology

The specificity of HDAC inhibitors has been of high interest as both a method to better design HDAC inhibitors with minimal side effects as well as to understand the specific role of each individual HDAC in the context of development and disease. Many *in vitro* siRNA experiments have lent significant support for class I HDACs as the main target for anti-tumor therapies. Through knockdown and gene deletions in multiple animal models, we are beginning to understand the specific roles of individual HDACs *in vivo*.

Lessons from yeast, invertebrates, and zebrafish Surprisingly, null mutations of the *RPD3* gene in yeast (*S. cerevisiae*) are viable unlike its higher eukaryotic ortholog. However, *RPD3* mutants exhibit multiple phenotypes, including reduced potassium dependency (for which it is named), mating defects, and derepression of acid phosphatase (Vidal and Gaber 1991; Dora et al. 1999). As expected, deletion of *RPD3* results in increased histone

acetylation, but there is also a paradoxical increase in repression of telomeric heterochromatin (Rundlett et al. 1996).

Mutations of the *C. elegans* homolog of yeast RPD3, *hda-1*, have been characterized and also cause a variety of defects. Both mutational and RNAi studies demonstrate HDA-1 is necessary for viability, is required for proper gonadal and vulval development, and is necessary for efficient cell migration and axon pathfinding (Shi and Mello 1998; Zinovyeva et al. 2006). Microarray analysis of *C. elegans* embryos fed RNAi against *hda-1* demonstrated HDA-1 regulates a number of extracellular matrix genes as well as tissue-specific genes (Whetstine et al. 2005). The total percentage of genes changed was roughly 2.2%, very similar to the number of genes altered after HDAC inhibitor treatment.

Studies in *Drosophila* provided significant evidence for the role of HDACs as transcriptional repressors. Strong hypomorphic mutations result in embryonic lethality and segmentation phenotypes due to defects in transcriptional repression (Mannervik and Levine 1999). Additional mutational analyses have demonstrated a set of dominant negative mutations in which genes silenced by position effect variegation (PEV) become activated due to a "poisoning" effect on the deacetylase complex (Mottus et al. 2000).

Mutational analyses of HDAC1 in zebrafish have resulted in an array of phenotypes ranging from abnormalities in neural differentiation to cardiovascular development. The *colgate(hdac1)* mutant shows defects in body axis extension and branchiomotor neuronal migration (Nambiar et al. 2007). The *add(hdac1)* mutant is unable to differentiate into neurons and glial cells, blocking differentiation of retinal progenitors (Yamaguchi et al. 2005). Using an *hdac1*-morpholino, it was shown that HDAC1 mutants exhibit defects in neuronal specification, reduced brain size, and pericardial edema (Cunliffe 2004).

Furthermore, another *hdac1* homozygous mutant showed defects in oligodendrocyte specification, consistent with the earlier studies on other neuronal cell types (Cunliffe and Casaccia-Bonnefil 2006). Collectively, these studies support HDAC1 as a necessary component of the transcriptional machinery required to promote a variety of neuronal specifications in the developing zebrafish.

Lessons from mice The analyses performed in lower eukaryotes provide insight into the role of HDACs, but because of the few HDAC enzymes, it is difficult to translate these roles to human pathologies and delineate the roles of individual HDACs. Mice and humans share all 10 class I and II HDACs and are highly homologous in their amino acid sequence. Because of this, knockout mice for individual HDACs can yield insight into the role of individual HDACs in normal physiology and disease states.

Deletion of HDAC1 results in embryonic lethality before E10.5, presumably due to proliferative defects from the up-regulation of the CDK inhibitors p21 and p27 (Lagger et al. 2002). However, deletion of p21 and p27 were unable to rescue the lethality associated with loss of HDAC1 (C. Seiser, personal communication). Interestingly, loss of HDAC1 resulted in increased expression of both *HDAC2* and *HDAC3*, however this was unable to compensate. Mice with global deletion of HDAC2 have been reported to be partially viable and the surviving mice able to block cardiac hypertrophy (Trivedi et al. 2007a), however our HDAC2 null mutation caused lethality by postnatal day 1 (Montgomery et al. 2007). These mice are born at Mendelian ratios, but showed both proliferative and apoptotic cardiomyocytes and died within 24 hours. The discrepancies between the two alleles remain unclear, however our line was generated through conventional homologous recombination, while the Trivedi et al. line was generated using a gene trap insertion line which frequently

display variable phenotypes due to alternative splicing within the mutant locus (Voss et al. 1998). Additionally, different regions of the HDAC2 protein were targeted. Our group targeted the amino terminal region of HDAC2 that contains key histidine residues necessary for activity (Finnin et al. 1999), whereas the gene trap insertion ablates the carboxy terminus. Regardless, the global deletions of HDAC1 and HDAC2 demonstrate interesting possibilities for these enzymes in development. The lethality shows these enzymes are either non-redundant during development or they are not coexpressed in every cell type and the resultant phenotype is due to lack of expression of the other redundant enzyme.

While global deletion of either HDAC1 or HDAC2 results in lethality, the potential redundancy of HDAC1 and HDAC2 is evident through the tissue-specific deletions of these enzymes. Deletion of HDAC1 or HDAC2 in cardiomyocytes, brain, skeletal muscle, neural crest, chondrocytes, smooth muscle, or endothelial cells using conditional floxed alleles results in viable offspring that show no gross abnormalities (Montgomery et al. 2007). However, deletion of HDAC1 and HDAC2 results in embryonic lethality (in early cardiomyocytes, smooth muscle, or endothelial cells) or lethality soon after birth (in late cardiomyocytes, brain, skeletal muscle, or chondrocytes) (Chapter IV). The robust phenotypes and lethality associated with deleting both enzymes, but not with either individually, implicates these enzymes as redundant regulators in many cell types during development.

Deletion of HDAC3 has not been published, however we have used a conditional floxed allele of HDAC3 to delete it in a variety of tissues (Chapter III). Global deletion of HDAC3 is embryonically lethal before E9.5 due to defects in gastrulation. The role of HDAC3 in individual tissues is just now beginning to be investigated, however striking

phenotypes are apparent thus far in a variety of tissues including defects in cardiac energetics from the cardiac specific deletion of HDAC3. Given the role of HDAC3 in mediating nuclear hormone dependent transcription, the continued analysis of these knockouts will prove vital to the pursuit of HDAC therapeutics.

The analysis of the gene deletions of class IIa HDACs has also given insight into the biological and physiological functions of these proteins in development and disease. The class IIa HDACs are expressed predominantly in brain, heart, and skeletal muscle (McKinsey et al. 2002), however HDAC7 shows an endothelial cell restricted expression pattern (Chang et al. 2006). These proteins function as repressors by binding to MEF2 and other transcription factors to mediate gene expression. Deletion of HDAC4 results in premature chondrocyte hypertrophy and early onset ossification through the rampant expression of Runx2 dependent genes (Vega et al. 2004b). HDAC5 and HDAC9 knockout mice show redundant phenotypes in exacerbating the cardiac hypertrophic response (Zhang et al. 2002; Chang et al. 2004). Deletion of HDAC7 shows embryonic lethality due to defects in vascular integrity (Chang et al. 2006). The generation of these mice has made the question of specificity much easier to ascertain. The use of individual knockouts or compound deletions, both *in vitro* and *in vivo*, in the presence and absence of HDAC inhibitors will not only lead to a better understanding of which isozymes are responsible for HDAC inhibitor-mediated outcomes, but also allow for a more vigorous analysis toward off-target complications.

Histone deacetylases in cardiac hypertrophy

As mentioned, HDACs and HDAC inhibitors are well known for their potential roles as anti-tumor targets and agents, respectively. However, the potential for HDACs as therapeutic

targets extends well beyond cancer. In fact, HDAC inhibitors have been shown to ameliorate a multitude of pathologies including muscle dystrophy, atrophy, multiple sclerosis, diabetes, neurodegeneration, and asthma (Steffan et al. 2001; Camelo et al. 2005; Choi et al. 2005; Minetti et al. 2006; Tsai et al. 2006; Lee et al. 2007). Additionally, genetic and inhibitor studies have shed light on the roles of histone deacetylases in cardiac hypertrophy.

Stress-dependent cardiac remodeling In response to stress signals from a variety of cardiovascular disorders including hypertension and myocardial infarction, the heart enlarges due to cardiomyocyte hypertrophy. This is initially beneficial to sustain cardiac output, however prolonged hypertrophy often leads to dilated cardiomyopathies and lethality (Chien 1999). The cellular hypertrophy is characterized by an increase in cell size, augmented protein synthesis, higher organization of the sarcomere, and re-activation of the fetal gene program (Frey and Olson 2003). Multiple pathways have been identified that transmit extrinsic signals to the genome to activate the hypertrophic response (Figure 1.4). Many of these are dependent upon intracellular calcium concentrations such as calcineurin and CAMKII, however whether or not these pathways converge at nodal points to activate downstream targets remains to be elucidated.

The stressed myocardium responds to these signals by transcriptional reprogramming of the cardiomyocyte to a more fetal-like gene state. This includes the well studied switch in myosin heavy chain isoforms (Ng et al. 1991). During hypertrophy, the heart up-regulates the expression of the fetal isoform, βMHC, and down-regulates the adult isoform, αMHC, resulting in diminished myofibrillar ATPase activity (Kurabayashi et al. 1990). Additional hallmark genes of cardiac hypertrophy include induction of atrial natriuretic peptide (ANP) and brain natriuretic peptide (BNP) and down-regulation of sarcoplasmic reticulum Ca^{2+}-

ATPase (SERCA) (Saito et al. 1989; Hasegawa et al. 1993; Matsui et al. 1995). Identification of the transcription factors mediating the hypertrophic response is still under intense investigation. GATA4, NFAT, CREB, and MEF2 are among the numerous transcription factors implicated in regulating hypertrophic gene activation (Frey and Olson 2003).

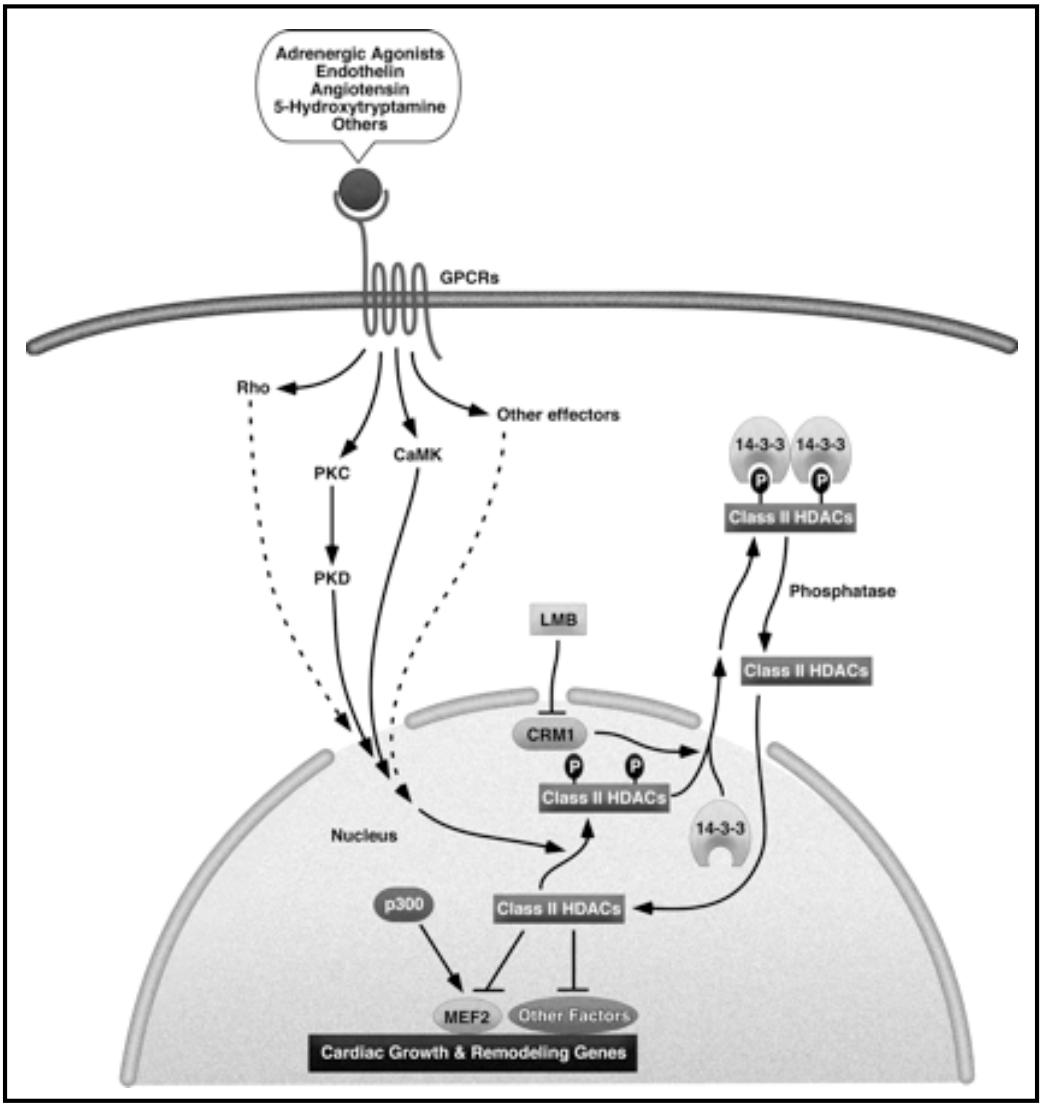

Figure 1.4. Intracellular cardiac hypertrophy pathways. Multiple pathways that active remodeling genes have been defined. Many of these converge on Class II HDACs and MEF2. Numerous kinases phosphorylate class II HDACs resulting in their nucleocytoplasmic shuttling. This allows derepression of MEF2 and activation of remodeling genes. (Adapted from (Backs and Olson 2006)

Class II HDACs and cardiac growth MEF2 is among a number of transcription factors whose expression remains constant during hypertrophy, but MEF2 activity is greatly increased (Passier et al. 2000; Zhang et al. 2002). This is due to regulation by the class IIa HDACs (HDAC4, HDAC5, HDAC7, and HDAC9). These proteins contain an amino-terminal extension that mediates interaction with various transcription factors. Mice with genetic deletion of HDAC5 or HDAC9 are viable, however these mice begin to show cardiac abnormalities at about 6 months of age (Zhang et al. 2002; Chang et al. 2004). Additionally, these mice are hypersensitive to certain calcium-dependent stresses such thoracic aortic constriction, showing an exacerbated hypertrophic response. The early lethality associated with loss of HDAC4 or HDAC7 has precluded the analysis of these proteins in modulating the hypertrophic program, however conditional deletions are underway to examine such effects (Vega et al. 2004b; Chang et al. 2006).

The exacerbation of the hypertrophic response resulting from the loss of HDAC5 or HDAC9 is presumably due to increased activity of the transcription factor MEF2. Under normal physiological conditions, class IIa HDACs bind to MEF2 and block MEF2-dependent gene activation. Extrinsic stress signals are able to activate various intracellular kinases such as CaMKII and PKD that directly phosphorylate class IIa HDACs at 2 conserved serine residues (Vega et al. 2004a; Backs et al. 2006). This phosphorylation results in the binding of the chaperone 14-3-3, nucleocytoplasmic shuttling by CRM1, and derepression of MEF2 and other transcription factors (Grozinger and Schreiber 2000; McKinsey et al. 2000b). The loss of HDAC5 or HDAC9 results in an imbalance of MEF2 activity within the myocytes and subsequent activation of the hypertrophic response.

HDAC inhibitors and class I HDACs in hypertrophy Given the loss of function phenotypes of HDAC5 or HDAC9, one might predict treatment of cardiomyocytes with HDAC inhibitors would result in cardiac hypertrophy. Paradoxically, HDAC inhibitors such as TSA and sodium butyrate are able to block the hypertrophic response and dose-dependently block activation of the fetal gene program (Antos et al. 2003; Kong et al. 2006). Moreover, treatment of mice with an HDAC1 and HDAC2 specific inhibitor is able to completely mimic the response seen with pan-HDAC inhibitors (Kee et al. 2006). Surviving mice from the gene-trap deletion of HDAC2 fail to undergo cardiac hypertrophy from aortic constriction and β-adrenergic stimulation, lending support for HDAC2 as a nodal point in the activation of the fetal gene program during hypertrophy (Trivedi et al. 2007a). Our lab, however, has shown that HDAC1 and HDAC2 act redundantly in the pathological setting of hypertrophy as cardiac-specific deletion of HDAC1 or HDAC2 is not able to block the hypertrophic response (Montgomery et al. 2007). Cardiac-specific deletion of both HDAC1 and HDAC2 results in neonatal lethality, precluding adult hypertrophy analysis. However, we have recently generated an adult cardiac-specific deletion of HDAC1 and HDAC2 using an inducible cardiac Cre line and these mice handle the loss of HDACs very well and are showing promise in the blockade of hypertrophic signals from β-adrenergic stimulation. These studies have implicated class I HDACs as critical regulators of the hypertrophic response. Interestingly, these enzymes appear to play opposing roles to class II HDACs during pathological hypertrophy (Figure 1.5). Because of this, the design of more specific inhibitors against class I HDACs remains a promising approach for the treatment of cardiac hypertrophy and heart failure.

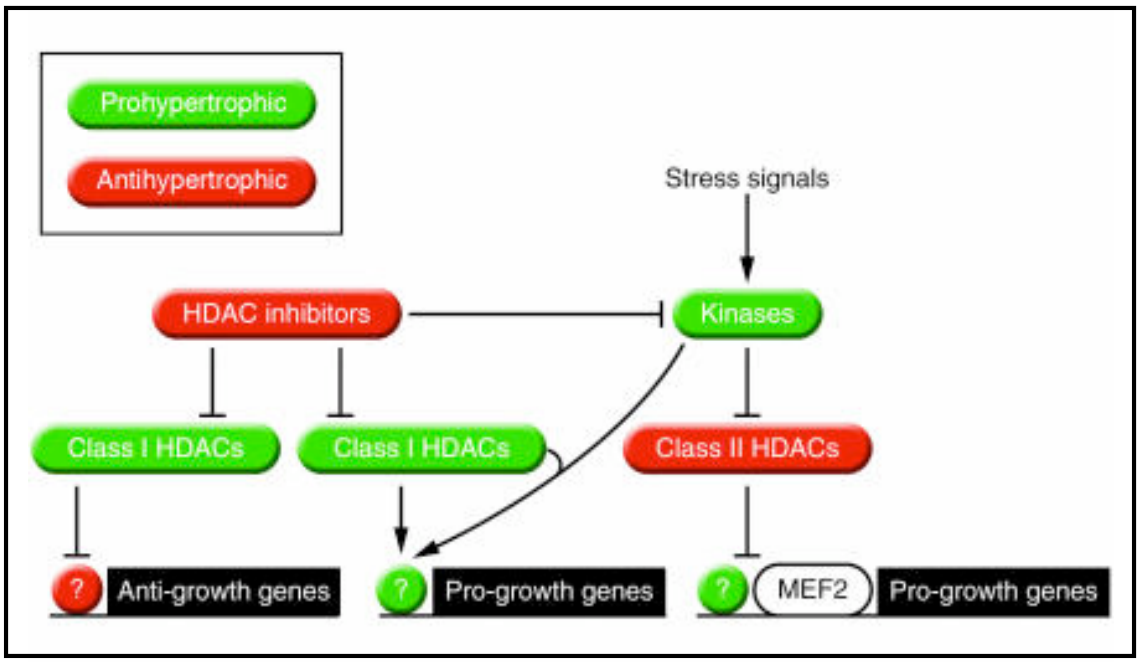

Figure 1.5. Schematic diagram of opposing roles of class I and II HDACs in hypertrophy. Class II HDACs are anti-hypertrophic through the repression of MEF2 and other transcription factors. Class I HDACs are pro-hypertrophic, possibly through the repression of anti-growth genes. (McKinsey and Olson 2005)

Concluding remarks

Over the last 15 years, covalent modifications of histones have become one of the most attractive therapeutic targets for a variety of disease states. With the recent approval of Vorinostat by the FDA, histone deacetylases and HDAC inhibitors will continue to lead the way in targeting histone modifications for clinical malignancies. Genetic and pharmacologic studies have demonstrated HDACs to have vast potential beyond cancer and have paved the way to identify new small molecule inhibitors that selectively inhibit individual HDAC isozymes. Furthermore, the continued generation and analysis of knockout mice from various HDACs will help identify specific functions for these enzymes in development and disease. Thus, what began as simple screens to induce differentiation of transformed cells

has uncovered some of the most promising compounds in not only cancer, but muscular dystrophies, neurodegeneration, multiple sclerosis, and heart disease as well.

Chapter II

Histone Deacetylases 1 and 2 Redundantly Regulate Cardiac Morphogenesis, Growth, and Contractility

ABSTRACT

Histone deacetylases (HDACs) tighten chromatin structure and repress gene expression through the removal of acetyl groups from histone tails. The class I HDACs, HDAC1 and HDAC2, are expressed ubiquitously, but their potential roles in tissue-specific gene expression and organogenesis have not been defined. To explore the functions of HDACs 1 and 2 in vivo, we generated mice with conditional null alleles of both genes. Whereas global deletion of HDAC1 results in death by embryonic day 9.5, mice lacking HDAC2 survive until the perinatal period when they succumb to a spectrum of cardiac defects including obliteration of the lumen of the right ventricle, excessive hyperplasia and apoptosis of cardiomyocytes, and bradycardia. Cardiac-specific deletion of either HDAC1 or 2 does not evoke a phenotype, whereas cardiac-specific deletion of both genes results in neonatal lethality, accompanied by cardiac arrhythmias, dilated cardiomyopathy, and up-regulation of genes encoding skeletal muscle-specific contractile proteins and calcium channels. Our results reveal cell autonomous and non-autonomous functions for HDAC1 and 2 in the control of myocardial growth, morphogenesis and contractility, which reflect partially redundant roles of these enzymes in tissue-specific transcriptional repression.

INTRODUCTION

Chromatin modifying enzymes control gene expression through reversible post-translational modifications of histone tails within nucleosomes (Jenuwein and Allis 2001). Histone acetyltransferases catalyze the transfer of acetyl groups from acetyl-Coenzyme A to ε-amino groups of lysine residues of histone tails. Acetylation results in a loss of positive charge, relaxing chromatin structure and allowing access of transcription factors to their target genes (Roth et al. 2001). Histone deacetylases (HDACs) oppose the activity of histone acetyltransferases by catalyzing the removal of acetyl groups from histone tails, resulting in compaction of chromatin and transcriptional repression (Grozinger and Schreiber 2002).

There are 4 classes of HDACs that comprise an ancient enzyme family conserved from bacteria to humans (Gregoretti et al. 2004). Class I HDACs (HDAC1, 2, 3 and 8) are highly homologous to the yeast HDAC RPD3 and are ubiquitously expressed (Yang et al. 1997). Class II HDACs (HDAC4, 5, 6, 7 and 9) are homologous to the yeast protein HDA1 and are enriched in muscle and neural tissues (Grozinger et al. 1999; Verdin et al. 2003). Class II HDACs regulate tissue growth through signal-dependent repression of MEF2 and other transcription factors (Lu et al. 2000). Class III HDACs or sirtuins require NAD for deacetylation and are related to the yeast repressor Sir2 (Grozinger and Schreiber 2002). Class IV HDACs, a recently identified family of deacetylases, share homology to human HDAC11 (Gao et al. 2002).

The functions of class I HDACs in mammals have been largely inferred from studies in cultured cells, but relatively little is known of their potential roles *in vivo*. HDAC1 and HDAC2 share 85% amino acid homology and are found together in almost all repressive transcriptional complexes (Grozinger and Schreiber 2002). Mouse embryos deficient in

HDAC1 die before embryonic day (E) 10.5 due to proliferative defects (Lagger et al. 2002), precluding an analysis of its potential functions later in development or after birth. An HDAC2 mutant mouse generated from a lacZ insertion was recently reported to be viable (Trivedi et al. 2007b), although as discussed below, our findings differ from the conclusions of that study.

To examine the functions of HDAC1 and 2 in vivo, we generated mice with conditional null alleles for both genes. We show that global deletion of HDAC2 results in perinatal lethality with severe cardiac defects that appear to reflect a non-myocyte autonomous function of HDAC2, since cardiac-specific deletion of either HDAC1 or 2 alone has no discernable effect on cardiac function. However, cardiac deletion of both HDAC1 and 2 genes results in dilated cardiomyopathy, arrhythmias, and neonatal lethality, accompanied by up-regulation of genes encoding skeletal muscle-specific myofibrillar proteins and calcium channels. Our findings suggest that HDAC1 and HDAC2 are functionally redundant in cardiac growth and development and maintain cardiomyocyte identity and function, at least in part, through repression of genes encoding skeletal muscle-specific myofibrillar proteins and calcium channels.

RESULTS

Conditional deletion of *HDAC1*

The mouse *HDAC1* gene contains 14 exons and spans 30 kilobases of DNA (Khier et al. 1999). We generated a conditional null allele of *HDAC1* by introducing *loxP* sites upstream of exon 5 and downstream of exon 7 through homologous recombination in ES cells (Figure 2.1). This deletion eliminates several key histidine and aspartic acid residues required

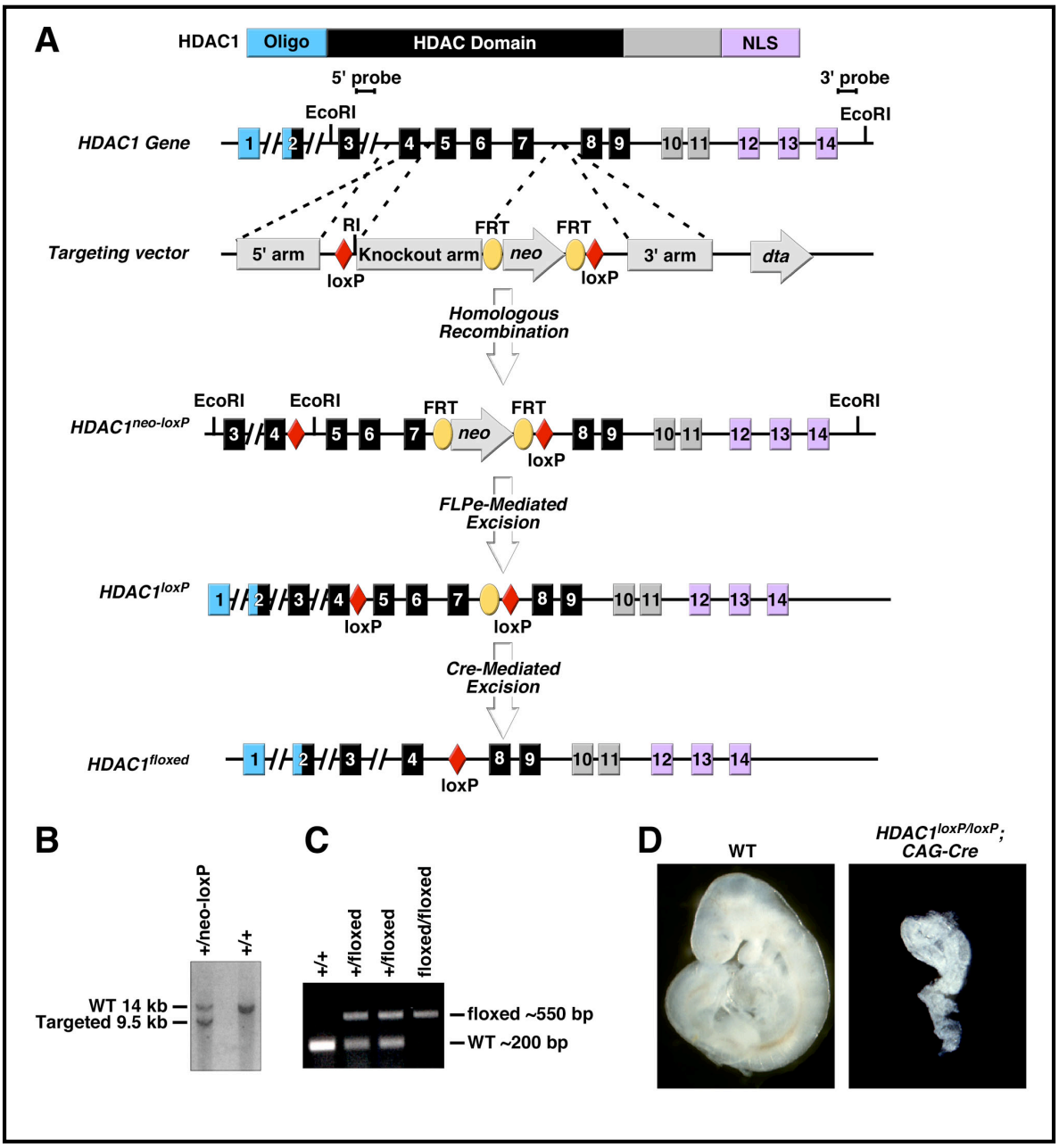

Figure 2.1. Generation of a conditional *HDAC1* allele. (*A*) Strategy to generate a conditional *HDAC1* allele. Protein, corresponding exonic structure, targeting vector, and targeted allele are shown. *loxP* sites were inserted into introns 4 and 7 through homologous recombination. The neomycin resistance cassette, flanked by FRT sites, was removed by crossing to transgenic animals expressing hACTB::FLPe in the germline. Cre-mediated excision results in one *loxP* site in the place of exons 5–7. (*B*) Southern blot analysis of agouti offspring from chimera/C57BL/6 intercrosses from targeted ES cells. Tail DNA was digested with EcoRI, and the corresponding wild-type (14 kb) and targeted (9.5 kb) bands are indicated for the 3' probe. (*C*) Genotyping of *HDAC1*^{floxed} mice by genomic PCR. Primer set includes three primers. One primer set flanks the 5' *loxP* site with the third primer downstream from the 3' *loxP* site. Global deletion by CAG-Cre removes the primer within the *loxP* sites, resulting in one 550-bp product for the *HDAC1*$^{floxed/floxed}$ animals. (*D*) Wild-type and *HDAC1*$^{loxP/loxP}$; *CAG-Cre* mutant embryos at E9.5. Recapitulation of the previously reported global KO is shown.

for catalytic activity (Hassig et al. 1998). Mice heterozygous for this *HDAC1*$^{neo\text{-}loxP}$ allele were bred to females expressing a CAG-Cre transgene, which deletes in the germline (Sakai and Miyazaki 1997), resulting in an *HDAC1*$^{+/-}$ allele. *HDAC1*$^{+/-}$ mice were intercrossed to generate *HDAC1*$^{-/-}$ mice on a 129/C57BL/6/CD1 mixed genetic background. Homozygosity of the *HDAC1* null allele resulted in embryonic lethality before E9.5, consistent with a prior description of the global *HDAC1* gene deletion (Lagger et al. 2002) (Figure 2.1D).

HDAC1$^{neo\text{-}loxP}$ mice were bred to FLPe transgenic animals to delete the neomycin cassette (Rodriguez et al. 2000), resulting in an *HDAC1*^{loxP} allele (Figure 2.1A). We deleted *HDAC1* specifically in the heart by breeding homozygous *HDAC1*$^{loxP/loxP}$ mice to transgenic mice expressing Cre recombinase under the control of the *α-myosin heavy chain* (*αMHC*) promoter, which is expressed in differentiated cardiomyocytes pre- and postnatally (Agah et al. 1997). *HDAC1*$^{loxP/loxP}$; *αMHC-Cre* mice were phenotypically normal and displayed no cardiac abnormalities (Figure 2.2A). HDAC1 immunostaining of cardiomyocytes isolated from *HDAC1*$^{loxP/loxP}$; *αMHC-Cre* mice revealed no nuclear staining in cardiomyocytes positive for α-actinin, confirming efficient recombination *in vivo* (Figure 2.2B).

RT-PCR on RNA isolated from the hearts of *HDAC1*$^{loxP/loxP}$; *αMHC-Cre* mice confirmed the reduction in expression of the HDAC1 transcript (Figure 2.2C); residual transcript in the heart likely arises from fibroblasts and other non-myocytes in which the *αMHC-Cre* transgene is not expressed. Other class I HDAC levels were unchanged in the hearts of *HDAC1*$^{loxP/loxP}$; *αMHC-Cre* mice (Figure 2.2C), suggesting basal expression of other class I HDACs is sufficient to compensate for the loss of HDAC1. We also deleted *HDAC1* in the neural crest, skeletal muscle, central nervous system, endothelium, smooth

muscle, and secondary heart field using the appropriate Cre transgenic lines (Table 2.1). All of these mutant mice were viable.

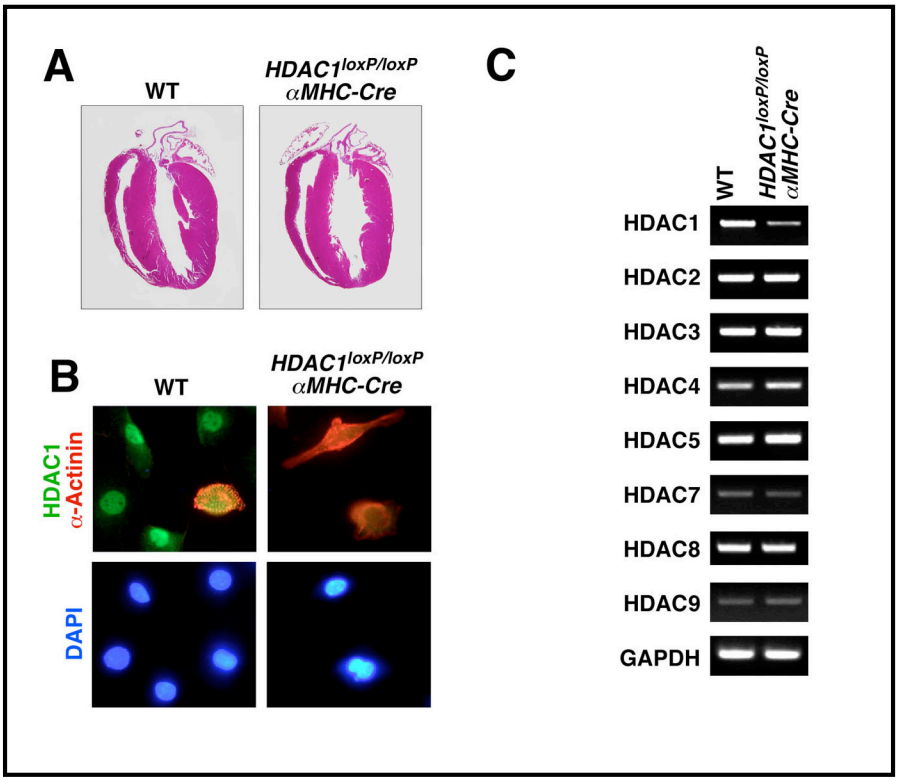

Figure 2.2. Cardiac-specific deletion of HDAC1. (*A*) Wild-type and *HDAC1*$^{loxP/loxP}$; *MHC-Cre* mice at 6 wk of age. Cardiac-specific deletion of HDAC1 was achieved by crossing *HDAC1*$^{loxP/loxP}$ mice to mice harboring a transgene for MHC-Cre. Hematoxylin and eosin (H&E)-stained hearts at 6 wk of age show no gross abnormalities. (*B*) Immunostaining for HDAC1 (green) and -actinin (red) on cardiomyocytes isolated from wild-type and *HDAC1*$^{loxP/loxP}$; *MHC-Cre* neonatal mice. Note cardiac fibroblasts positive for HDAC1 that are negative for -actinin. Immunostaining for HDAC1 in Cre-positive myocytes shows no positive staining for HDAC1. (*C*) Transcript analysis of cardiac-specific deletion of HDAC1. Transcript levels were analyzed by semiquantitative RT–PCR for *HDAC*s *1–5* and *HDAC*s *7–9*. *GAPDH* levels were detected as a control. *HDAC1* transcript levels are not entirely lost due to high expression in contaminating cardiac fibroblasts, as seen in *B*.

Cre-mediated deletion of HDAC1 and HDAC2

Cre Recombinase Driver	Expression Pattern	Results
α-MHC	Cardiomyocyte (late)	Viable
Nkx2.5 KI	Cardiomyocyte (early)	Viable
Wnt1	Neural crest	Viable
Myogenin	Skeletal muscle	Viable
hGFAP	Central nervous system	Viable
Tie2	Endothelial cell	Viable
SM22	Smooth muscle	Viable
Tbx1	Secondary heart field	Viable

Table 2.1. Table of Cre recombinase drivers used to delete HDAC1 or HDAC2. All cre recombinase transgenes tested resulted in viable offspring.

Conditional deletion of *HDAC2*

Given the persistent expression of other class I HDACs in the hearts of *HDAC1*$^{loxP/loxP}$; *αMHC-Cre* mice and the high homology between HDAC1 and 2, we addressed the possible functional redundancy of these HDACs by generating a conditional allele for *HDAC2*. We introduced *loxP* sites upstream of exon 2 and downstream of exon 4 of the mouse *HDAC2* gene, which contains 14 exons and spans 36 kilobases (Figure 2.3A, B). This mutation deletes a portion of the oligomerization domain and residues in the catalytic domain required for enzymatic activity (Hassig et al. 1998). Mice heterozygous for the *HDAC2*$^{neo\text{-}loxP}$ allele were crossed to CAG-Cre transgenic mice (Sakai and Miyazaki 1997) to generate an *HDAC2*$^{+/-}$ allele, and *HDAC2*$^{+/-}$ mice were intercrossed to generate

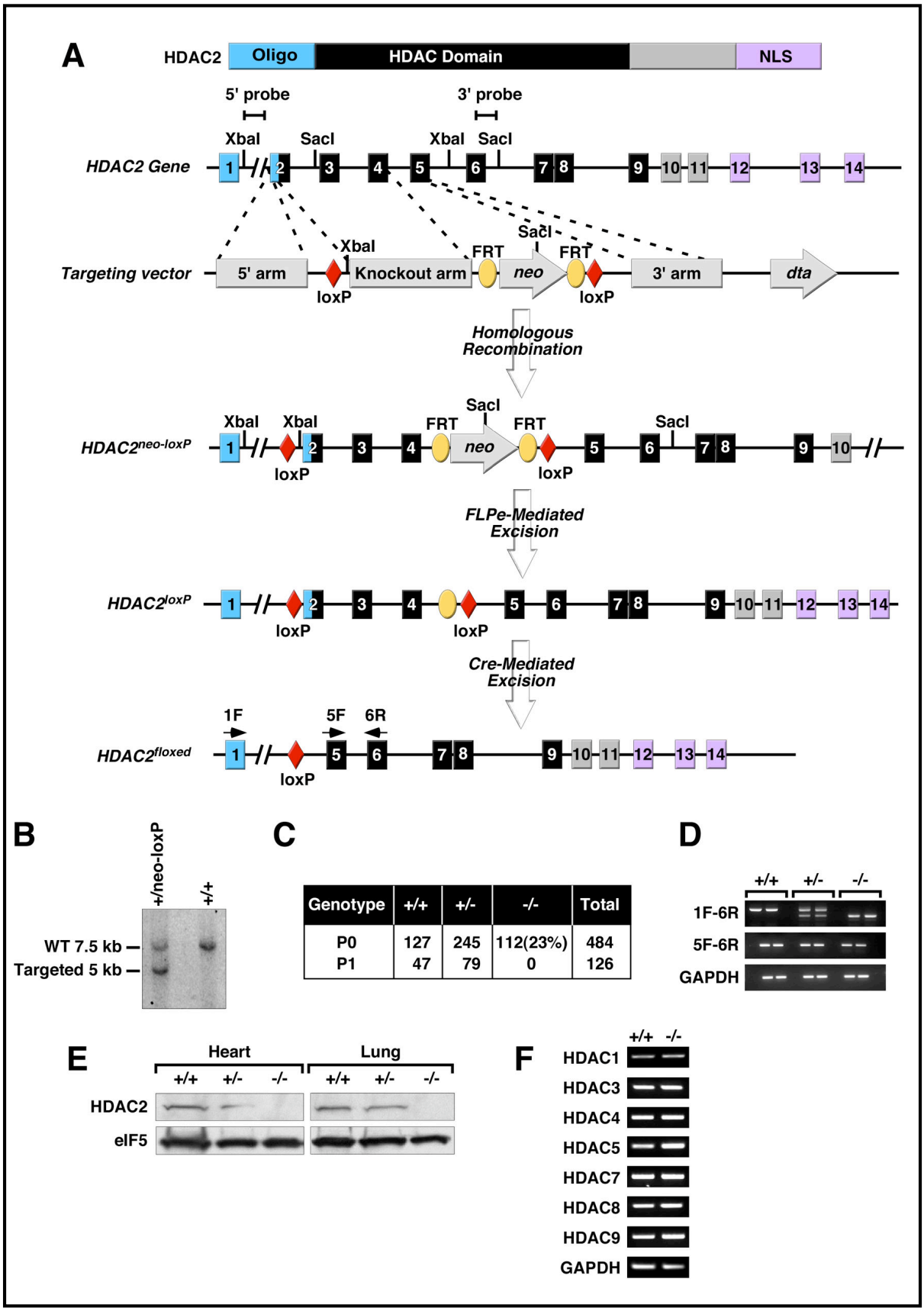
A
HDAC2
Oligo
HDAC Domain
NLS
5' probe
3' probe
XbaI
SacI
XbaI
SacI
HDAC2 Gene
1
2
3
4
5
6
7
8
9
10
11
12
13
14
Targeting vector
5' arm
XbaI
loxP
Knockout arm
FRT
neo
SacI
FRT
loxP
3' arm
dta
Homologous Recombination
HDAC2neo-loxP
XbaI
XbaI
loxP
FRT
neo
SacI
FRT
loxP
SacI
FLPe-Mediated Excision
HDAC2loxP
loxP
loxP
Cre-Mediated Excision
1F
5F
6R
HDAC2floxed
loxP
B
+/neo-loxP
+/+
WT 7.5 kb
Targeted 5 kb
C
Genotype
+/+
+/-
-/-
Total
P0
127
245
112(23%)
484
P1
47
79
0
126
D
+/+
+/-
-/-
1F-6R
5F-6R
GAPDH
E
Heart
Lung
+/+
+/-
-/-
+/+
+/-
-/-
HDAC2
eIF5
F
+/+
-/-
HDAC1
HDAC3
HDAC4
HDAC5
HDAC7
HDAC8
HDAC9
GAPDH

Figure 2.3. Generation of a conditional *HDAC2* allele. (*A*) Strategy for targeting of *HDAC2*. Exonic structure, targeting vector, and targeted allele for *HDAC2* are shown. *loxP* sites were introduced upstream of exon 2 and downstream from exon 4. Flanking FRT sites allowed for the neomycin resistance cassette to be removed by crossing to FLPe recombinase transgenic animals. Cre excision results in one *loxP* site in the place of exons 2–4. Probes for Southern analysis and primer positions for RT–PCR are shown. (*B*) Southern blot analysis for *HDAC2*. Tail DNA from agouti offspring was digested with SacI and probed with the indicated 3' probe. Wild-type (7.5 kb) and targeted (5 kb) bands indicate proper transmission of targeted allele. (*C*) Table of offspring from *HDAC2* heterozygous intercrosses. *HDAC2*-null mice were born at near Mendelian ratios, but showed 100% lethality within the first 24 h. (*D*) Transcript analysis of *HDAC2* by RT–PCR. Genotypes of animals are shown at *top*, and primer positions from *A* are shown to the *left*. *GAPDH* levels were detected as a control. (*E*) Western blot analysis to show deletion of HDAC2. Western blot analysis on heart and lung tissue isolated from P1 wild-type, heterozygous, and *HDAC2* homozygous-null neonates. eIF5 was detected as a loading control. (*F*) Transcript analysis on *HDAC2*-null mice. mRNA transcript levels were analyzed by semiquantitative RT–PCR for *HDAC*s *1*, *3–5*, and *7–9*. *GAPDH* was detected as a control.

HDAC2$^{-/-}$ mice on a 129/C57BL/6/CD1 mixed genetic background. *HDAC2*$^{-/-}$ mice were born at near expected Mendelian ratios, however, 100% of null mice derived from two independent ES cell clones became cyanotic and died within the first 24 hours after birth (Figure 2.3C). At birth, *HDAC2*$^{-/-}$ offspring were indistinguishable from wild type littermates, but most failed to nurse and even those that did nurse succumbed within the same time period as mutants that lacked milk in their stomachs. The complete lethality of these *HDAC2* null mice contrasts with the conclusions of a recent study reporting that the majority of mice homozygous for a lacZ insertion mutation in *HDAC2*, reputed to be a null allele, were viable (Trivedi et al. 2007b).

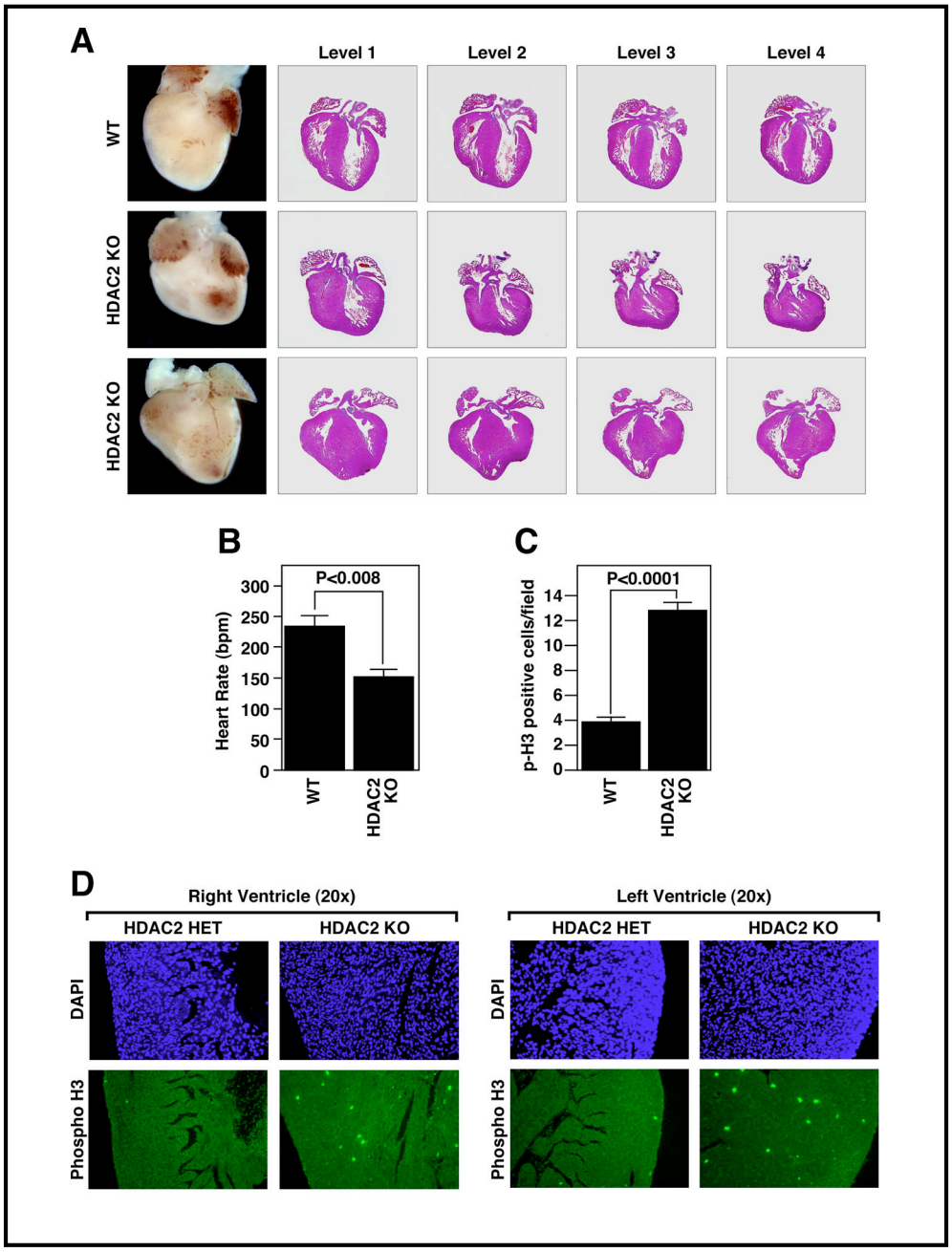

Figure 2.4. Cardiac defects in HDAC2$^{-/-}$ neonates. (*A*) Structural abnormalities in the hearts of *HDAC2*-null neonates. Hearts from mice of the indicated genotypes at P1 are shown at the *left*. H&E-stained sections at four successive levels of wild-type and *HDAC2*-null hearts are shown. The myocardium of *HDAC2*-null animals displays a thicker septum and diminished or dislocated right ventricular lumen. (*B*) Heart rates of *HDAC2*-null neonates. EKGs show reduced heart rate in the *HDAC2*-null mice. (*C*) Increased proliferation of cardiomyocytes in *HDAC2*-null mice. Immunohistochemistry for phospho-histone H3 was performed on heart sections from P1 mice. Quantification of phospho-histone H3-positive cells was performed on six sections from three individual hearts and averaged. (*D*) Immunohistochemistry of heterozygous and *HDAC2*-null hearts at 20x magnification. DAPI (blue) and phospho-histone H3 (green) staining show increased proliferation in both the right and left ventricles.

RT-PCR using primers upstream and downstream of the *loxP* sites showed a complete absence of HDAC2 mRNA encoding exons 2 through 4 in the homozygous *HDAC2* mutant animals, whereas primers downstream of the *loxP* sites revealed near normal levels of transcript in the mutant mice (Figure 2.3D). Sequencing of the mutant transcript showed two splice variants of the mutant *HDAC2* allele, an in-frame transcript from exon 1 to exon 5 and an out-of-frame transcript from exon 1 to exon 6. However, we were unable to detect any expression of mutant HDAC2 protein from lung or heart tissue by western blot using an HDAC2 antibody against the carboxy-terminus (Figure 2.3E), suggesting that the truncated mRNA is inefficiently translated or the truncated protein is unstable. Other class I and II HDACs were expressed at normal levels in the hearts of *HDAC2*-null mice (Figure 2.3F).

Cardiac abnormalities in *HDAC2* mutant neonates

Histological analysis of wild type and *HDAC2*$^{-/-}$ neonates revealed no obvious defects in the brain, liver, lung, or skeletal muscle (data not shown). However, the hearts of mutant mice displayed unusual morphological abnormalities of the right ventricular chamber (Figure 2.4A). In some *HDAC2* mutant neonates, there was an almost complete loss of the right ventricular lumen, as revealed by serial sectioning of the heart. In other mutant hearts, we observed the right ventricle to be completely dorsal to the left ventricle. In addition, the interventricular septum was thickened in all mutant hearts (Figure 2.4A). Gross observation and serial sections of E18.5 and P1 pups indicated proper partitioning of the great vessels and closure of the ductus arteriosis (Figure 2.5 and data not shown). Histological analysis

showed no evidence of fat deposition or fibrosis in the myocardium of HDAC2 mutant neonates (data not shown).

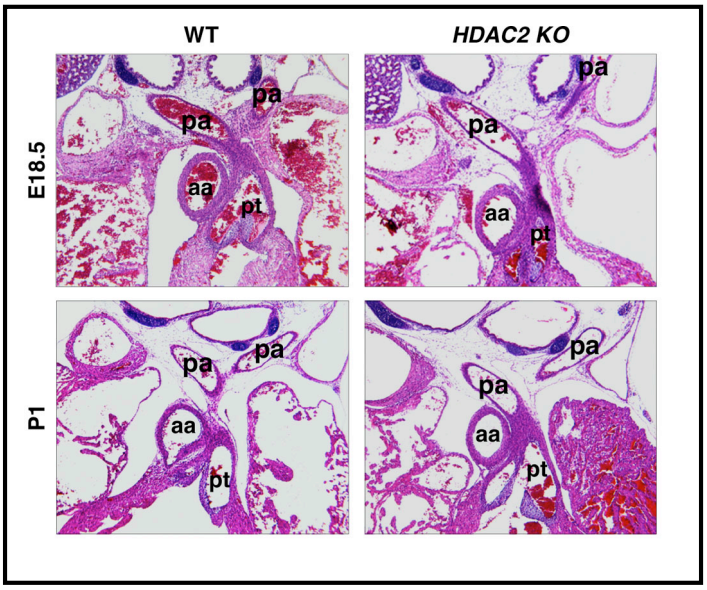

Figure 2.5. Partitioning of the outflow tract of *HDAC2* mutant mice. H&E stained transverse sections of wild-type and HDAC2 null mice at E18.5 and P1 to show normal partitioning of outflow tract. aa, ascending aorta, pa, pulmonary artery, pt, pulmonary trunk.

ECGs on mice at P1 showed an average decreased heart rate of 152 +/- 14 beats per minute (bpm) compared to 235 +/- 20 bpm in wild type littermates (Figure 2.4B). While all *HDAC2*$^{-/-}$ mice were bradycardic, we never observed arrhythmias or defects in atrioventricular conduction in the mutant animals. In all ECGs and rhythm strips taken from knockout mice, normal p-wave morphology was observed (data not shown). Moreover, all p-waves were upright in lead II, suggesting that the location of the pacemaker lies high in the right atrium in or near the sinus node. These observations suggest that these mice are most likely in normal sinus rhythm.

Increased cardiac apoptosis and proliferation in *HDAC2* mutant mice

Given the diminished right ventricular lumen and increased interventricular wall thickness of *HDAC2*$^{-/-}$ mice, we performed phospho-histone H3 staining to distinguish between cardiomyocyte hyperplasia and hypertrophy. Mutant hearts displayed a 3-fold increase in phospho-histone H3 staining compared to wild type hearts at P1 (Figure 2.4C, $p<0.0001$). Enhanced phospho-histone H3 staining was observed throughout the right ventricle, as well as the interventricular septum and left ventricular free wall (Figure 2.4D). Increased proliferative activity was not observed in any other tissue examined, including brain, lung, liver, thymus, or skeletal muscle (data not shown).

Terminal deoxynucleotidyl Transferase biotin-dUTP Nick End Labeling (TUNEL) analysis revealed increased apoptosis in both right and left ventricular walls as well as the interventricular septum (data not shown), which was most pronounced at the base of the interventricular septum of mutant hearts at P1 (Figure 2.6). TUNEL analysis on extra-cardiac tissue showed no differences between wild type and mutant animals (data not shown).

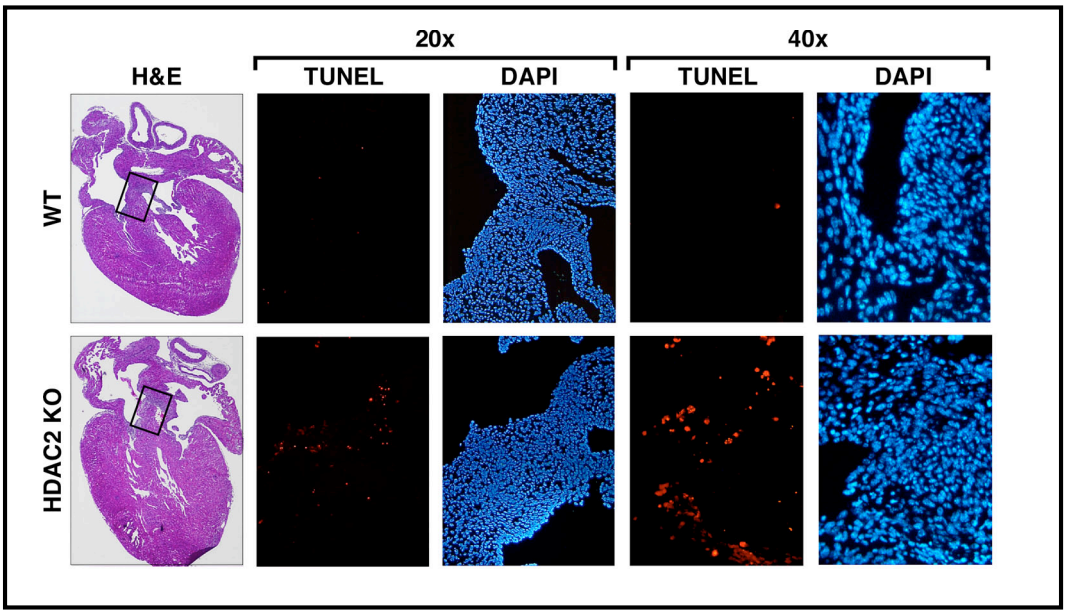

Figure 2.6. TUNEL analysis of HDAC2 mutant mice. Increased apoptosis in HDAC2 null mice. H&E, TUNEL, and DAPI staining at 20x and 40x of wild-type and HDAC2 null mice to show increased apoptosis at the base of the ventricular septum.

Cardiac deletion of *HDAC2*

To determine if the neonatal lethality of *HDAC2* null mice was due solely to a cardiomyocyte autonomous function of HDAC2, we deleted *HDAC2* specifically in the heart by breeding homozygous $HDAC2^{loxP/loxP}$ mice to the *αMHC-Cre* transgenic line. In contrast to the global deletion of *HDAC2*, $HDAC2^{loxP/loxP}$; *αMHC-Cre* mice were viable to adulthood and showed no gross cardiac abnormalities (data not shown). HDAC2 immunostaining of cardiomyocytes from $HDAC2^{loxP/loxP}$; *αMHC-Cre* mice confirmed the absence of HDAC2 protein in cardiomyocytes (Figure 2.7).

We further crossed mice bearing the conditional *HDAC2* allele to a variety of Cre lines to delete the gene in the neural crest, skeletal muscle, central nervous system, endothelium, smooth muscle, and secondary heart field (Table 2.1). No Cre line homozygous for $HDAC2^{loxP/loxP}$ was able to phenocopy the global deletion of *HDAC2*, suggesting that the lethal cardiac abnormalities of $HDAC2^{-/-}$ mice reflected functions of HDAC2 in multiple cell types within the heart.

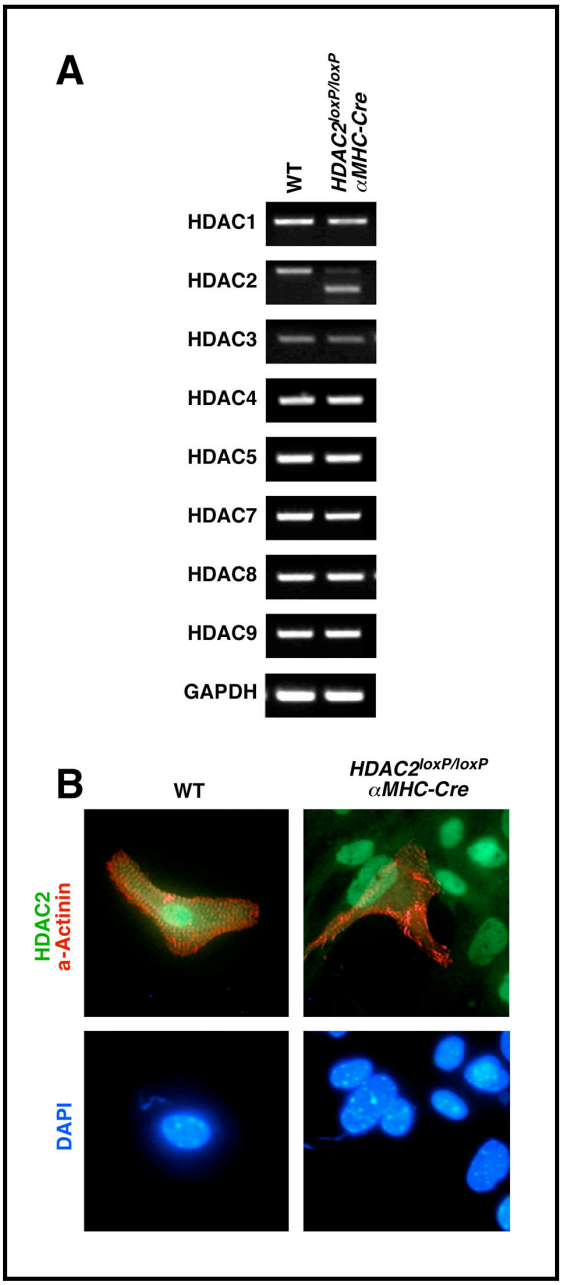

Figure 2.7. Cardiac-specific deletion of HDAC2. (A) Transcript levels were analyzed by semi-quantitative RT-PCR for HDACs 1-5 and HDACs 7-9. GAPDH levels were detected as a control. HDAC2 transcript levels show loss of exons 2 through 4 and residual wild-type expression due to contaminating cardiac fibroblasts as seen in (B). (B) Immunostaining for HDAC2 (green) and α-actinin (red) on cardiomyocytes isolated from wild-type and *HDAC2*$^{loxP/loxP}$*; αMHC-Cre* neonatal mice. Note cardiac fibroblasts positive for HDAC2 that are negative for α-actinin. Immunostaining for HDAC2 in Cre positive myocytes show no positive staining for HDAC2.

Cardiac deletion of *HDAC1* and *HDAC2* causes heart failure and aberrant gene expression

To test for possible functional redundancy between HDAC1 and 2 in cardiomyocytes, we generated cardiac-specific deletions of both genes using *αMHC-Cre*. A single copy of either allele was sufficient for viability, whereas double deletion of *HDAC1* and *HDAC2* by *αMHC-Cre* (designated dCKO for double conditional cardiac knockout) resulted in postnatal lethality by 14 days (Figure 2.8A). Hearts from dCKO mice appeared grossly normal at P8, but displayed cardiac arrhythmias by P10 and severe right and left ventricular dilatation by P11 (Figure 2.8B, C). TUNEL staining revealed approximately a 3-fold increase in apoptosis in the hearts of dCKO mice compared to wild type or $HDAC1^{loxP/loxP}$; $HDAC2^{loxP/+}$; *αMHC-Cre* littermates ($p<0.0001$, Figure 2.8D-2.8E).

We examined multiple markers of the cardiac stress response in dCKO mice and found the cardiac stress markers ANF, BNP, βMHC, α-skeletal actin, and MLC-2a to be dramatically up-regulated at P11, consistent with the heart failure phenotype of these mice (Figure 2.8F).

To further understand the primary cause of the observed heart failure phenotype, we performed expression profiling of dCKO hearts at P8. At this time-point, hearts were morphologically normal (Figure 2.8B) and cardiac stress markers were either unchanged or only mildly induced (data not shown). Surprisingly only a small portion of the transcriptome was dysregulated with 0.94 % (162 genes) of unique and annotated transcripts up-regulated and 0.58 % (100 genes) down-regulated when a cutoff of two-fold change was applied (data not shown).

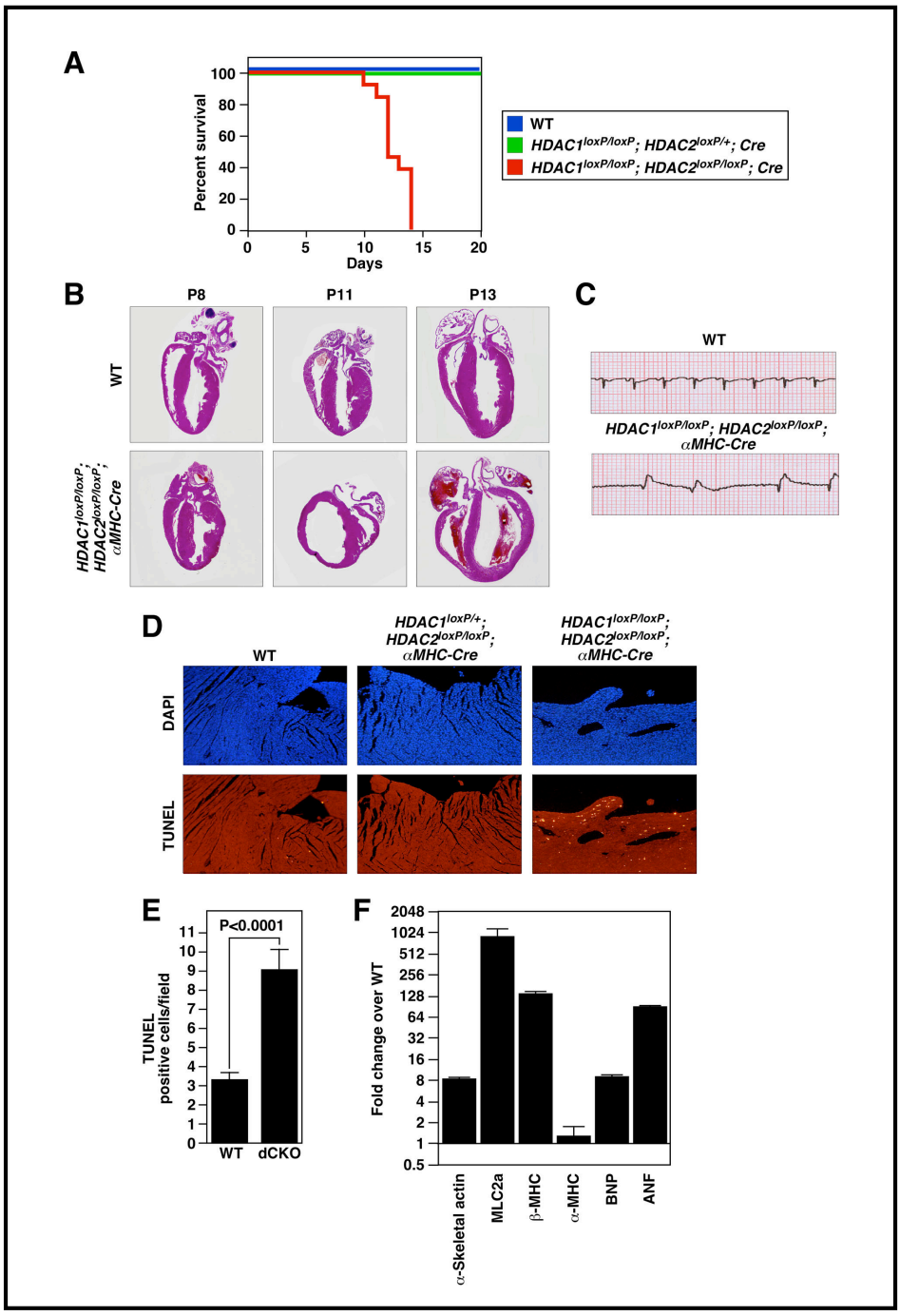

Figure 2.8. Cardiac defects resulting from cardiac deletion of HDAC1 and HDAC2. (*A*) Kaplan-Meier survival curves for cardiac deletion of HDAC1 and HDAC2 by *MHC-Cre*. Note that one copy of *HDAC2* is sufficient for 100% viability. (*B*) H&E-stained sections of wild-type and dCKO mice at P8, P11, and P13. Deletion of both HDAC1 and HDAC2 results in severe dilated cardiomyopathy by P11. (*C*) ECGs performed on wild-type and dCKO mice at P10. Deletion of HDAC1 and HDAC2 in cardiomyocytes leads to cardiac arrhythmia by P10. (*D*) Apoptosis in dCKO mice. TUNEL staining of wild-type and dCKO ventricular sections showed enhanced apoptosis in dCKO mice at P10. (*E*) Quantification of apoptosis in dCKO hearts. TUNEL-positive cells were quantified from six individually stained sections at 40x and averaged; $P < 0.0001$. (*F*) Expression of cardiac stress markers in dCKO mice at P11. mRNA transcript levels were detected by real-time RT–PCR and normalized to 18S RNA.

To analyze if certain pathways or biological processes were especially sensitive to the loss of HDAC1 and 2 in the heart, a Gene Ontology analysis (Thomas et al. 2003) was performed on the dysregulated transcripts. This analysis indicated that the most significantly enriched up-regulated genes participate in cell structure and motility (Figure 2.9A). Up-regulated genes falling in this group were further analyzed for their annotated biological function, showing that the majority of the up-regulated genes encode either cytoskeletal proteins or ion channels (Figure 2.9B).

Up-regulation of calcium channel genes resulting from cardiac deletion of HDAC1 and 2

Microarray analysis of hearts from dCKO mice at P8 revealed inappropriate up-regulation of specific L-type and T-type calcium channel subunit genes. $Ca_V3.2$, a T-type channel encoded by *CACNA1H*, is normally expressed in embryonic hearts and is down-regulated after birth (Yasui et al. 2005). Microarray analysis revealed a 3.5-fold increase in expression of $Ca_V3.2$, which was confirmed by real-time PCR at P8, and even greater up-regulation at P11 (Figure 2.9C). Induced expression of $Ca_V3.2$ in dCKO hearts was also detected by western blot analysis (Figure 2.9D). The L-type calcium channel subunit $\alpha 2\delta 2$, encoded by *CACNA2D2*, was also up-regulated 8.6-fold at P8 and to even higher levels at P11 in dCKO mice (Figure 2.9C). These genes appeared to be specific targets for repression by HDAC1 and 2, as there were no significant changes in expression of other regulators of calcium handling, including the sarco(endo)plasmic reticulum Ca^{2+}-ATPase, SERCA2, the ryanodine receptor 2, RyR2, or the Na^+/Ca^{2+} exchanger, NCX1 (Figure 2.9C and data not shown). In addition, analysis of transcript levels for *CACNA1H* and *CACNA2D2* in

HDAC1$^{loxP/loxP}$; *αMHC-Cre* and *HDAC2*$^{loxP/loxP}$; *αMHC-Cre* showed no significant increase in expression (Figure 2.9C), suggesting HDAC1 and HDAC2 redundantly regulate the expression of L-type and T-type calcium channel subunits during postnatal development.

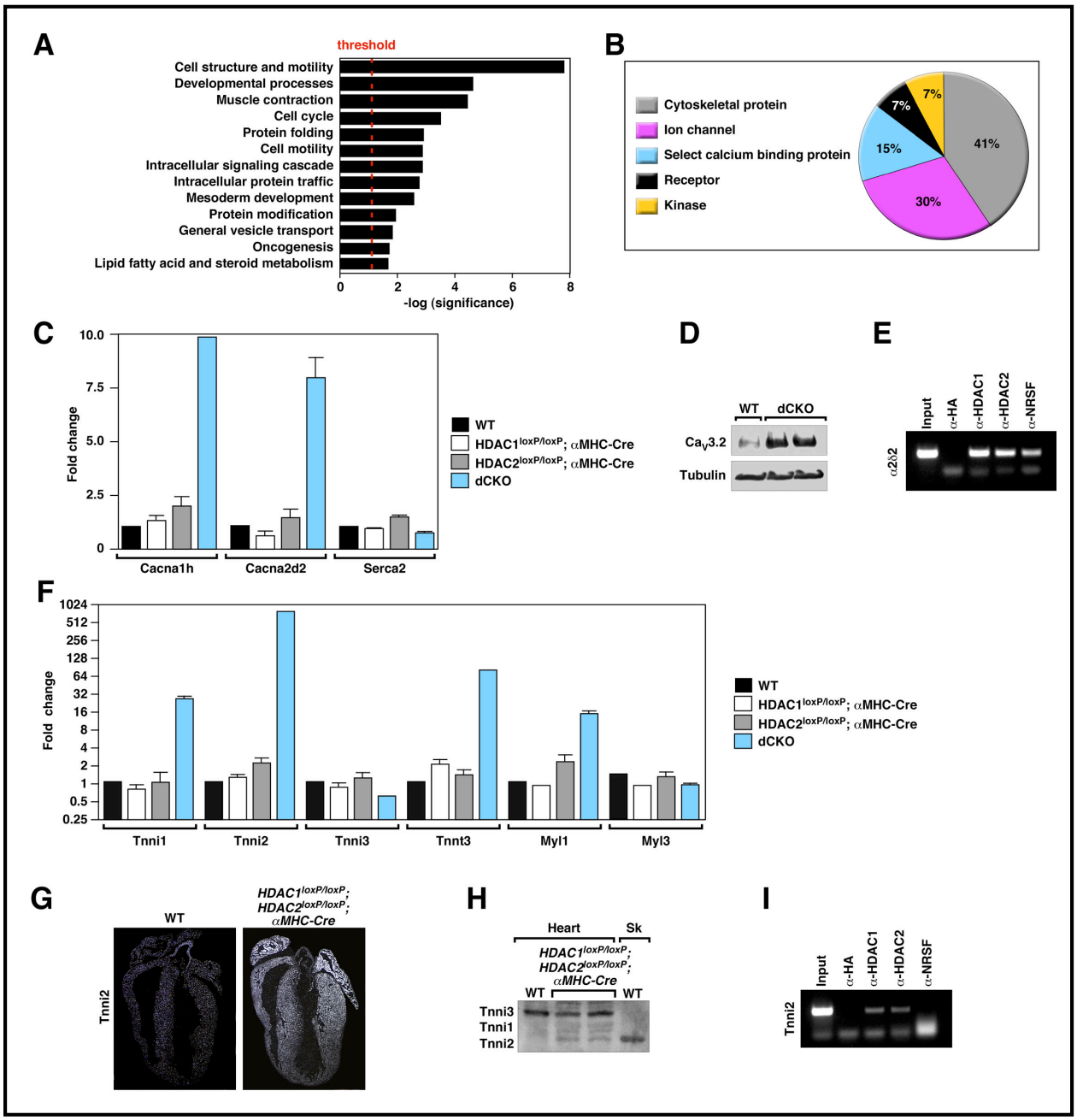

Figure 2.9. Aberrant cardiac gene expression resulting from cardiac deletion of HDAC1 and HDAC2. (*A*) Gene ontology analysis was performed with PANTHER. Significantly ($P < 0.05$) enriched biological processes are shown. Plotted is the –log (*P* value) with the threshold set to 1.3 [log(0.05)]. (*B*) Molecular functions were assigned to the genes that fall in the most significantly enriched process, "cell structure and motility" ($P < 0.00000005$). (*C*) Calcium channel subunit dysregulation in the hearts of dCKO mice. Real-time RT–PCR analysis of transcript levels from wild-type, cardiac-specific HDAC1 KO, cardiac-specific HDAC2 KO, and dCKO hearts at P11. L-type and T-type calcium subunits were dysregulated in the dCKO hearts. Error bars indicate standard deviation. (*D*) $Ca_V3.2$ expression in dCKO hearts. Western blot analysis was performed on hearts from P11 wild-type (lane *1*) and dCKO (lanes *2*,*3*) mice. dCKO mice show increased expression of $Ca_V3.2$. Tubulin was detected as a loading control. (*E*) ChIP assays were performed from neonatal rat ventricular myocytes. Chromatin was immunoprecipitated with antibodies against HA as a negative control, HDAC1, HDAC2, or NRSF. Primers were designed around the NRSE within intron 1 of *CACNA2D2*, and precipitated DNA was analyzed by PCR. PCR was also performed from a nonimmunoprecipitated sample as an input control. (*F*) Specific dysregulation of skeletal myofibrillar proteins in the hearts of dCKO mice. Real-time RT–PCR analysis of transcript levels from wild-type, cardiac-specific HDAC1 KO, cardiac-specific HDAC2 KO, and dCKO hearts at P11. Error bars indicate standard deviation. (*G*) RNA in situ hybridization of *Tnni2* transcripts on wild-type and dCKO hearts. (*H*) Troponin isoform expression in dCKO heats. Western blot analysis was performed on hearts from P11 wild-type (lane *1*) and dCKO (lanes *2*,*3*) mice. dCKO mice show heterogeneity in troponin isoform expression. Lane *4* is wild-type skeletal muscle as a control for Tnni2. (*I*) ChIP assays were performed on the IRE of *Tnni2* in neonatal rat ventricular myocytes. Chromatin was immunoprecipitated with antibodies against HA, HDAC1, HDAC2, and NRSF. Precipitated DNA was analyzed by PCR using primers flanking the IRE. HDAC1 and HDAC2, but not NRSF, mediate repression of *Tnni2* at basal levels. PCR was performed prior to immunoprecipitation as an input control.

$Ca_V3.2$ has been shown to be repressed by neuron-restrictive silencing factor (NRSF), and up-regulation of $Ca_V3.2$ has been shown to render the heart susceptible to cardiac arrhythmias and sudden death (Kuwahara et al. 2003). To investigate whether HDAC1 and HDAC2 also regulate $\alpha 2\delta 2$ in an NRSF dependent manner, we performed chromatin immunoprecipitation (ChIP) on neonatal rat ventricular myocytes. Immunoprecipitation of HDAC1, HDAC2, or NRSF, pulled down the NRSE-containing region within intron 1 of *CACNA2D2*, whereas anti-HA as a negative control did not recognize this regulatory DNA sequence. These findings suggest that a repressive complex containing

NRSF/HDAC1/HDAC2 normally represses ventricular expression of α2δ2 under basal conditions (Figure 2.9E).

Up-regulation of skeletal muscle contractile protein genes resulting from cardiac deletion of HDAC1 and 2

Cardiac stress is often accompanied by the up-regulation of skeletal muscle contractile protein genes in the heart, which alters calcium handling and increases cardiac contractility. Indicative of heart failure, the expression of α-skeletal actin (Acta1), myosin light chain 1F (MLC1f), and sketelal isoform of troponin T (Tnnt3) was up-regulated in dCKO mice (Figure 2.8F and 2.9F). Notably, the ventricular isoform of myosin light chain, MLC1v, was not induced, arguing against a global dysregulation of contractile proteins.

Strikingly, troponin I (TnI), an inhibitory subunit of the heterotrimeric troponin complex, that allows for the binding of actin to myosin in response to influxes of Ca^{2+}, resulting in sarcomeric activation and contraction (Parmacek and Solaro 2004), was the most dramatically up-regulated gene in the mutant heart. There are three mammalian isoforms of TnI, a cardiac TnI (Tnni3), and a slow and fast skeletal TnI (Tnni1 and Tnni2, respectively). Both skeletal muscle isoforms were induced in the dCKO mice at P11. Remarkably, the fast skeletal isoform, Tnni2, was induced over 500-fold (Figure 2.9F). In addition, the levels of the cardiac specific isoform were unchanged, if not moderately down. Analysis of transcript levels in hearts with cardiac specific deletions of either HDAC1 or 2 showed no significant changes in skeletal muscle myofibril proteins (Figure 2.9F), further suggesting HDAC1 and 2 as redundant regulators of myofibril gene expression.

RNA *in situ* hybridization on P8 hearts confirmed the induced expression of Tnni2, not only in the ventricles, but in the atria of dCKO mice as well (Figure 2.9G). Cardiac expression of all three isoforms of troponin I was also detected by western blot analysis using a pan-troponin antibody (Figure 2.9H). The skeletal muscle specific isoforms of troponin I are not typically induced during cardiac hypertrophy or failure (Sasse et al. 1993; Bodor et al. 1997), suggesting the induction of Tnni1 and Tnni2 is not compensatory, but represents a primary defect contributing to the cardiac arrhythmia leading to sudden death.

ChIP assays on neonatal rat cardiomyocytes showed that HDAC1 and HDAC2 were localized to the homologous internal regulatory element (IRE) (Figure 2.9I), which has been shown to direct skeletal muscle-specific expression of Tnni2 (Lin et al. 1991). Although there is an NRSF binding site within the IRE of the Tnni2 gene, NRSF was not detected on this element in neonatal rat cardiomyocytes (Figure 2.9I), suggesting that HDAC1 and 2 repress Tnni2 through an NRSF-independent mechanism.

Hypertrophic response to adrenergic stimulation and aortic constriction

Based on the ability of HDAC inhibitors to blunt hypertrophic growth of cardiomyocytes in response to stress (Antos et al. 2003; Kee et al. 2006; Kong et al. 2006), we tested whether cardiac deletion of HDAC1 or 2 diminished the hypertrophic growth response to chronic infusion of isoproterenol, a β-adrenergic agonist that induces cardiac hypertrophy, or thoracic aortic constriction (TAC), which induces cardiac hypertrophy through increased afterload on the heart. As shown in Figure 2.10, *HDAC1*$^{loxP/loxP}$; *αMHC-Cre* mice and *HDAC2*$^{loxP/loxP}$; *αMHC-Cre* mice displayed a hypertrophic response to isoproterenol that was comparable to that of wild-type littermates. Similarly, *HDAC1*$^{loxP/loxP}$;

αMHC-Cre mice showed no statistical difference in heart weight/body weight (HW/BW) or heart weight/tibia length (HW/TL) ratios compared to *HDAC1*$^{loxP/loxP}$ littermates not expressing Cre recombinase following TAC (Figure 2.10B). Histological analyses were also indistinguishable between *HDAC1*$^{loxP/loxP}$; *αMHC-Cre* mice and littermate controls (Figure 2.10C).

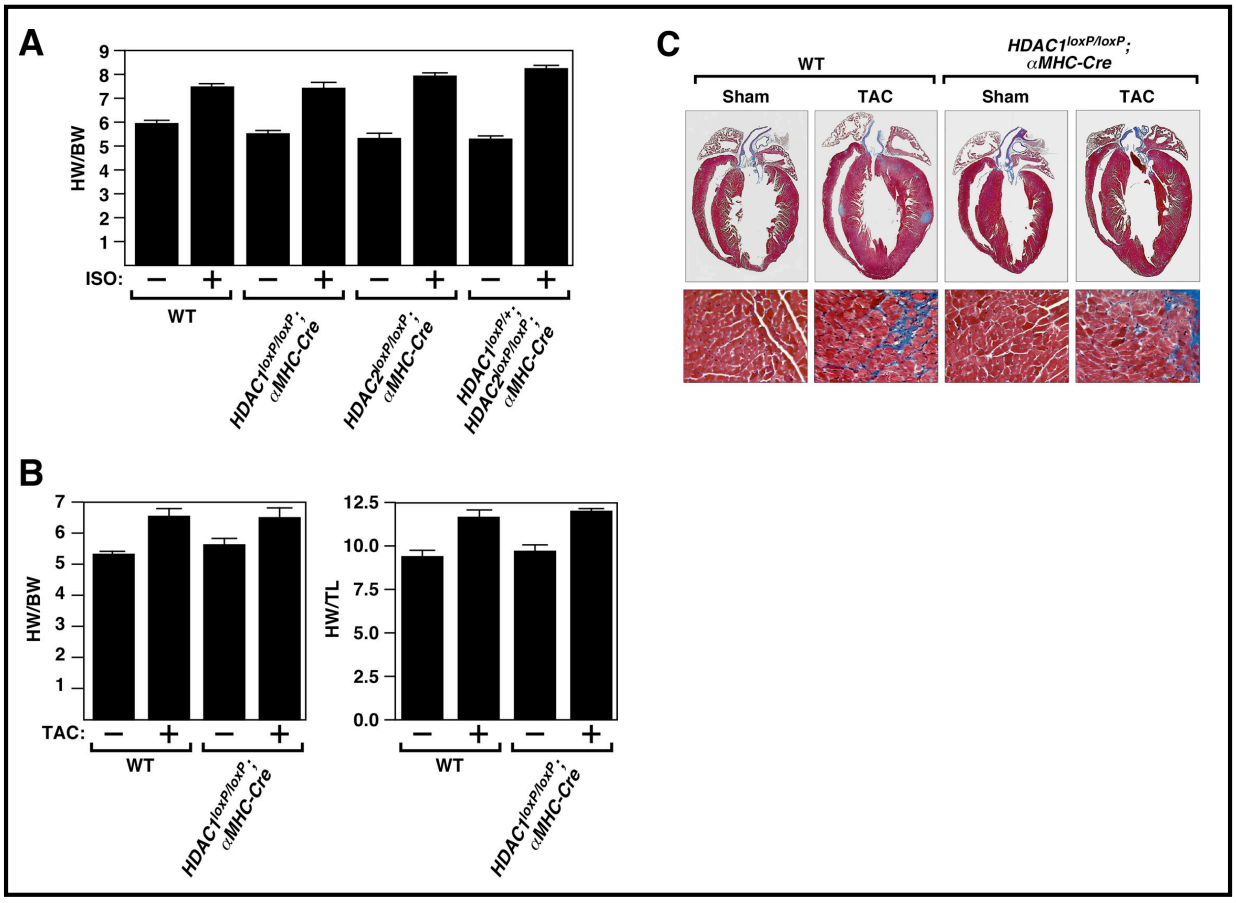

Figure 2.10. Stress-dependent cardiac hypertrophy in mice lacking cardiac expression of HDAC1 and HDAC2. (*A*) Wild-type, *HDAC1*$^{loxP/loxP}$; *MHC-Cre, HDAC2*$^{loxP/loxP}$; *MHC-Cre,* and *HDAC1*$^{loxP/+}$; *HDAC2*$^{loxP/loxP}$; *MHC-Cre* mice at 8 wk of age were subjected to isoproterenol or saline infusion. Mice were sacrificed after 7 d, and cardiac hypertrophy was evaluated by heart weight/body weight ratios. (*B*) Wild-type and *HDAC1*$^{loxP/loxP}$; *MHC-Cre* mice were subjected to TAC or sham operation. Heart weight/body weight ratios and heart weight/tibia length ratios were determined after 21 d. (*C*) Histological sections of representative hearts from *B* are shown stained with Masson Trichome. *Bottom* panels are 40x magnifications of the *above* hearts to show fibrosis.

DISCUSSION

Class I HDACs are expressed ubiquitously and are thought to function as global repressors of transcription. The results of this study provide the first glimpse of the functions of HDAC1 and 2 in postnatal tissues in vivo and reveal specialized and redundant roles of these HDACs in the control of cardiac growth and function.

Roles of HDAC1 and 2 in cardiac growth and function

Mice homozygous for an HDAC1 null allele die at gastrulation from a block to cell proliferation due, at least in part, to up-regulation of the cell cycle inhibitor p21 (Lagger et al. 2002). Thus, the potential functions of HDAC1 at later stages of embryogenesis or after birth have remained enigmatic. Our results show that HDAC1 can be deleted in a wide range of tissues, including cardiac, skeletal and smooth muscle, neural crest, endothelial cells and the central nervous system, without affecting viability. The essential early role of HDAC1 is, therefore, likely to reflect a specific requirement at gastrulation rather than a general requirement in cell proliferation per se.

Our results show that HDAC2 is essential for normal growth and morphogenesis of the heart. Global deletion of HDAC2 results in a highly specific cardiac phenotype associated with uncontrolled proliferation of ventricular cardiomyocytes, which lead to obliteration of right ventricular chamber, causing perinatal lethality with complete penetrance. These defects appeared to be superficially similar to many known congenital heart abnormalities including hypoplastic right heart syndrome, right ventricular dysplasia, and transposition of the great arteries. However, histological analysis at the cellular level showed no infiltration of fat and no signs of fibrosis in the HDAC2 mutant neonate, which

typically accompany RV dysplasia. In addition, there were no signs of pulmonary valve atresia, a common defect in hypoplastic right heart syndrome. The finding that conditional deletion of HDAC2 in cardiomyocytes, smooth muscle, endothelial cells and neural crest does not phenocopy the cardiac defects observed in HDAC2 null mice suggests that HDAC2 may be required in multiple cell types for normal heart development.

The neonatal lethal phenotype we observed for *HDAC2* null mice contrasts with that of another recent study in which mice homozygous for a gene trap insertion mutation in *HDAC2*, purported to create a null allele, were viable (Trivedi et al. 2007b). We cannot explain the basis for these differing phenotypes, but there are several possibilities. LacZ insertion lines frequently display variable phenotypes due to alternative splicing within the mutant locus (Voss et al. 1998). Thus, it is conceivable that the mutation described by Trivedi et al. is a hypomorphic allele, rather than a true null, and generates sufficient levels of HDAC2 for viability of a subset of mutant animals. The mutation we introduced into the HDAC2 locus deleted many key residues required for deacetylase activity (Finnin et al. 1999), whereas that gene trap insertion ablates the carboxy-terminus of the protein which, to date, has unknown function (Gregoretti et al. 2004). Different genetic backgrounds of the mice tested in the two studies could also contribute to the differing phenotypes. The mice in our study were from a mixed 129/C57BL/6/CD1 background while the background of the mice generated by Trivedi et al. (2007) was not specified.

Our findings also differ from those of Trivedi et al. with respect to the role of HDAC2 in mediating stress-dependent cardiac growth. Diverse stresses including neurohormonal signaling and pressure-overload promote pathological cardiac hypertrophy, which often culminates in heart failure and lethal cardiac arrhythmias. HDAC inhibitors have

shown efficacy both *in vitro* and *in vivo* in blunting the hypertrophic response (Antos et al. 2003; Kee et al. 2006; Kong et al. 2006). Our results demonstrate that cardiac deletion of either HDAC1 or HDAC2 is not sufficient to block hypertrophy in response to chronic administration of isoproterenol or aortic constriction. In contrast, Trivedi et al. reported that the lacZ insertional mutation in HDAC2 prevented cardiac hypertrophy in response to these stimuli (Trivedi et al. 2007).

The finding that cardiac deletion of either HDAC1 or 2 has no apparent effect on cardiac development or function, whereas deletion of both genes in the heart results in lethal cardiac abnormalities strongly suggests that these HDACs act in a redundant manner to regulate cardiac gene expression. Based on the high sequence homology between HDAC1 and 2 and the cardiac phenotype resulting from the combined deletion of these genes, it is likely that these genes play redundant roles in many tissues. Double tissue-specific gene deletions to address this issue are underway.

Abnormalities in gene expression resulting from HDAC1 and 2 deletion

Deletion of two global transcriptional repressors such as HDAC1 and 2 might be expected to result in rampant ectopic gene activation. Instead, the consequences of HDAC1 and 2 loss-of-function in the heart were remarkably specific and resulted in selective induction of genes involved in calcium influx, calcium handling and contraction.

In cardiomyocytes, the thin filaments, together with the myosin-containing thick filaments, regulate Ca^{2+} sensitivity, contractility and relaxation. The thin filament, which is composed of actin, tropomyosin, and the heterotrimeric troponin complex, responds to intracellular Ca^{2+} fluxes from Ca^{2+} channels to control cardiac contractility (Kobayashi and

Solaro 2005). The troponin complex is comprised of a Ca^{2+} binding troponin C (TnC), a tropomyosin binding troponin T (TnT), and an inhibitory subunit (TnI) that blocks actin-myosin binding at low Ca^{2+} levels (Parmacek and Solaro 2004). The absence of HDAC1 and 2 results in the up-regulation of T- and L-type Ca^{2+} channels as well as robust expression of the skeletal muscle-specific isoforms of troponin I (ssTnI and fsTnI), which exhibit varying sensitivities to intracellular Ca^{2+} and are regulated independently through phosphorylation (Parmacek and Solaro 2004).

Expression of the T-type calcium channel $Ca_V3.2$ is regulated by the transcriptional repressor NRSF (Kuwahara et al. 2003), which recruits class I HDACs (Roopra et al. 2000). By ChIP assays, we identified HDAC1, HDAC2, and NRSF on the NRSE in intron 1 of *CACNA2D2* in neonatal rat cardiac myocytes, suggesting class I HDACs actively repress the expression of CACNA2D2 during normal cardiac growth. HDAC1 and 2 were also localized to the IRE of *Tnni2*, however this appears to be in an NRSF independent manner. We postulate that the increased expression of Ca^{2+} channel subunits results in a pathological influx of Ca^{2+} into cardiomyocytes, which, coupled with a heterogeneous population of Ca^{2+} sensitive troponin I, results in a dysregulation of sarcomeric activation, contraction, and relaxation, resulting in cardiac arrhythmia and sudden death.

Implications for human disease

HDACs have been implicated in a wide range of cellular processes and disease states based on the ability of HDAC inhibitors to ameliorate various disease pathologies (Bolden et al. 2006; Minucci and Pelicci 2006). However, an important issue that has been difficult to resolve is whether the effects of HDAC inhibitors in vivo reflect the combined inhibition of

multiple HDACs or specific functions of individual HDACs in different tissues. The conditional alleles of class I HDACs will allow the detailed analysis of the functions of these chromatin-remodeling enzymes in diverse tissues during development and in the settings of disease. Moreover, by testing the responses to HDAC inhibitors of cells isolated from these mutant mice, it should be possible to identify the specific HDAC isoforms that mediate the actions of HDAC inhibitors in vivo.

METHODS

Generation of *HDAC1* and *HDAC2* mutant mice

Both *HDAC1* and *HDAC2* targeting vectors were constructed using the pGKNEO-F2L2DTA vector, which contains a neomycin resistant gene, flanked by frt and loxP sites, and a diphtheria toxin gene cassette. The 5' arm, KO arm, and 3' arm of the targeting construct for *HDAC1* were generated by high fidelity PCR amplification (Roche Expand High Fidelity Long Template) of 129SvEv genomic DNA and correlate to a 2kb fragment in intron 4, a 2kb fragment harboring exons 5 through 7, and a 4kb fragment in intron 7, respectively. For the targeting construct of *HDAC2*, a 4kb fragment in intron 1, a 4kb fragment harboring exons 2 through 4, and a 2kb fragment in intron 4 was generated correlating to the 5' arm, KO arm, and 3' arm, respectively. Both targeting vectors were linearized with PvuI and electroporated into 129SvEv-derived ES cells. 1000 (for HDAC1) and 400 (for HDAC2) ES cell clones were isolated and analyzed for homologous recombination by Southern blotting. 5' loxP incorporation for *HDAC1* was confirmed using a 5' probe following digestion with EcoRI. *HDAC2* Long arm and 5' loxP recombination was confirmed using a 5' probe following digestion with XbaI. Short arm and 3' loxP confirmation was performed using a 3' probe after EcoRI or SacI digestion for *HDAC1* and *HDAC2*, respectively. Three clones with a properly targeted *HDAC1* or *HDAC2* allele were injected into 3.5 day C57BL/6 blastocysts and the resulting chimeras were crossed to C57BL/6 females to achieve germline transmission of the targeted allele.

Histology, immunohistochemistry and RNA in situ hybridization

Tissues were fixed in 4% paraformaldehyde, embedded in paraffin, and sectioned at 5μm intervals. Sections were stained with hematoxylin and eosin using standard procedures (Shelton et al. 2000). TUNEL assay was performed according to standard protocol (Roche) and immunohistochemistry using an anti-rabbit phospho-histone H3 antibody was performed as described (Xin et al. 2006). ^{35}S-labeled RNA probes were generated using Maxiscript kit (Amersham).

RT-PCR, microarray and gene ontology analysis

Total RNA was purified from tissues using TRIzol reagent according to manufacturer's instructions. For RT-PCR, total RNA was used as a template for reverse transcriptase using random hexamer primers. Primer sequences are available upon request. Quantitative real time PCR was performed using Taqman probes purchased from ABI. For microarray, RNA was extracted from either 3 wild-type or dCKO hearts and subsequently pooled prior to analysis. All heart RNA was from ventricle tissue only. Microarray analysis was performed by the UT Southwestern Microarray Core Facility using the Mouse Genome 430 2.0 Array (Affymetrix) as described (Davis et al. 2006). Gene ontology analysis with PANTHER (Thomas et al. 2003) was performed essentially as described (Matsuoka et al. 2007). Briefly, 1586 probe spots were flagged as significantly up-regulated by the Affymetrix analysis software GeneChip. The corresponding Entrez Gene IDs (Maglott et al. 2007) were uploaded to PANTHER and 1176 unique and annotated genes could be identified from this dataset, which then could be assigned to 197 different biological processes. This distribution was compared to a reference list (NCBI: M. musculus genes, version 1-16-2007 (Maglott et al. 2007)) and significant enrichment of the experimental dataset in a given process was

calculated using binomial testing with Bonferroni correction for multiple testing as described (Thomas et al. 2006). Only processes with a significant (< 0.05) enrichment were used for further analysis. The process with the highest significance score was then analyzed for molecular function using PANTHER. Only families with more then one gene in a given family were considered.

The percentage of gene changes was calculated by uploading the Entrez Gene IDs of the Mouse Genome 430 2.0 Affymetrix annotation file to PANTHER, leading to the identification of 17201 unique and annotated transcripts. These were then compared to the statistically significantly dysregulated unique and annotated transcripts (ESTs excluded) as identified by GeneChip using a cutoff at 2-fold change. Similar results were obtained when non-annotated transcripts were included in the analysis (data not shown).

Indirect immunofluorescence

Hearts were extracted from 2-3 day-old wild-type and dCKO mice, minced in DMEM (Cellgro), washed in PBS, and digested with collagenase type II (0.2% w/v, Worthington Biochemical) and glucose (0.1% w/v, Sigma). Cells were resuspended in DMEM containing fetal bovine serum (FBS) (10%), L-glutamine (2mM), and penicillin-streptomycin. Cells were pre-plated twice for 2 hours each to separate adherent fibroblasts from cardiomyocytes. Cardiomyocytes were plated on gelatin coated glass coverslips in 6-well dishes (4×10^5 cell/well). After 24 hours, cells were fixed with ice-cold methanol, permeabilized, and blocked with PBS containing Nonidet P-40 (PBS-N) (0.1%) and bovine serum albumin (BSA) (3%) and incubated in the same solution for primary antibodies for HDAC1 (rabbit polyclonal, 1:2000 dilution, Abcam), HDAC2 (rabbit polyclonal, 1:2000 dilution, Abcam),

and sarcomeric α-actinin (mouse monoclonal, 1:500 dilution, Sigma). Coverslips were washed five times with PBS-N and incubated with fluorescein (HDAC1 or HDAC2) and texas red (α-actinin) conjugated secondary antibodies (1:500 dilution, Vector Laboratories). Coverslips were washed five times with PBS-N, mounted on glass slides using Vectashield mounting medium with DAPI (Vector Laboratories), and visualized with a fluorescence microscrope.

Western blotting

Heart and lung tissue was homogenized in lysis buffer (50mM Tris, pH7.4/150mM NaCl/1% Triton X-100/1mM EDTA) supplemented with protease inhibitors (Complete Mini, EDTA-free, Roche), centrifuged at 14,000 x *g* for 5 minutes and supernatant recovered. Equal amounts were resolved by SDS/PAGE on a 10% acrylamide gel and analyzed by western blot using primary antibody for HDAC2 (rabbit polyclonal, 1:5000 dilution, Abcam) followed by goat anti-rabbit IgG HRP-conjugated secondary antibody (Bio-Rad) and detected by enhanced chemiluminescence (Western Blot Luminol Reagent, Santa Cruz). Membranes were reprobed with a primary antibody against eIF5 (rabbit polyclonal, 1:1000 dilution, Santa Cruz) to serve as a loading control.

For detection of $Ca_V3.2$, heart tissue was homogenized in lysis buffer (50mM HEPES, pH7.5/250mM NaCl/0.1% NP40/5mM EDTA/1% β-mercaptoethanol) supplemented with protease inhibitors (Complete Mini, EDTA-free, Roche), centrifuged at 14,000 x g for 3 minutes and supernatant recovered. Equal amounts were resolved by SDS/PAGE on a 4-20% acrylamide gel and analyzed by western blot using a primary antibody against CaV3.2 (rabbit polyclonal, 1:500 dilution, Santa Cruz) followed by goat

anti-rabbit IgG HRP-conjugated secondary antibody (Bio-Rad) and detected by enhanced chemiluminescence (Western Blot Luminol Reagent, Santa Cruz). Membranes were reprobed with a primary antibody against tubulin (mouse monoclonal, 1:1000 dilution, Sigma) to serve as a loading control.

For detection of troponin isoforms, myofibril preparations were performed as described (Thys et al. 2001). Equal amounts were resolved by SDS/PAGE on a 4-20% acrylamide gel and analyzed by western blot using a primary antibody against troponin I (goat polyclonal, 1:1000 dilution, Santa Cruz) followed by a donkey anti-goat IgG HRP-conjugated secondary antibody (1:5000 dilution, Santa Cruz) and detected by enhanced chemiluminescence (Western Blot Luminol Reagent, Santa Cruz).

Chromatin immunoprecipitation

Neonatal rat ventricular myocytes were prepared as described (Antos et al. 2003). Following 24 hours incubation, chromatin was harvested as described (Nelson et al. 2006). Briefly, cells were formaldehyde cross-linked, lysed, and chromatin was sheared by sonication to ~500bp fragments. Sheared chromatin was immunoprecipitated with antibodies for HA (Sigma), HDAC1 (Abcam), HDAC2 (Abcam), or NRSF (Upstate) and DNA was isolated and analyzed by PCR with primers flanking binding sites for indicated response element of each gene. Primers are available upon request.

Electrocardiography

Electrocardiography (ECG) was performed on sedated neonatal mice using Accutac Diaphoretic ECG Electrodes (ConMed Corp). Mice were allowed to adapt to environment

prior to recording. Pads were attached to all 4 limbs and leads I, II, III, aVR, aVL, and aVF were recorded using PageWriter XLs (Hewlett Packard). Traces were recorded using identical settings between dCKO and wild type mice (50mm/s; 20mm/mV).

Isoproterenol administration and aortic constriction

Hypertrophic agonist Isoproterenol (Sigma) (8.8mg/kg/day) or saline were administered using miniosmotic pumps (Model 2001, Alzet) dorsally implanted subcutaneously in 8 to 10-week-old male mice. Mice were sacrificed 7 days after isoproterenol infusion and cardiac hypertrophy was assayed by heart weight, body weight, and tibia length. Cardiac hypertrophy was also induced by pressure overload. 8-week-old WT or *HDAC1*$^{loxP/loxP}$; *αMHC-Cre* male mice underwent a sham operation or were subjected to thoracic aortic constriction (TAC) as described (Hill et al. 2000).

Statistical methods

Values are presented as ± SEM unless otherwise noted. Gene expression was normalized to 18S Ribosomal RNA and calculated as relative change. Statistics were calculated with Excel. A p-value of <0.05 was considered to be statistically significant.

Chapter III

Control of Cardiac Energy Metabolism by Histone Deacetylase 3

ABSTRACT

HDAC inhibitors show remarkable therapeutic potential for a variety of disorders such as cancer (Bolden et al. 2006), neurological disease and cardiac hypertrophy (McKinsey and Olson 2004). However, the specific HDAC isoforms that mediate their actions are unclear, as are the physiological and pathological functions of individual HDACs in vivo. To explore the role of HDAC3 in the heart, we generated mice with a conditional HDAC3 null allele. Whereas global deletion of HDAC3 results in lethality by E9.5, mice with a cardiac specific deletion of HDAC3 survive until 3-4 months of age when they show massive cardiac hypertrophy and up-regulation of genes associated with fatty acid uptake, fatty acid oxidation, and electron transport/oxidative phosphorylation, accompanied by fatty acid-induced myocardial lipid accumulation and elevated triglyceride levels. These abnormalities in cardiac metabolism appear to be attributable to excessive activity of the nuclear receptor PPARα and mimic the metabolic derangements associated with diabetic cardiomyopathies. Our results reveal distinct roles for class I histone deacetylases in maintaining cardiac function and identify HDAC3 as a critical regulator of myocardial energy metabolism.

RESULTS and DISCUSSION

Conditional deletion of *HDAC3*

The four class I HDACs, (1, 2, 3 and 8) are widely expressed, but little is known of their individual functions *in vivo.* Previously, we showed that cardiac deletion of either HDAC1 or HDAC2 in the heart did not affect cardiac structure or function, whereas deletion of both of these HDACs resulted in perinatal lethality from cardiac arrhythmias, accompanied by dilated cardiomyopathy, and up-regulation of genes encoding skeletal muscle-specific contractile proteins and calcium channels. To investigate the potential functions of HDAC3 in the heart, we generated a conditional null allele of HDAC3 by introducing *loxP* sites upstream of exon 11 and downstream of exon 14 through homologous recombination (Figure 3.1A). This mutation deletes almost all of the nuclear import sequence and a carboxy-terminal region that is necessary for repression (Guenther et al. 2001). Germline transmission was detected by Southern blot and deletion of HDAC3 was confirmed at the genetic and RNA level (Figure 3.1B-D). $HDAC3^{neo\text{-}loxP}$ mice were bred to CAG-Cre (Sakai and Miyazaki 1997) transgenic mice, which express Cre recombinase ubiquitously, allowing for the generation of $HDAC3^{+/-}$ mice. $HDAC3^{+/-}$ mice were intercrossed to obtain $HDAC3^{-/-}$ mice, which died before E9.5 due to defects in gastrulation (data not shown).

Cardiac deletion of *HDAC3* causes cardiac hypertrophy

To circumvent embryonic lethality, we deleted HDAC3 specifically in the heart by breeding homozygous $HDAC3^{loxP/loxP}$ mice to transgenic mice expressing Cre recombinase under the control of the *α-myosin heavy chain* (*αMHC)* promoter (Agah et al. 1997). Cardiomyocyte-restricted deletion of HDAC3 (designated HDAC3cKO for HDAC3 cardiac

knock-out) was confirmed by RT-PCR (Figure 3.1D). HDAC3cKO mice were born at Mendelian ratios, however signs of cardiac hypertrophy assessed by heart weight to body weight ratios (HW/BW) were apparent by 4 weeks of age and were exacerbated by 12 weeks of age, resulting a 72% increase in HW/BW ratios compared to wild type littermates (Figure 3.2A). Cardiac deletion of HDAC3 resulted in 100% lethality by 16 weeks of age, with significant lethality occurring between 12 and 14 weeks (Figure 3.2B). Hearts of HDAC3cKO mice were hypertrophic and showed enlargement of both right and left atria (Figure 3.2C). Histology confirmed cardiomyocyte hypertrophy, especially in the left ventricular free wall and septum, and interstitial fibrosis in HDAC3cKO mice compared to wild type littermates (Figure 3.2C). Cardiac stress markers ANF, BNP, and α-skeletal actin levels were significantly up-regulated as early as 8 weeks of age in mutant mice, consistent with the hypertrophic response seen by histological sectioning (Figure 3.2D). Expression of p21, shown to be repressed by class I HDACs in a variety of cell types, was also significantly up-regulated, supporting the role of class I HDACs as transcriptional repressors of p21.

Ultrastructural analysis of the left ventricular free wall of the adult myocardium revealed that the normal juxtaposition of sarcomeres to mitochondria, which facilitates efficient myofibrillar contraction and relaxation in normal cardiomyocytes (Figure 3.2E), was aberrant in HDAC3 mutants. Instead, cardiac deletion of HDAC3 resulted in disorganized and fragmented myofibrils, associated with intracellular debris and disarrangement of mitochondria that showed reduced cristae density (Fig. 3.2E).

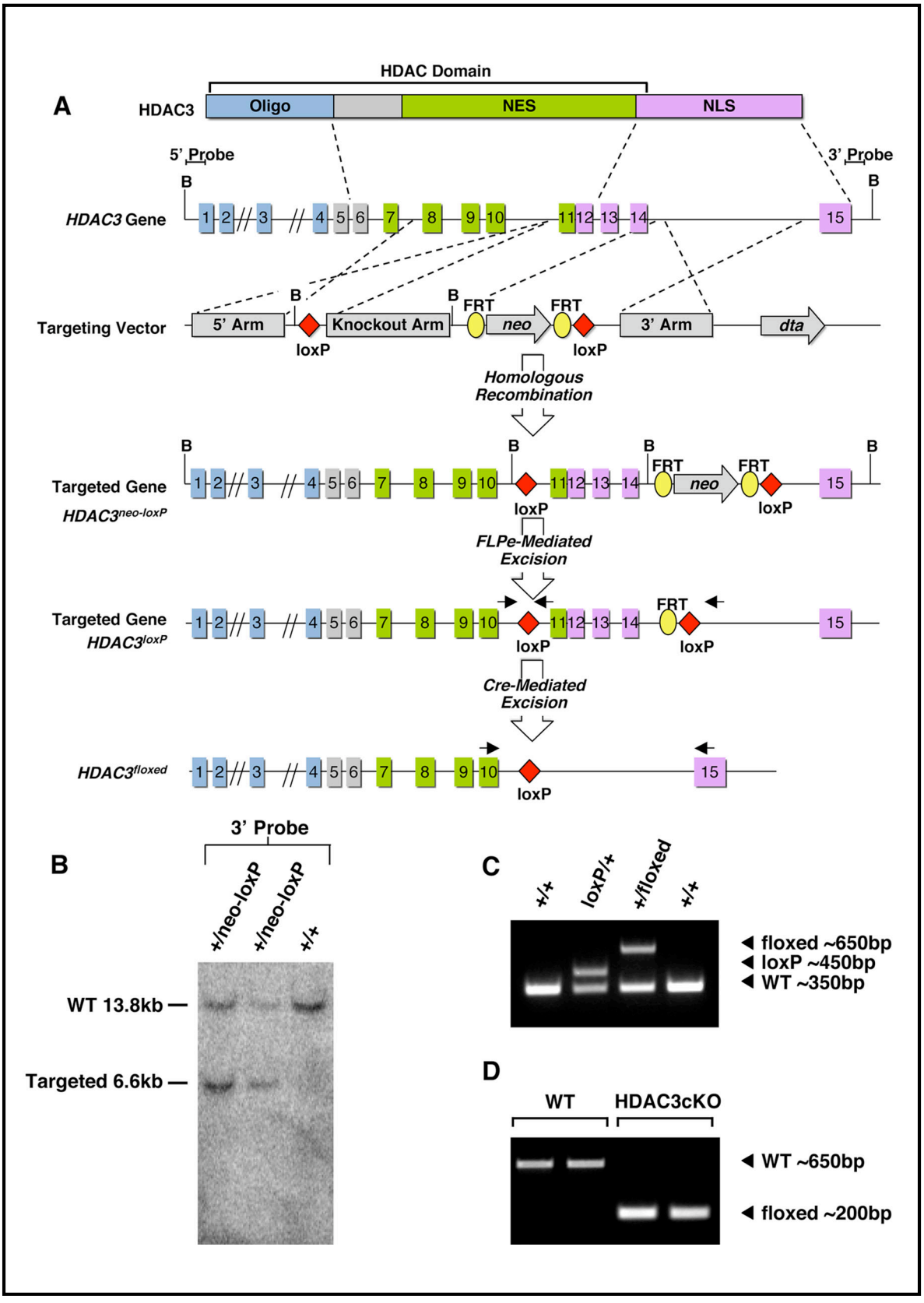
A
HDAC Domain
HDAC3
Oligo
NES
NLS
5' Probe
3' Probe
B
HDAC3 Gene
1 2 3 4 5 6 7 8 9 10 11 12 13 14 15
Targeting Vector
5' Arm
loxP
Knockout Arm
FRT
neo
FRT
loxP
3' Arm
dta
Homologous Recombination
Targeted Gene
HDAC3neo-loxP
FLPe-Mediated Excision
Targeted Gene
HDAC3loxP
Cre-Mediated Excision
HDAC3floxed
B
3' Probe
+/neo-loxP
+/neo-loxP
+/+
WT 13.8kb
Targeted 6.6kb
C
+/+
loxP/+
+/floxed
+/+
floxed ~650bp
loxP ~450bp
WT ~350bp
D
WT
HDAC3cKO
WT ~650bp
floxed ~200bp

Figure 3.1. Generation of a conditional *HDAC3* allele. (A) Strategy to generate a conditional *HDAC3* allele. Protein, genomic structure, targeting vector, and targeting allele are shown. *loxP* sites were inserted upstream of exon 11 and downstream of exon 14. The neomycin cassette was removed by crossing to FLPe transgenic mice. Cre-mediated excision leaves one *loxP* site in place of exons 11 through 14. (B) Representative Southern blot of genomic DNA to show germline transmission. WT (~13.8kb) and targeted (~6.6kb) bands are indicated. (C) Genotyping of HDAC3 conditional mice by genomic PCR. Primer triplex includes one set flanking the 5' *loxP* site and a third primer downstream of the 3' *loxP* site. Global deletion by CAG-Cre removes the primer within the *loxP* sites, resulting in once ~650-bp fragment. (D) Cardiac specific deletion of HDAC3. Semi-quantitative RT-PCR showing HDAC3 transcript levels in wild-type and HDAC3cKO mice using primers in exon 10 forward and exon 15 reverse. Cardiac deletion of HDAC3 results in deletion of exons 11 through 14. Primers are shown in (A).

Functional analyses of wild-type and HDAC3cKO mice were performed at 8 weeks of age by echocardiography. As shown in Table 3.1, HDAC3cKO mice showed significantly reduced contractility as indicated by reduced fractional shortening (39.25 ± 0.75 vs. 78.65 ± 4.35 for WT) and increased left ventricular chamber dilatation as assessed by systolic and diastolic internal diameters, LVIDs and LVIDd, respectively.

	LVIDd(mm)	LVIDs(mm)	FS (%)	HR (min^{-1})
Wild-type	**1.80 ± 0.04**	**0.38 ± 0.03**	**78.65 ± 4.35**	**632 ± 40.59**
HDAC3cKO	**2.67 ± 0.21**	**1.64 ± 0.14**	**39.25 ± 0.75**	**354 ± 12.49**

Table 3.1. Echocardiographic data of HDAC3cKO mice. Values show severe ventricular dysfunction in HDAC3cKO hearts. Values represent mean (±SEM). LVIDd, LV internal diameter at diastole; LVIDs, LV internal diameter at systole; FS, fractional shortening; HR, heart rate.

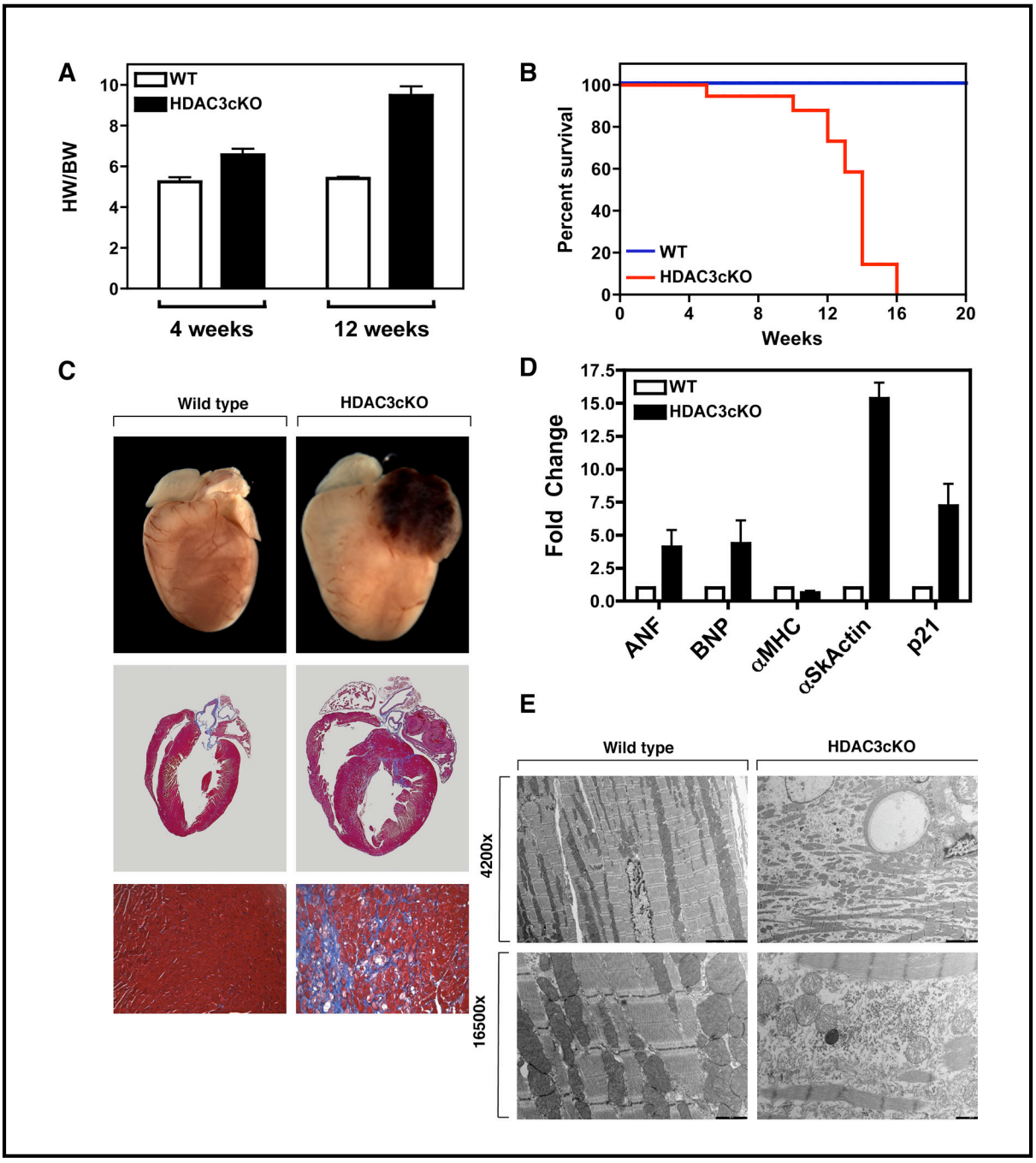

Figure 3.2. Cardiac defects resulting from cardiac deletion of HDAC3. (A) HW/BW ratios of WT and HDAC3cKO showing progression of cardiac hypertrophy. (B) Kaplan-Meier survival curve showing lethality by 16 weeks in HDAC3cKO mice. (C) Masson's trichrome stained sections of wild-type and HDAC3cKO mice. Deletion of HDAC3 results in cardiac hypertrophy, left atrial thrombus, and cardiac fibrosis seen in blue. (D) Expression of cardiac stress markers in HDAC3cKO mice at 8 weeks. mRNA transcript levels were detected by real-time RT-PCR and normalized to 18S ribosomal RNA. (E) Electron Microscopy of left ventricle tissue from WT and HDAC3cKO hearts. Bar represents 5000 nm at 4200x and 1000 nm at 16500x.

Up-regulation of myocardial energetic genes from cardiac deletion of *HDAC3*

In an effort to more precisely understand the primary cause of cardiomyopathy in HDAC3 mutant hearts, we performed microarray analysis on left ventricles from 5-week-old mice. At this timepoint, mutant hearts showed moderate increases in heart weight to body weight ratios and relatively minor changes in cardiac stress markers (Figure 3.2A and data not shown). Gene ontology analysis was performed on significantly up-regulated transcripts to identify specific biological processes altered in HDAC3cKO mice. This analysis revealed a dramatic dysregulation of cardiac metabolism in the mutant hearts (Figure 3.3A)

Cardiac energetics is tightly regulated by the peroxisome proliferator-activated receptor (PPAR) and the estrogen-related receptor (ERR) families of nuclear hormone receptors (Huss and Kelly 2004). PPARα and PPARδ have been shown to function as central regulators of cardiac mitochondrial fatty acid metabolism (Kersten et al. 1999; Watanabe et al. 2000; Finck et al. 2002; Cheng et al. 2004). Cardiac overexpression of PPARα causes increased expression of genes associated with mitochondrial uncoupling, fatty acid uptake and oxidation, and concomitant decreased expression of genes associated with glucose uptake (Finck et al. 2002), mimicking diabetic cardiomyopathy. HDAC3, together with the NCoR/SMRT or the Rb complex, is specifically recruited by PPARs to the promoters of target genes to facilitate the transcriptional repression by nuclear receptors (Fajas et al. 2002; Guan et al. 2005). To determine if the cardiac hypertrophy and ventricular dysfunction in HDAC3 mutant mice resulted from rampant nuclear receptor-dependent gene activation, we assayed known PPARα target genes in ventricles of HDAC3cKO mice. PPARα has been shown to regulate expression of the mitochondrial uncoupling proteins, UCP2 and UCP3 (Young et al. 2001). Accordingly, transcript levels for both UCP2 and

UCP3 were significantly up-regulated at baseline (6.5-fold and 2.9-fold, respectively) and this induction was increased upon administration of Wy14,643, a synthetic PPARα-agonist (Figure 3.3B).

Real-time PCR analysis of genes encoding fatty acid import, transport, and esterification (fatty acid transport protein [Slc27a1], CD36, and fatty acyl-CoA synthetase [Acsl1]) showed modest to insignificant changes at baseline. Following administration of the PPARα agonist Wy14,643, these levels were only slightly up-regulated (Figure 3.3C). The modest response at baseline is not surprising given previous studies that have shown PPAR ligands to be rate-limiting under physiological conditions (Finck et al. 2002). Additionally, the level of induction is much lower than that of the uncoupling proteins, however fatty acid import genes such as CD36 show a delayed response to PPARα ligands (Sato et al. 2002).

The expression of PPARα-responsive genes involved in fatty acid oxidation was also analyzed by real time PCR. Similar to the expression of PPARα dependent genes involved in fatty acid import, induction of genes involved in fatty acid oxidation was modest at baseline. Surprisingly, expression levels of muscle carnitine palmitoyl transferase-1 (mCPT-1) were unchanged in HDAC3cKO mice compared to wild-type mice and Wy14,643 treatment had no effect on mCPT-1 transcript levels in wild-type or HDAC3cKO hearts (Figure 3.3D). Conversely, acyl-CoA oxidase 1 (ACOX1) was significantly increased in HDAC3cKO hearts and was further up-regulated in response to Wy14,643 (Figure 3.3D and data not shown). ACOX1 is the first enzyme in peroxisomal fatty acid β-oxidation, suggesting HDAC3cKO hearts have a greater fatty acid oxidation potential than wild-type littermates.

Decreased expression of genes involved in glucose utilization from cardiac deletion of *HDAC3*

In diabetic cardiomyopathies, increased expression of genes involved in fatty acid import and mitochondrial fatty acid oxidation is coupled to a decreased utilization of the glucose oxidation pathway (Stanley et al. 1997). To determine if HDAC3cKO mice show defects in glucose uptake and utilization, we examined expression levels of the glucose transporters, GLUT1 and GLUT4. GLUT1 levels were relatively unchanged in HDAC3cKO mice compared to wild-type (data not shown), whereas GLUT4 expression was significantly down-regulated in HDAC3cKO mice (Figure 3.3E) and was further decreased in response to Wy14,643 (Figure 3.3E). GLUT1 controls basal glucose uptake while GLUT4 regulates glucose transport in an insulin-sensitive dependent manner. Down-regulation of GLUT4 in HDAC3cKO mice is consistent with the phenotype resulting from PPARα overexpression and diabetic cardiomyopathies.

Pyruvate dehydrogenase kinase 4, PDK4, regulates the pyruvate dehydrogenase (PDH) complex through phosphorylation and subsequent inactivation. PDK4 levels and activity are increased in diabetic hearts (Glyn-Jones et al. 2007). Similarly, HDAC3cKO mice showed an increase in expression of PDK4 that was further elevated upon administration of Wy14,643 (Figure 3.3E).

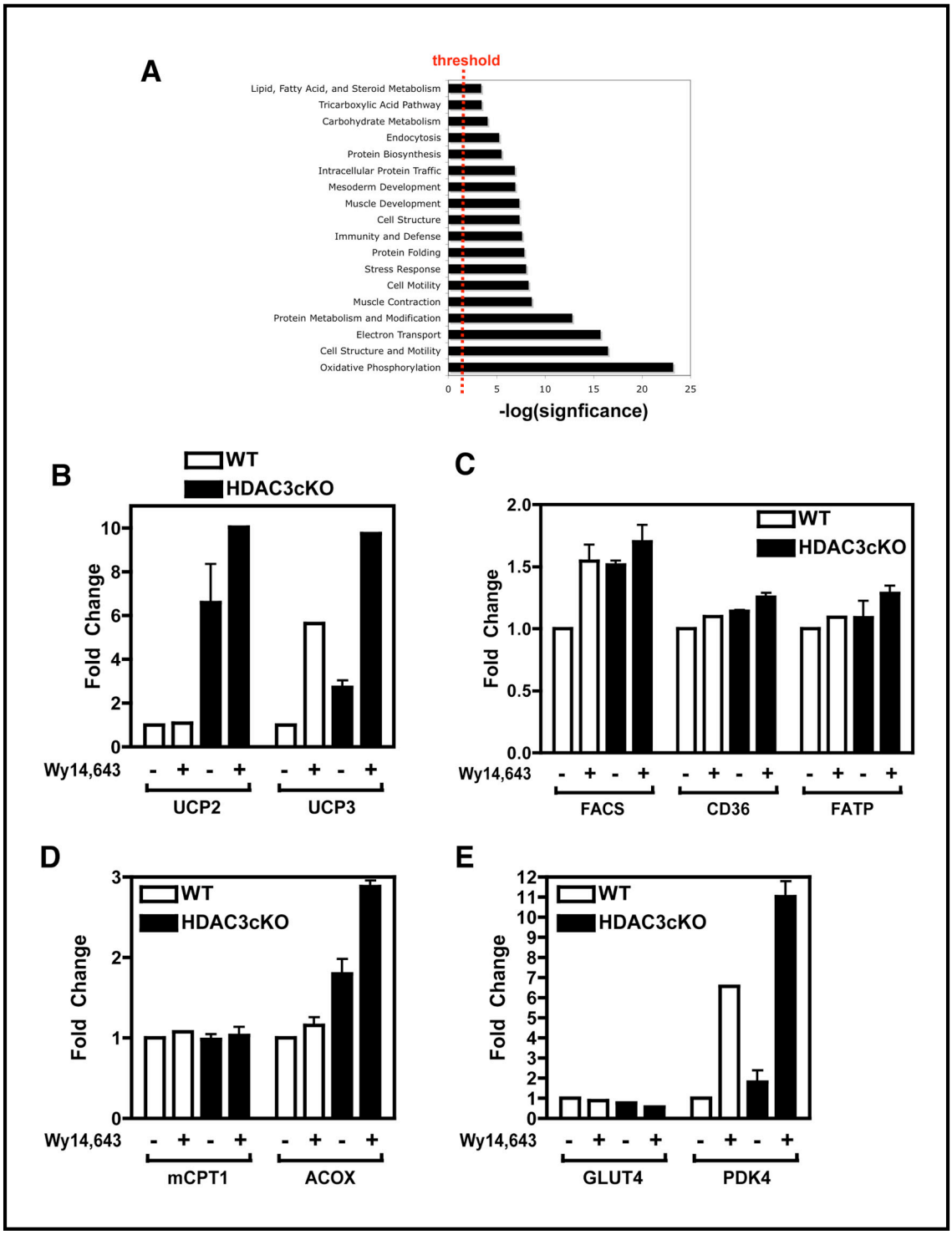

Figure 3.3. Aberrant expression of cardiac metabolism genes from cardiac deletion of HDAC3. (A) Gene ontology analysis was performed with PANTHER. Significantly enriched biological processes are shown and plotted as the –log(*P* value). (B) PPAR-regulated mitochondrial uncoupling genes are increased in HDAC3cKO mice. (C and D) Fatty acid uptake and oxidation genes are moderately increased in HDAC3cKO hearts. (E) Glucose metabolism is decreased in HDAC3cKO hearts. For (B-D), real-time RT-PCR was performed from LV RNA on wild-type and HDAC3cKO mice in absence or presence of Wy14,643. Error bars represent standard deviation.

Cardiac deletion of *HDAC3* shows ligand-induced lipid accumulation

The ligand-inducible activation of multiple PPAR-responsive genes in cardiomyocytes of HDAC3cKO mice suggests these mice are sensitive to increased fatty acids in the circulation. A hallmark of the diabetic heart is lipid accumulation in myocytes due to augmented fatty acid import (Murthy and Shipp 1977). To determine if HDAC3 mutant mice show myocardial lipid accumulation following increases in the circulating fatty acids, we subjected HDAC3cKO and wild-type mice to a 24-hour fast, which induces circulating fatty acids that can subsequently serve as ligands for PPARs. After fasting, hearts were excised and triglycerides were quantified. Mice fed ad libitum showed no significant difference in triglyceride content between HDAC3cKO and wild-type mice (Figure 3.4A). However, HDAC3cKO fasted mice showed a robust increase in myocardial triglycerides compared to wild-type controls (Figure 3.4A). Quantification of serum fatty acid and triglyceride levels showed there to be no significant difference between wild-type and HDAC3cKO mice (data not shown). Consistent with these findings, oil red O staining of histological sections from fed and fasted wild-type and HDAC3cKO hearts showed no significant staining in fed mice for either wild-type or HDAC3cKO mice (data not shown), whereas fasted myocytes from cardiac specific deletion of HDAC3 showed a substantial increase in neutral lipid accumulation (Figure 3.4B). Neutral lipids could be easily visualized throughout both ventricular free walls as well as the ventricular septum, however the atria remained free of lipids. These results are consistent with observations from diabetic cardiomyopathies and further suggest HDAC3 as a central regulator of PPAR and other transcription factors that govern myocardial energy metabolism.

Mitochondrial dysfunction resulting from cardiac deletion of *HDAC3*

To further define the metabolic abnormalities resulting from cardiac specific deletion of HDAC3, we assayed mitochondrial function from wild-type and HDAC3cKO mice. Mitochondrial dysfunction is intimately linked to diabetic cardiomyopathy through defects in glucose utilization and increased fatty acid oxidation (Boudina and Abel 2007). The increased fatty acid oxidation results in increased reducing equivalents to the electron transport chain, which in turn generates free radicals and leads to mitochondrial uncoupling (Boudina and Abel 2006). Free fatty acids are able to directly promote free radical production through the inhibition of complex I of the electron transport chain (Cocco et al. 1999; Loskovich et al. 2005; Schonfeld and Reiser 2006). Consistently, HDAC3cKO mice showed a 25% reduction in complex I activity accompanied by a 39% reduction in NADH oxidase activity (Figure 3.4C). Additionally, free radical production was increased two-fold in HDAC3cKO mice compared to wild-type littermates (Figure 3.4C). Given the increase in expression of genes involved in oxidative phosphorylation and electron transport from the microarray analysis, this data suggests a feedback mechanism is activating these genes to compensate for the electron transport chain inhibition and reduction in cardiac efficiency.

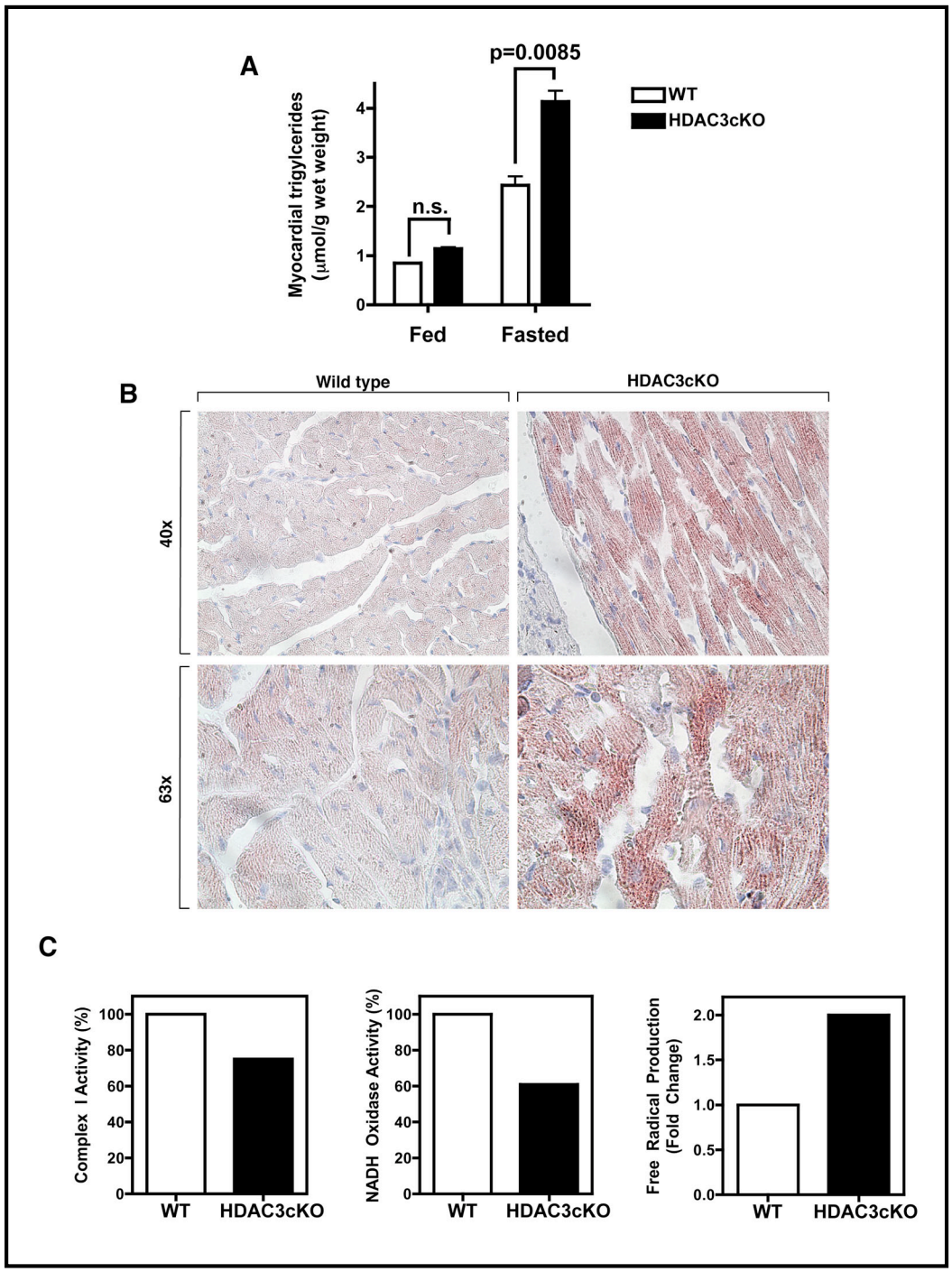

Figure 3.4. Myocardial lipid accumulation and mitochondrial dysfunction in HDAC3cKO mice. (A) Increased triglycerides in HDAC3cKO hearts after fasting. Triglycerides were extracted from wild-type and HDAC3cKO hearts and quantified. (B) Oil red O staining of wild-type and cardiac deletion of HDAC3 following a 24 hour fast. Red droplets indicate neutral lipids. HDAC3cKO mice show substantial lipid accumulation. (C) HDAC3cKO hearts show impaired mitochondrial function. Complex I activity, NADH oxidase activity, and free radicals were determined as described.

The results of this study, together with those of prior studies, point to HDAC3 as a unique regulator of cardiac gene expression. In contrast to the severe hypertrophy and metabolic abnormalities associated with deletion of HDAC3, cardiac deletion of HDAC1 or 2 does not evoke a phenotype, whereas deletion of both results in ventricular dilatation without metabolic abnormalities. Thus, despite the high degree of homology between HDACs 1, 2 and 3, HDAC3 clearly plays a unique role in maintenance of cardiac function. The phenotype of HDAC3 mutant mice also underscores the need to develop specific pharmacological inhibitors that avoid HDAC3 inhibition so as to avoid cardiac toxicity from systemic delivery of HDAC inhibitors.

METHODS

Generation of a conditional *HDAC3* allele

HDAC3 targeting vector was generated using the pGKNEO-F2L2-DTA vector. This vector contains a neomycin resistance cassette flanked by frt and loxP sites and a diphtheria toxin gene cassette. The arms for homologous recombination were generated by high fidelity PCR amplification (Roche Expand High Fidelity) of 129SvEv genomic DNA. The targeting vector was linearized with PvuI and electroporated into 129SvEv-derived ES cells. 500 ES cell clones were screened for homologous recombination by Southern blot analysis. Genomic DNA was digested with BamHI and successful loxP site incorporation was confirmed with both a 5' and 3' probe. Targeted ES cells were injected into the blastocysts of C57BL/6 females to generate chimeric mice. Chimeras were crossed to C57BL/6 females to achieve germline transmission.

Histology, immunohistochemistry, and electron microscopy

Tissues were fixed in 4% paraformaldehyde, embedded in paraffin, and sectioned at 5μm intervals. Sections were stained with hematoxylin and eosin or Masson's trichrome using standard procedures. For neutral lipid staining, hearts were fixed in 4% paraformaldehyde, cryo-embedded, and stained with oil red O and counterstained with hematoxylin. For transmission electron microscropy, left ventricular tissue was minced and fixed in 2% paraformaldehyde, 2.5% glutaraldehyde, 0.1M cacodylate buffer, prepared according to standard protocol and visualized on a Tecnai G2 Spirit 120KV TEM.

RT-PCR and microarray

Total RNA was purified using TRIzol reagent according to manufacturer's instructions. For RT-PCR, total RNA was used for reverse transcriptase using random hexamer primers. Primer sequences are available upon request. Quantitative real time PCR was performed using Taqman probes purchased from ABI. For microarray, RNA was extracted from either 3 wild-type or *HDAC3*$^{loxP/loxP}$*; aMHC-Cre* hearts and subsequently pooled prior to analysis. Microarray analysis was performed using the Mouse Genome 430 2.0 Array (Affymetrix). All heart RNA is from ventricle tissue only. Microarray analysis was performed by the UT Southwestern Microarray Core Facility using the Mouse Genome 430 2.0 Array (Affymetrix) as described (Davis et al. 2006).

Echocardiography

Cardiac function was analyzed by 2-dimensional echocardiography on nonsedated mice using a Vingmed System (GE Vingmed Ultrasound) and a 11.5-MHz linear array transducer. M-mode tracings were used to measure anterior and posterior wall thicknesses at end diastole and end systole. LV internal diameter (LVID) was measured as the largest anteroposterior diameter in either diastole (LVIDd) or systole (LVIDs). A single observer blinded to mouse genotypes analyzed the data. LV FS was calculated according to the following formula: FS (%) = [(LVIDd – LVIDs)/LVIDd] × 100.

Myocardial triglyceride levels

Lipids were extracted from ventricular tissue using a modified Bligh and Dyer technique (REF). Briefly, tissue was homogenized in an ice-cold chloroform/methanol/water (2:1:0.8) solution. Additional chloroform and water was added to separate layers and mixture was centrifuged at 12,000 x *g*. Following centrifugation, chloroform layer was extracted,

evaporated, and resultant residue was resuspended in 0.5ml isopropanol. Triglyceride content was quantified using a triglyceride quantification kit (Sigma).

Animal studies

For fasting studies, male HDAC3cKO and wild-type littermates were fasted for 24 hours. After 24 hours, mice were sacrificed, hearts extracted, and prepared for Oil Red O staining. Control mice were allowed standard chow ad libitum. Wy14,643 (Biomol) (50mg/kg body weight) in 50% DMSO/saline was administered as a single intraperitoneal injection. Control littermates were administered vehicle and hearts were extracted 8 hours after injection.

Mitochondrial function assays

8 week old wild-type and HDAC3cKO hearts were perfused in mannitol sucrose buffer and snap frozen under liquid nitrogen. Mitochondrial function assays were performed as described (Yu et al. 2007).

Statistical methods

Values are presented as ± SEM unless otherwise noted. Gene expression was normalized to 18S Ribosomal RNA and calculated as relative change. Statistics were calculated with Excel. A p-value of <0.05 was considered to be statistically significant.

Chapter IV

Functional Redundancy of Histone Deacetylases 1 and 2 in Multiple Cell Types

ABSTRACT

Histone deacetylases antagonize histone acetyltransferases to modulate gene expression by catalyzing the removal of acetyl groups from histone tails. The ensuing charge on histone lysines results in chromatin compaction and subsequent gene repression. HDACs have become therapeutic targets for a variety of disease states however the function of individual HDACs in specific tissues has not been defined. We have previously shown HDAC1 and HDAC2 act redundantly in the control of cardiac growth and morphogenesis. To explore the role of HDAC1 and HDAC2 in additional stages of heart development and disease, as well as multiple cell types, we generated conditional deletions of HDAC1 and HDAC2 in the adult myocardium, early differentiating cardiomyocytes, endothelial cells, and neuronal precursors. Surprisingly, deletion of HDAC1 and HDAC2 in the adult myocardium has no deleterious effect on the heart. In fact, loss of HDAC1 and HDAC2 blunts β-adrenergic induced hypertrophy. Conversely, deletion of both HDAC1 and HDAC2 in prenatal cardiomyocytes, endothelial cells, or neuronal precursors results in lethality. Deletion of HDAC1 and HDAC2 in developing neurons results in loss of the hippocampus, absence of cerebellar foliation, and disorganization of cortical neurons. Additionally, loss of HDAC1 and HDAC2 in neuronal precursors blocks differentiation of neurons. These results identify HDAC1 and HDAC2 as required redundant regulators of development in a variety of cell types, but are dispensable, if not beneficial, in post-mitotic cells.

RESULTS and DISCUSSION

Adult cardiac-specific deletion of HDAC1 and HDAC2

The class I HDACs (HDAC1, HDAC2, HDAC3, and HDAC8) are ubiquitously expressed and provide the enzymatic basis for transcriptional repression. Transcription factors recruit HDACs, either individually, or in repressive complexes to deacetylate lysine residues on histone tails and repress gene expression. While much has been learned through *in vitro* and inhibitor studies, little is known about the biological function of these individual enzymes *in vivo*. We have previously shown HDAC1 and HDAC2 redundantly regulate cardiac growth and morphogenesis, however the lethality associated with postnatal deletion of HDAC1 and HDAC2 precludes studies in the adult heart. To circumvent this lethality, we generated adult cardiac-specific deletion of HDAC1 and HDAC2 by crossing homozygous *HDAC1*$^{loxP/loxP}$*; HDAC2*$^{loxP/loxP}$ mice to *αMHC-MerCreMer* transgenic mice (Sohal et al. 2001; Montgomery et al. 2007). The *αMHC-MerCreMer* mice express a fusion of Cre recombinase and the mutated estrogen receptor ligand-binding domain that is sensitive to tamoxifen but not estrogen and driven by the *α-myosin heavy chain* (*αMHC)* promoter (Agah et al. 1997; Sohal et al. 2001). Deletion of HDAC1 and HDAC2 by *αMHC-MerCreMer* showed no lethality or deleterious effects on the heart (data not shown). Real-time PCR analysis of calcium channels and skeletal muscle contractile genes up-regulated in the *HDAC1*$^{loxP/loxP}$*; HDAC2*$^{loxP/loxP}$; *αMHC-Cre* (or dCKO) hearts showed no change 10 days after tamoxifen treatment compared to wild-type littermates (Figure 4.1A). These results suggest HDAC1 and HDAC2 are involved in repressing these embryonic isoforms during postnatal development, but are no longer required for repression in adult post-mitotic cardiomyocytes.

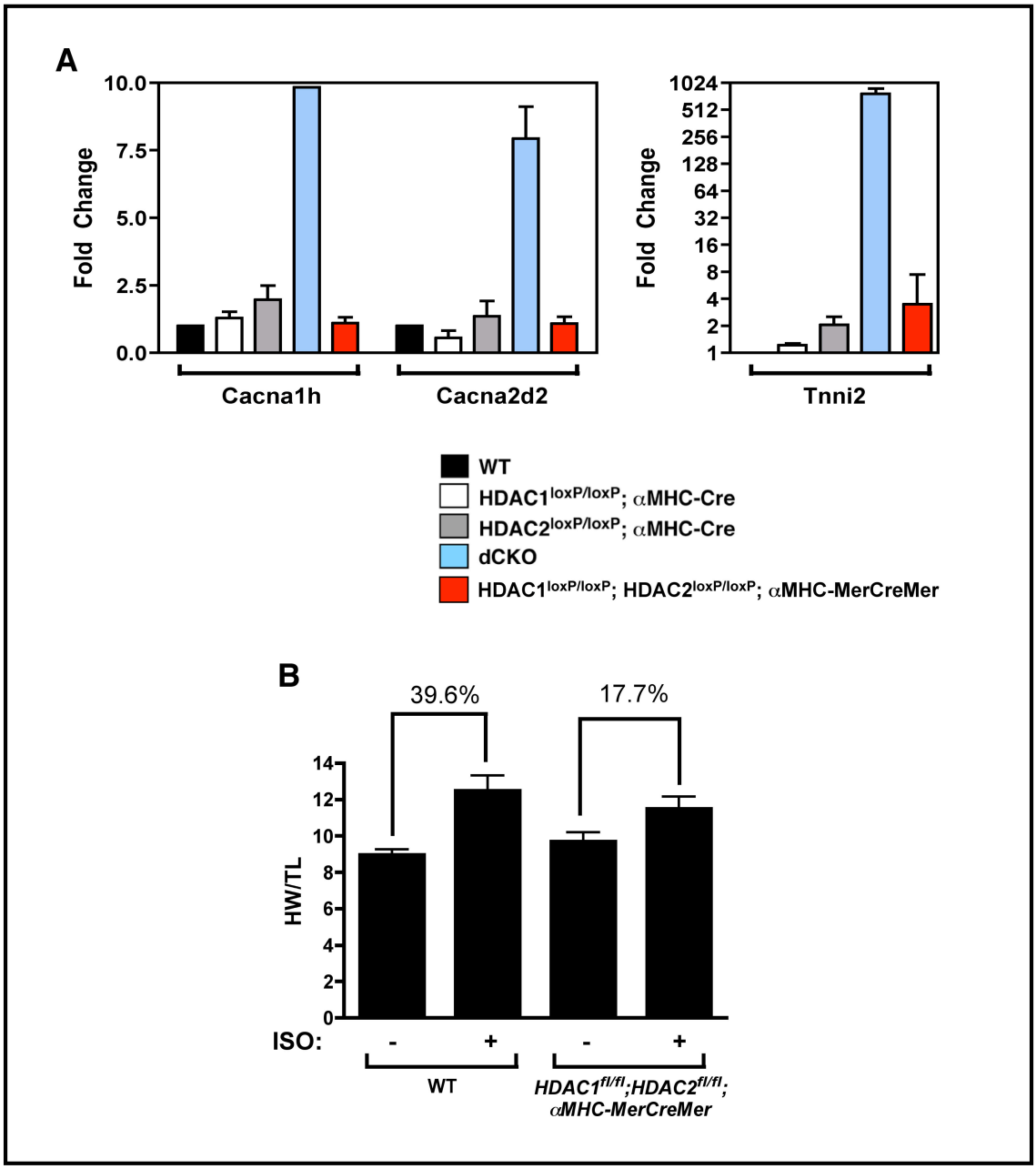

Figure 4.1. Adult cardiac-specific deletion of HDAC1 and HDAC2 blunts hypertrophy. (A) Real-time PCR analysis of multiple HDAC1 and HDAC2 mutants showing adult cardiac-specific deletion has no effect on calcium channels and skeletal muscle-specific genes up-regulated in dCKO mice. (B) HW/TL ratios of WT and *HDAC1$^{loxP/loxP}$; HDAC2$^{loxP/loxP}$;αMHC-MerCreMer* mice subjected to isoproterenol. Loss of HDAC1 and HDAC2 in adult myocytes blunts the hypertrophic response.

Class I HDAC inhibition is able to block the hypertrophic response (Antos et al. 2003; Kee et al. 2006; Kong et al. 2006) and global genetic deletion of HDAC2 using a gene-

trap line blunts cardiac hypertrophy (Trivedi et al. 2007a), however cardiac-specific deletion of HDAC1 or HDAC2 does not prevent the hypertrophic program (Montgomery et al. 2007). To determine if loss of HDAC1 and HDAC2 in adult cardiomyocytes can blunt the hypertrophic response, we treated wild-type and *HDAC1$^{loxP/loxP}$; HDAC2$^{loxP/loxP}$; αMHC-MerCreMer* with tamoxifen or vehicle and subjected them to isoproterenol, a β-adrenergic agonist, to induce hypertrophy. Compared to wild-type controls, which showed a 39.6% increase in HW/TL ratios, loss of HDAC1 and HDAC2 in adult myocytes resulted in a 17.7% increase in HW/TL ratios following isoproterenol-induced hypertrophy. These results suggest HDAC1 and HDAC2 also act as redundant regulators of the pro-hypertrophic response and targeting HDAC1 and HDAC2 together could be beneficial for heart failure therapeutics.

HDAC1 and HDAC2 are redundant in multiple cell types

To further investigate the role of HDAC1 and HDAC2 in the development of multiple tissues, we crossed *HDAC1$^{loxP/loxP}$; HDAC2$^{loxP/loxP}$* mice to *Nkx2.5KI-Cre*, *Tie2-Cre*, and *GFAP-Cre* to mediate cre recombination of HDAC1 and HDAC2 in early differentiating cardiomyoctes, endothelial cell, and neuronal precursors, respectively (Kisanuki et al. 2001; Moses et al. 2001; Zhuo et al. 2001). Surprisingly, only one copy of either HDAC1 or HDAC2 was sufficient for viability in all three cell types, however loss of all four alleles resulted in embryonic or postnatal lethality (Figure 4.2 and data not shown). *HDAC1$^{loxP/loxP}$; HDAC2$^{loxP/loxP}$*; *Nkx2.5KI-Cre* mice showed embryonic lethality by day E11.5 with dramatic pericardial effusion (Figure 4.2A). Loss of HDAC1 and HDAC2 in endothelial cells also resulted in embryonic lethality by day E11.5 (Figure 4.2B). *HDAC1$^{loxP/loxP}$; HDAC2$^{loxP/loxP}$*; *Tie2-Cre* embryos showed enlarged dorsal aortae and hemorrhaging throughout the midgut,

while embryos with only one copy of HDAC1 or HDAC2 showed normal development (Figure 4.2B and data not shown). *HDAC1*$^{loxP/loxP}$*; HDAC2*$^{loxP/loxP}$; *GFAP-Cre* mice were born at normal Mendelian ratios, but died within the first week, accompanied by a reduced brain size, "butterfly" shaped telencephalic lobes, and a compact cerebellum (Figure 4.2C). Again, one copy of either HDAC1 or HDAC2 was sufficient for neural development and viability. Together, these results define HDAC1 and HDAC2 as central redundant regulators of multiple developmental paradigms.

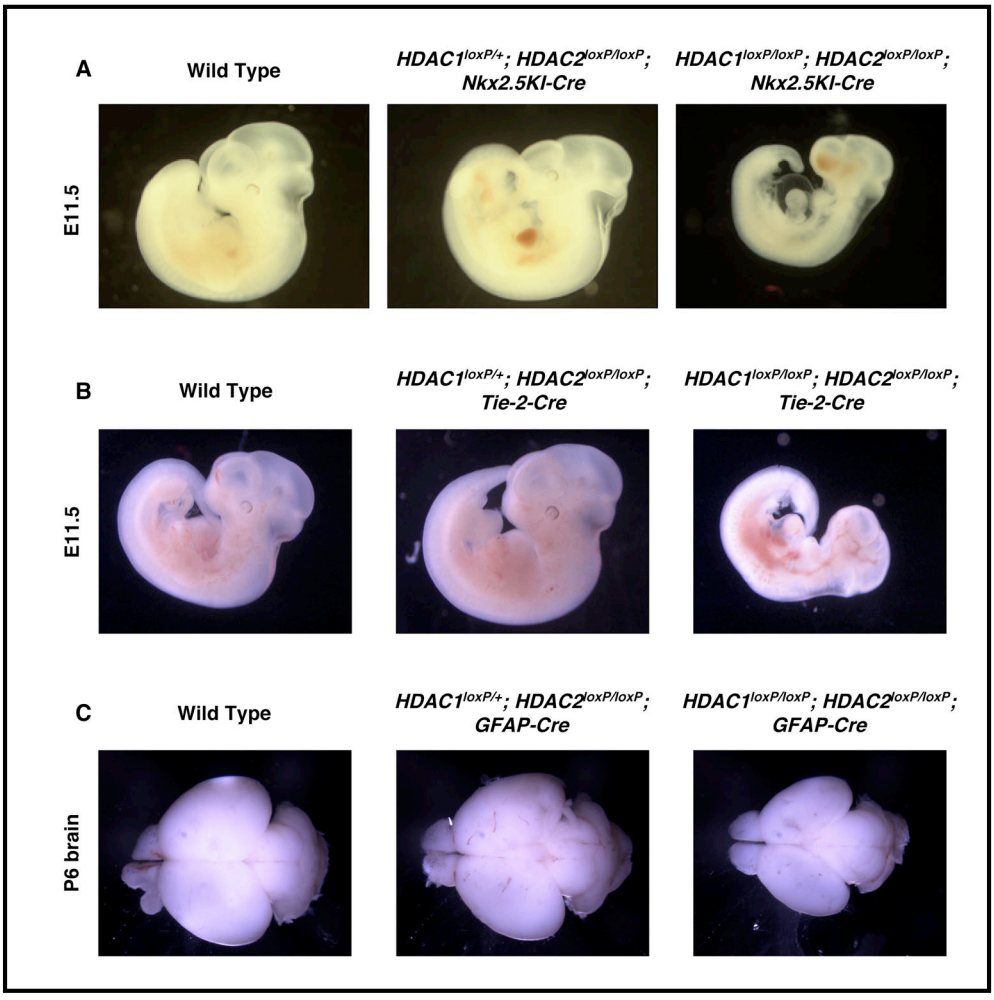

Figure 4.2. Functional redundancy of HDAC1 and HDAC2 in multiple lineages. Conditional deletion of HDAC1 and HDAC2 in early cardiomyocytes (A), endothelial cells (B), or neural precursors (C) results in lethality. One copy of HDAC1 is sufficient for viability in all three cell types.

Neuronal abnormities in brain deletion of HDAC1 and HDAC2

To further delineate the defects associated with loss of HDAC1 and HDAC2 in the developing central nervous system, we performed histological analysis on 6 day-old pups. Histoarchitectural findings on wild-type, *HDAC1*$^{loxP/+}$*; HDAC2*$^{loxP/loxP}$; *GFAP-Cre,* and *HDAC1*$^{loxP/loxP}$*; HDAC2*$^{loxP/loxP}$; *GFAP-Cre* mice showed dramatic defects localized to the hippocampus and the cerebellum. Deletion of HDAC1 and HDAC2 together resulted in severe deficiencies in cortical laminar organization, a loss of all hippocampal structures, and a lack of foliation in the cerebellum (Figure 4.3). Mice with only one copy of HDAC1 showed reduced cerebellar foliation (Figure 4.3B), however these mice survived to adulthood. Behavior studies are currently underway to determine if HDAC1 and HDAC2 have non-redundant roles in adult neurons. Histological timepoint analyses showed the neuronal defects to originate between E14.5 and E16.5, a timepoint when neurogenesis and neuronal migration are high (data not shown).

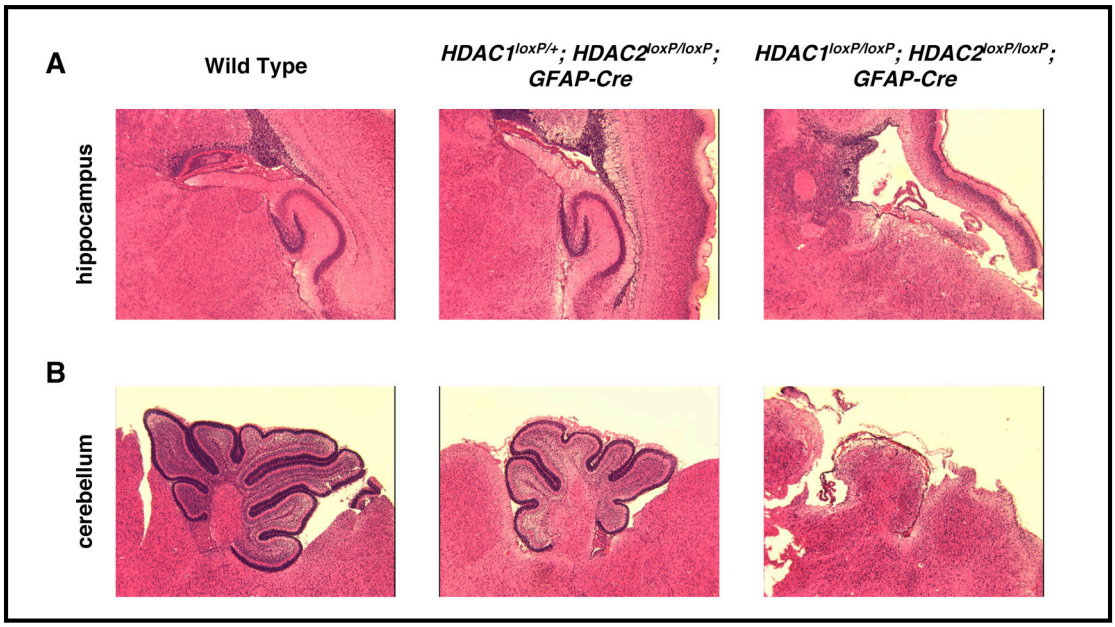

Figure 4.3. HDAC1 and HDAC2 deletion causes severe hippocampal and cerebellar abnormalities. (A) Hippocampus and (B) cerebellum sections from wild-type, *HDAC1*$^{loxP/+}$*; HDAC2*$^{loxP/loxP}$; *GFAP-Cre,* and *HDAC1*$^{loxP/loxP}$*; HDAC2*$^{loxP/loxP}$; *GFAP-Cre* mice stained with hematoxylin and eosin showing loss of hippocampus and loss of foliation in cerebellum of double HDAC1 and HDAC2 mutants.

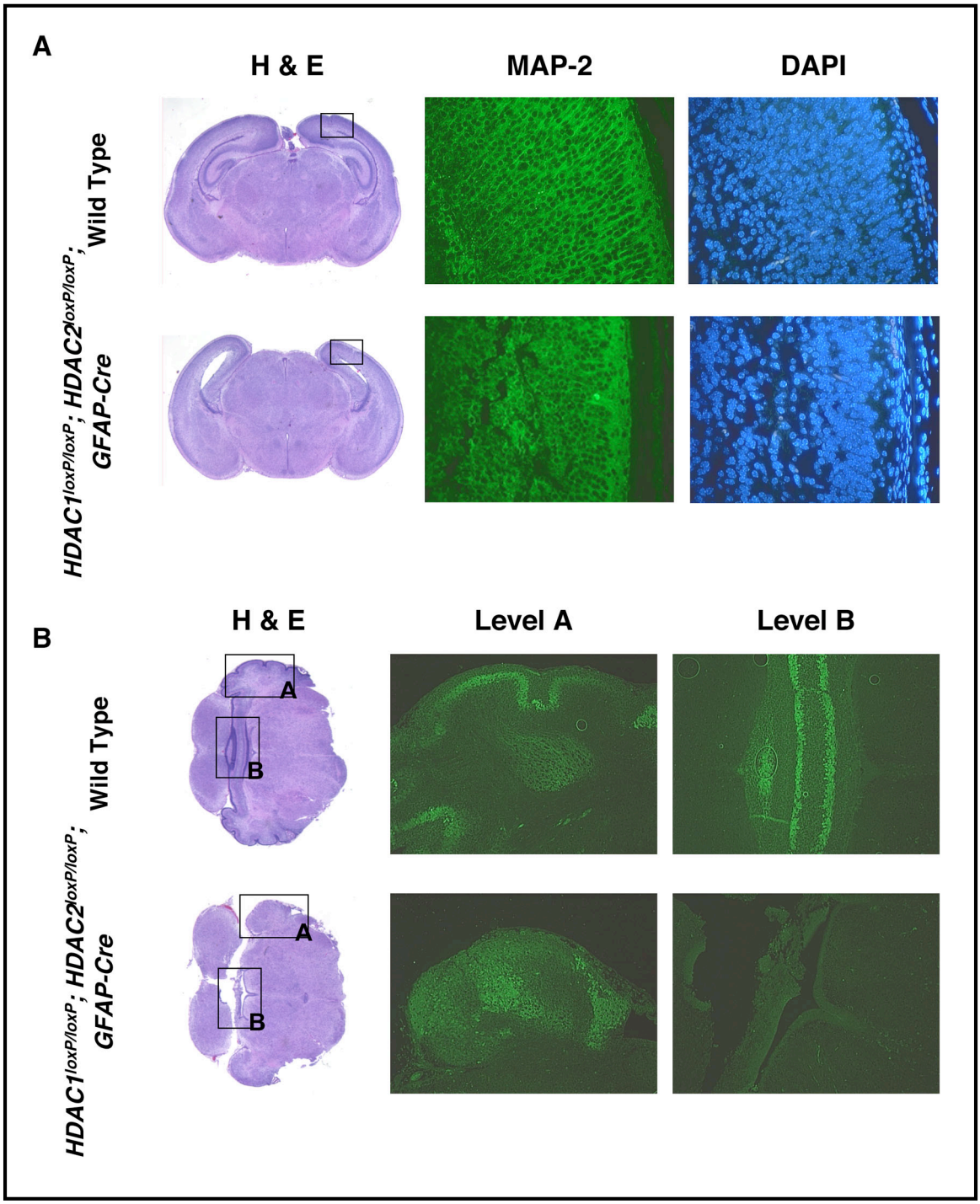

Figure 4.4. Neuronal defects in *HDAC1*$^{loxP/loxP}$; *HDAC2*$^{loxP/loxP}$; *GFAP-Cre* mice. (A) Immunohistochemical staining of MAP-2 on the neocortex of wild-type and mutant mice. Mutant mice show a lack of dendritic extensions compared to control. (B) Immunohistochemical staining for calbindin on wild-type and mutant cerebellum. Mutant cerebellum shows Purkinje cells have failed to migrate and remain among the deep cerebellar nuclei.

Defects in cerebral neurons and Purkinje cells resulting from loss of HDAC1 and HDAC2 in neurons

To further investigate the hippocampal and cerebellar abnormalities, we performed immunohistochemistry at postnatal day 1 to detect microtubule-associated protein 2 (MAP-2) and calbindin, respectively. MAP-2 is a neuronal marker highly expressed in dendritic extensions, whereas calbindin stains Purkinje cells in the cerebellum. In wild-type mice, MAP-2 staining of the neocortex showed proper dendritic extensions between cortical layers, whereas *HDAC1*$^{loxP/loxP}$*; HDAC2*$^{loxP/loxP}$; *GFAP-Cre* mice showed a complete disorganization of cortical neurons with a complete absence of dendritic extensions (Figure 4.4A). Similarly, calbindin staining of wild-type and *HDAC1*$^{loxP/loxP}$*; HDAC2*$^{loxP/loxP}$; *GFAP-Cre* cerebellum revealed distinct neuronal malformations. At postnatal day 1, cerebellar development is still on going; the Purkinje cells have not yet formed the tight single-cell layer present in later stages. Consistently, wild-type mice showed proper organization of Purkinje cells and normal foliation, whereas *HDAC1*$^{loxP/loxP}$*; HDAC2*$^{loxP/loxP}$; *GFAP-Cre* mice showed Purkinje cells failed to migrate and remained within the deep nuclei of the cerebellum. The lack of migration by the Purkinje cells is detrimental to the development of the cerebellum as the overlaying granule cell layer requires proliferative signals from the Purkinje cells for proper cerebellar growth (Chizhikov and Millen 2003).

Defective cortical laminar organization resulting from brain deletion of HDAC1 and HDAC2

Because HDACs are involved in regulation of the cell cycle (Wang et al. 2001) and have been shown to control cell migration (Whetstine et al. 2005; Zinovyeva et al. 2006), we

speculated the observed phenotypes could be due to inefficient neuronal migration and/or defective progenitor specification. We first examined the potential role HDAC1 and HDAC2 in neuronal migration. The development of the cerebral cortex is an intricate process that involves sequential neurogenesis and migration. Neurogenesis occurs in the ventricular zone and new post-mitotic neurons migrate outwardly along radial glial fibers to populate a region called the preplate around E10.5. Newly generated and migrating neurons split the preplate into the superficial marginal zone and the subplate. As the cortex develops, all newly generated neurons migrate past the older neurons to populate the cortical plate just below the marginal zone in a classical inside-out pattern (Hatten 1999). Multiple mutants have been characterized that show defects in neuronal migration and show defective hippocampal, cerebral cortex, and cerebellar development, including the *reeler* and *scrambler* mutations, as well as the Cdk5 knockout and VLDLR and ApoER2 double knockout (D'Arcangelo et al. 1995; Ohshima et al. 1996; Howell et al. 1997; Sheldon et al. 1997; Trommsdorff et al. 1999).

We performed immunohistochemistry to detect chondroitin sulfate proteoglycans (CSPGs) on both the hippocampus and overlaying neocortex for wild-type and mutant mice. CSPGs are molecular marker for the subplate and marginal zone in the cerebral cortex and the subplate of the hippocampus. In wild-type mice, by postnatal day 1, the cortical plate neurons have split the preplate into two layers, the superficial marginal zone and the subplate layer (Figure 4.5A). Immunohistochemical staining for CSPGs on *HDAC1*$^{loxP/loxP}$*; HDAC2*$^{loxP/loxP}$; *GFAP-Cre* mice also showed two distinct layers for the subplate and marginal zone, albeit much less pronounced. Additionally, the intermittent cortical plate is greatly reduced in the cortex suggesting either disorganization or compaction of the cortical

plate neurons or a reduced number of cortical plate neurons. Similarly, CSPG staining on the hippocampus of *HDAC1*$^{loxP/loxP}$; *HDAC2*$^{loxP/loxP}$; *GFAP-Cre* mice showed a complete disorganization of the hippocampal subplate compared to wild-type controls (Figure 4.5B).

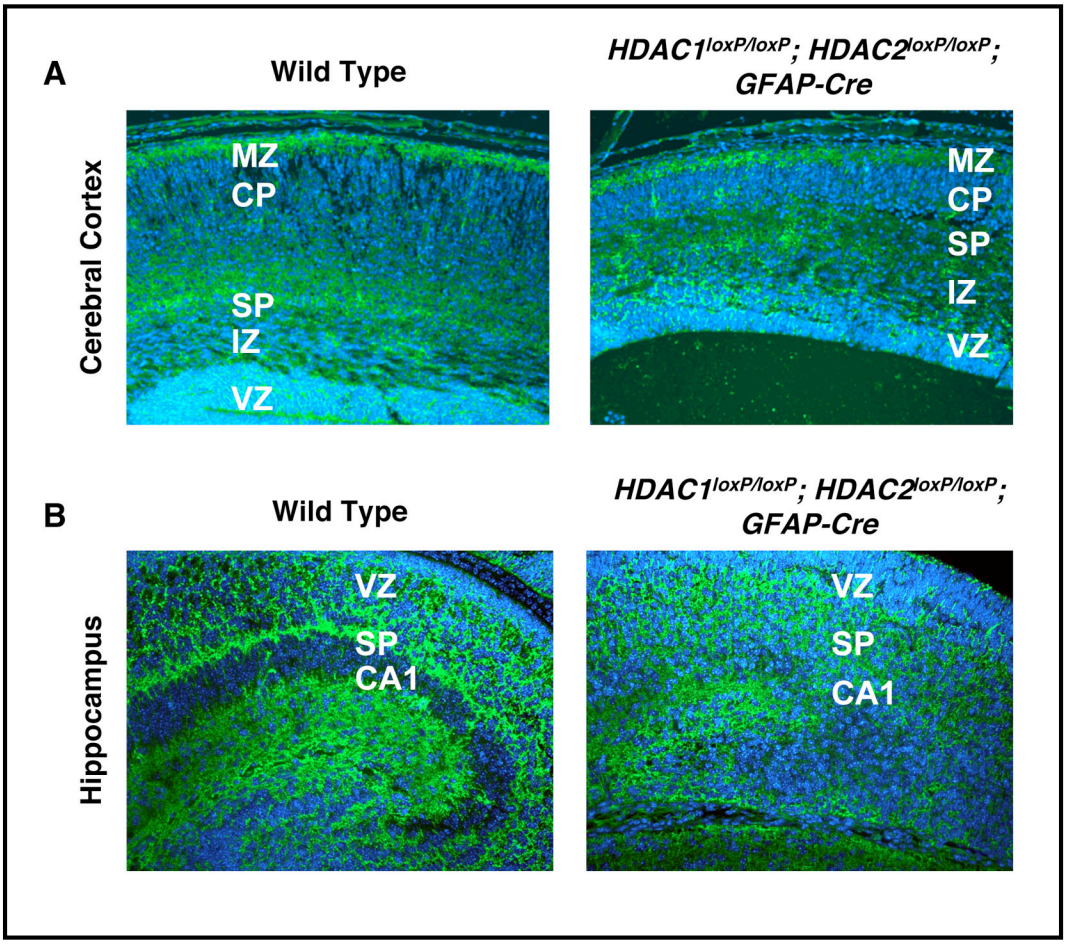

Figure 4.5. Defective laminar organization in cerebral cortex and hippocampus of *HDAC1*$^{loxP/loxP}$; *HDAC2*$^{loxP/loxP}$; *GFAP-Cre* mice. Immunohistochemistry of CSPGs (green) and Hoechst (blue) of wild-type and mutant cerebral cortex (A) and hippocampus (B). Deletion of HDAC1 and HDAC2 results in disorganization molecular layers. Hippocampal structures are unidentifiable in mutant mice. MZ, marginal zone; CP, cortical plate; SP, subplate; IZ, intermediate zone; VZ, ventricular zone.

Neuronal birth-date analysis of brain deletion of HDAC1 and HDAC2

To further determine if the defects in the cerebral cortex and hippocampus are due to aberrant neuronal migration, we performed neuronal birth data analysis at E12.5 and E14.5.

As mentioned, newly generated neurons will migrate outwardly from the ventricular zone along radial glial fibers and reside just superficially to more mature neurons. We injected pregnant females with a single intraperitoneal injection of bromodeoxyuridine (BrdU) at either E12.5 or E14.5 and sacrificed the embryos at E18.5. In wild-type mice, immunohistochemistry against BrdU detected neurons born at E12.5 at the base of the cortical plate (Figure 4.6A). *HDAC1*$^{loxP/loxP}$*; HDAC2*$^{loxP/loxP}$; *GFAP-Cre* mice also showed BrdU labeled neurons at the base of the cortical plate, indicating proper migration of neurons, however the number of mutant neurons born at E12.5 was considerably lower than that of wild-type controls. Consistently, BrdU labeled neurons born at E14.5 were visible in the cortical plate in both wild-type and *HDAC1*$^{loxP/loxP}$*; HDAC2*$^{loxP/loxP}$; *GFAP-Cre* mice, but again, the mutant mice showed a reduced number of BrdU-positive neurons (Figure 4.6B). These data suggest while neuronal migration of mutant neurons is intact, significantly fewer post-mitotic neurons exist in *HDAC1*$^{loxP/loxP}$*; HDAC2*$^{loxP/loxP}$; *GFAP-Cre* mice.

Brain deletion of HDAC1 and 2 results in increased proliferation of neuronal progenitors

Because of the reduced number BrdU-positive neurons, we suspected the developing neurons were either undergoing apoptosis or were failing to differentiate into neurons. Terminal deoxynucleotidyl Transferase biotin-dUTP Nick End Labeling (TUNEL) analysis revealed no significant difference in apoptosis between wild-type and *HDAC1*$^{loxP/loxP}$*; HDAC2*$^{loxP/loxP}$; *GFAP-Cre* brains (data not shown). To determine if neuronal proliferation/differentiation was affected in mutant mice, we injected pregnant females with a single intraperitoneal injection of BrdU at E14.5 and sacrificed the embryos one hour later.

Compared to wild-type mice, *HDAC1*$^{loxP/loxP}$*; HDAC2*$^{loxP/loxP}$; *GFAP-Cre* mice showed an increase in BrdU-positive neuronal precursors in the ventricular zone of the neocortex (Figure 4.7A) as well as in the developing hippocampus (Figure 4.7B). Additionally, Tuj1-positive cells, which labels neurons, appeared to be decreased in mutant mice compared to wild-type littermates, especially in the cortical plate region where neurons born at this timepoint would normally be migrating (Figure 4.7A).

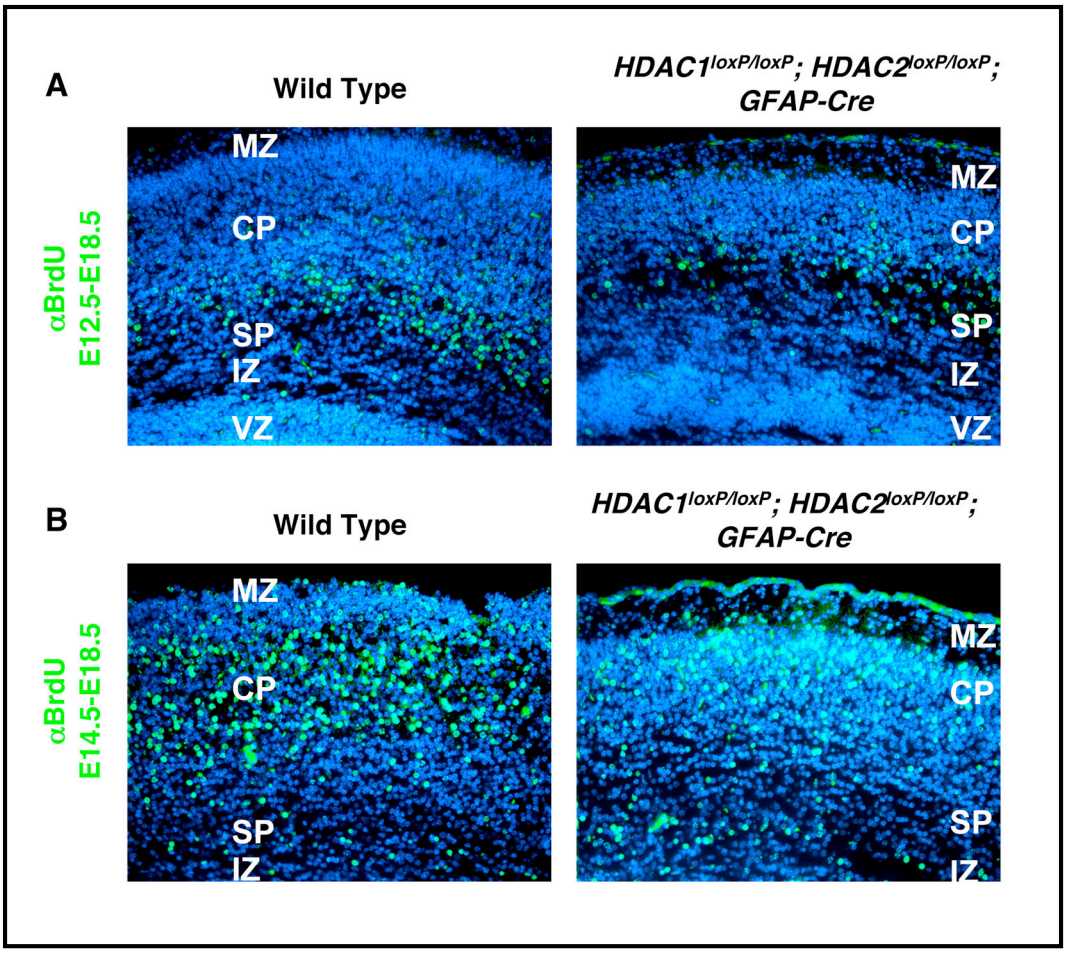

Figure 4.6. Neuronal birth date analysis of *HDAC1*$^{loxP/loxP}$*; HDAC2*$^{loxP/loxP}$*; GFAP-Cre* mice. Immunohistochemistry of BrdU (green) and Hoechst (blue) of wild-type and mutant cerebral cortex injected with BrdU at E12.5 (A) or E14.5 (B). Deletion of HDAC1 and HDAC2 results in normal neuronal migration but results in fewer differentiated neurons. MZ, marginal zone; CP, cortical plate; SP, subplate; IZ, intermediate zone; VZ, ventricular zone.

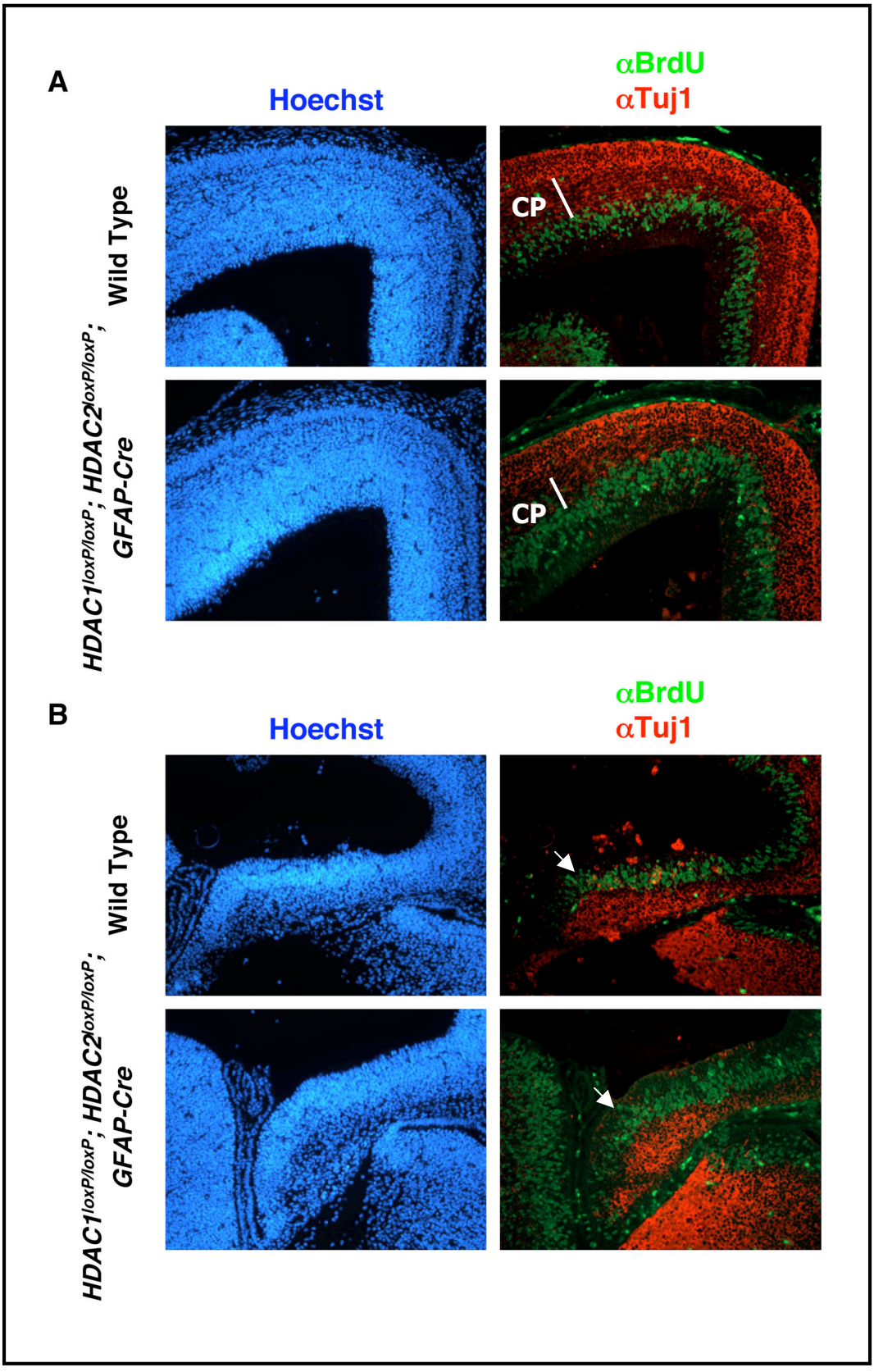
A
Hoechst
αBrdU
αTuj1
Wild Type
HDAC1loxP/loxP; HDAC2loxP/loxP; GFAP-Cre
CP
CP
B
Hoechst
αBrdU
αTuj1
Wild Type
HDAC1loxP/loxP; HDAC2loxP/loxP; GFAP-Cre

Figure 4.7. Aberrant neuronal proliferation in *HDAC1$^{loxP/loxP}$; HDAC2$^{loxP/loxP}$; GFAP-Cre* mice. Immunohistochemistry at E14.5 detecting Hoechst (blue), BrdU (green), and Tuj1 (red) on wild-type and mutant cerebrum cortex (A) and developing hippocampus (B). Deletion of HDAC1 and HDAC2 results in increased proliferation of neuronal precursors at the ventricular zone and reduced number of Tuj1-expressing neurons. Cortical plate, CP, is marked in (A) and arrow in (B) indicates developing hippocampus at E14.5.

Deletion of HDAC1 and HDAC2 in neuronal progenitors blocks neuronal differentiation

To better quantify the potential defect in cell fate specification, we prepared cortical neuronal precursors from E14.5 *HDAC1$^{loxP/loxP}$; HDAC2$^{loxP/loxP}$* mice and infected them with a lentivirus expressing Cre-GFP. Two days after infection, we withdrew FGF and added differentiation media. Surprisingly, deletion of HDAC1 and HDAC2 was able to completely block neuronal differentiation (Figure 4.8A) as no Tuj1-positive cell expressed GFP, whereas a significant number of noninfected cells expressed Tuj1. To quantify this, we infected lentivirus expressing Cre-GFP or GFP alone. The blockade of differentiation by deletion of HDAC1 and HDAC2 was robust, showing only 5% Tuj1-positive cells of the total GFP-positive cells in the Cre-GFP condition compared to 45% Tuj1-positive cells of the total GFP-positive cells in the GFP alone condition (Figure 4.8B).

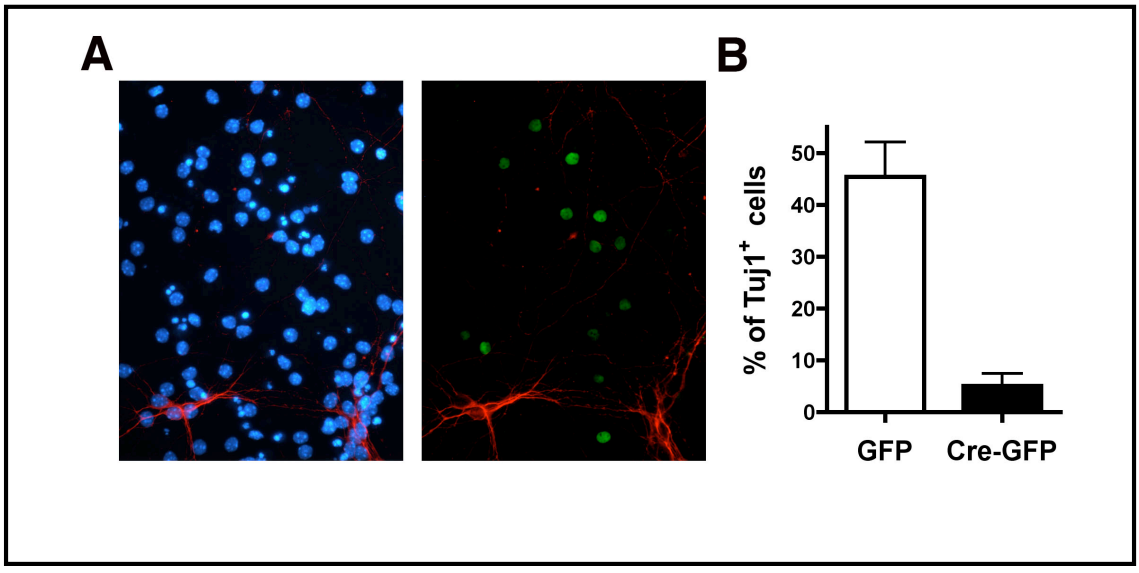

Figure 4.8. Deletion of HDAC1 and HDAC2 blocks neuronal differentiation. (A) Neuronal progenitors from E14.5 *HDAC1*$^{loxP/loxP}$*; HDAC2*$^{loxP/loxP}$ embryos infected with Cre-GFP. No GFP-positive cells express the neuronal marker Tuj1 (red). (B) Quantification of neuronal cultures infected with GFP alone or Cre-GFP. Graph is percentage of Tuj1-positive cells of total GFP-positive cells. Cre deletion of HDAC1 and HDAC2 blocks neuronal differentiation.

The results of this study have provided further genetic support that HDAC1 and HDAC2 act as redundant regulators of tissue development. Surprisingly, HDAC1 and HDAC2 have been shown to be only required during development, whereas deletion in post-mitotic cells appears to have no detrimental effect on the cell. The ability of deletion of HDAC1 and HDAC2 to blunt the hypertrophic response following β-adrenergic stimulation strengthens the designs of specific inhibitors against HDAC1 and HDAC2 for heart disease, as well as demonstrates HDAC1 and HDAC2 might be viable targets in all post-mitotic cells. The neuronal phenotype associated with loss of HDAC1 and HDAC2 is very surprising given that the effect is the exact opposite from the HDAC inhibitor studies (Hsieh et al. 2004b), however multiple zebrafish HDAC1 mutants have shown defective neuronal differentiation (Cunliffe 2004; Stadler et al. 2005; Cunliffe and Casaccia-Bonnefil 2006). While HDAC1 and HDAC2 appear to be the primary target for HDAC inhibitors in most tissues, these experiments suggest there are additional mechanisms controlling HDAC inhibitor-mediated induction of neuronal differentiation. Conversely, these results must be interpreted with caution as it pertains to drug therapies, as pharmacological inhibition does not equate to genetic deletion.

METHODS

Animal studies

Generation of HDAC1 and HDAC2 conditional alleles have been described (Montgomery et al. 2007). All transgenic Cre lines have been previously described (*αMHC-Cre,* Agah et al. 1997; *Tie2-Cre,* Kisanuki et al. 2001; *Nkx2.5KI-Cre,* Moses et al. 2001; *αMHC-MerCreMer,* Sohal et al. 2001; *hGFAP-Cre,* Zhuo et al. 2001). Tamoxifen (Sigma) (300 mg/kg BW in 95% sesame oil: 5% ethanol) was administered at 10 weeks of age by daily gavage for 5 consecutive days. Experiments were performed at a minimum of 10 days following treatment. For BrdU studies, pregnant females were injected with one single intraperitoneal injection of BrdU (Roche) (100 μg/g BW) at E12.5 or E14.5. For neuronal birthdate analysis, females were sacrificed at E18.5. For proliferation studies, pregnant females were sacrificed 1 hour after injection, embryos fixed in 4% paraformaldehyde, and sectioned for immunostaining.

Isoproterenol administration

Hypertrophic agonist Isoproterenol (Sigma) (8.8mg/kg/day) or saline were administered using miniosmotic pumps (Model 2001, Alzet) dorsally implanted subcutaneously in 10 to 12-week-old male mice. Mice were sacrificed 7 days after isoproterenol infusion and cardiac hypertrophy was assayed by heart weight and tibia length.

RT-PCR

Total RNA was purified using TRIzol reagent according to manufacturer's instructions. For RT-PCR, total RNA was used for reverse transcriptase using random hexamer primers.

Primer sequences are available upon request. Quantitative real time PCR was performed using Taqman probes purchased from ABI. All mRNA transcript levels were normalized to 18S ribosomal RNA.

Histology and immunohistochemistry

Tissues were fixed in 4% paraformaldehyde, embedded in paraffin, and sectioned at 5μm intervals. Sections were stained with hematoxylin and eosin using standard procedures (Shelton et al. 2000). TUNEL assay was performed according to standard protocol (Roche). Immunohistochemistry with the following primary antibodies: mouse anti-MAP2 (1:200; Sigma), mouse anti-calbindin (1:200; Sigma), mouse anti-CSPG (Sigma), and rabbit anti-Tuj1 (Covance) was performed according to protocol described (Xin et al. 2006). Immunohistochemistry using mouse anti-BrdU (Roche) was performed according to manufacturer's protocol.

In vitro differentiation analysis

Neuronal cortices were isolated from *HDAC1*$^{loxP/loxP}$; *HDAC2*$^{loxP/loxP}$ mice at E14.5 as described (Groszer et al. 2001) and neuronal differentiation was induced as described (Hsieh et al. 2004a). Briefly, neuronal precursors were isolated and placed in insulin-containing N2-supplemented (Invitrogen) DME:Ham's F12 (Omega Scientific) medium containing 20 ng/ml FGF-2 (PeproTech, Inc.). Retrovirus containing Cre-GFP or GFP alone was infected for 4 days. Following 4 days of infection, FGF-2 was withdrawn and neuronal differentiation media was added (N2 medium plus 1 μM RA and 5 μM forskolin (Sigma-Aldrich)). After 4

days, cells were fixed in 4% paraformaldehyde and immunostained for Tuj1 as described (Hsieh et al. 2004a).

Chapter V

Conclusions and Future Remarks

The dynamic process of histone acetylation and deacetylation has become an attractive therapeutic target because of the multitude of cellular processes it controls as well as the promising results shown in clinical trials for cancer. The first HDAC inhibitor was approved in 2006 for the treatment of cutaneous T-cell lymphoma and many more appear to be in the pipeline. While these drugs are showing potential, the question of target specificity remains. Mouse and human have 11 HDACs that have very similar "deacetylase domains" that most HDAC inhibitors target (class III HDACs are not inhibited by classical HDAC inhibitors). Furthermore, our lack of understanding of the biology of each individual enzyme has hindered the advancement of therapeutic design.

Histone Deacetylase 1 and 2 are redundant regulators of development

The results of these studies have given the first glimpse into the biological function of HDAC1, HDAC2, and HDAC3. HDAC1 and HDAC2 are redundant in the development of multiple tissues, however each appears to have autonomous functions as evident by the lethality associated with the global deletion of either one individually. We still do not know if the lethality is truly due to nonredundant functions or merely deletion in a specific cell type that only expresses HDAC1 or HDAC2. Further expression analyses are necessary to better characterize the expression patterns of HDAC1 and HDAC2 in development. The viability of adult cardiac-specific deletion of HDAC1 and HDAC2 suggests loss of HDAC1 and HDAC2 is tolerable in post-mitotic cells. Interestingly, the genes associated with lethality of the postnatal cardiac-specific deletion of HDAC1 and HDAC2 are not up-regulated in the adult cardiac-specific deletion suggesting HDAC1 and HDAC2 are necessary for the regulation of the complex transcriptional networks involved in proliferation and

differentiation but are dispensable post-mitotically. Preliminary results have shown that adult global deletion of HDAC1 or HDAC2 is viable, however adult global deletion of HDAC1 and HDAC2 results in lethality. Current experiments are underway to determine the cause of lethality by adult global double deletion of HDAC1 and HDAC2.

HDAC1 and HDAC2 as therapeutic targets for cardiac hypertrophy

Class I HDACs have become an increasingly attractive therapeutic target for cardiac hypertrophy due to HDAC inhibitor ability to block the hypertrophic program both in vitro and in vivo (Antos et al. 2003; Kee et al. 2006; Kong et al. 2006). Recently an HDAC2 gene trap mutant was reported to be partially viable and able to block cardiac hypertrophy from a number of stimuli (Trivedi et al. 2007a). We, however, were unable to recapitulate this data, as our global HDAC2 deletion causes lethality (Montgomery et al. 2007). Cardiac-specific deletions of HDAC1 or HDAC2 showed no difference compared to wild-type littermates in response to hypertrophic agonists, suggesting these enzymes are either redundant in the pathogenesis of hypertrophy or the persistent expression of HDAC1 or HDAC2 in cardiac fibroblasts and other non-Cre expressing cells is sufficient to mediate the hypertrophic response. To address this, we generated adult inducible cardiac-specific deletions of HDAC1 and HDAC2. Preliminary results show these mice are resistant to isoproterenol-induced cardiac hypertrophy. Current experiments are in progress to determine if this blunting of the hypertrophic response extends beyond β-adrenergic stimulation to additional models of hypertrophy such as thoracic aortic constriction. Given the loss of function phenotypes associated with class II HDACs and the ability of adult cardiac specific-deletion of HDAC1 and HDAC2 to potentially block hypertrophy, these results suggest designing new

hypertrophic therapeutics that directly target HDAC1 and HDAC2 specifically may be vastly beneficial to the treatment of heart disease.

HDAC1 and HDAC2 as redundant regulators of neuronal differentiation

The striking phenotype associated with loss of HDAC1 and HDAC2 in the developing central nervous system can at least be partially explained through HDAC1 and HDAC2 control of neuronal differentiation. Deletion of HDAC1 and HDAC2 in neuronal progenitor cells is able to completely block neuronal differentiation. This is surprising given inhibition of histone deacetylases with VPA induces neuronal differentiation, but also blocks astrocyte and oligodendrocyte differentiation (Hsieh et al. 2004b). However, multiple mutants of HDAC1 in zebrafish have shown HDAC1 is required for neuronal differentiation (Cunliffe 2004; Stadler et al. 2005). These results suggest a couple of possibilities. The effects seen by HDAC inhibitor treatment of neuronal precursors are possibly due to dominant effects of inhibition of other HDACs. This seems unlikely given the inhibitor used has shown strong preference towards class I HDACs (HDAC2 specifically). Additionally, HDAC1 and HDAC2 could potentially have non-enzymatic roles in neuronal differentiation that override loss of enzymatic activity in the deletion studies. Non-enzymatic functions have been seen in other cell types, such as overexpression of a "deacetylase dead" HDAC1 resulting in dilated cardiomyopathies. Continued analysis of these mutants as well as other HDAC mutants will continue to bring insight into the function of these enzymes during neuronal development. Through the generation of these alleles, we will now be able to narrow the target of HDAC inhibitors through experiments such as treating HDAC1 and HDAC2 deficient neuronal precursors with HDAC inhibitors to see if this promotes

differentiation. If so, it would suggest HDAC1 and HDAC2 are not the targets of HDAC inhibitors during neuronal differentiation. These experiments are currently in design.

Independent functions of HDAC3 during development

HDAC3 is roughly 50% identical to HDAC1 and HDAC2 in their amino acid sequence and share high homology in their deacetylase domains, however HDAC3 is normally found in different repressive complexes than HDAC1 and HDAC2. Likewise, the generation of an HDAC3 conditional allele has allowed us to more distinctly identify these individual functions of HDAC3. HDAC3 appears to show no redundancy with HDAC1 or HDAC2 during cardiac development as cardiac-specific deletion of HDAC3 results in massive cardiac hypertrophy accompanied by aberrant myocardial energetic transcripts, ligand-induced myocardial lipid accumulation, and mitochondrial dysfunction. The specific phenotype of cardiac-restricted HDAC3 deletion has furthered the necessity of specificity of HDAC inhibitors. It will be interesting to see if loss of HDAC3 in post-mitotic cardiomyocytes has similar detrimental effects on the tissue. These experiments are currently underway. Preliminary studies in additional cell types have also identified HDAC3 as a unique transcriptional regulator during development as deletion in endothelial cells is lethal by E12.5 and deletion in the central nervous system results in lethality by 3 weeks of age. Continued analysis of these mutants will provide pivotal information to the biological function of HDAC3 during development and disease as well as provide potential off-target effects from inadvertent pharmacological inhibition.

Class I HDAC inhibitors have shown great benefit in a variety of disease states. Through the generation and analysis of conditional alleles for HDAC1, HDAC2, and HDAC3, we hope therapeutic design and HDAC biological knowledge will continue to progress. We are certain compound deletions and pharmacological treatment of mutant cells in the years to come will uncover some of the most fascinating functions of these enzymes during developmental, physiological, and pathological settings.

References

Agah, R., Frenkel, P.A., French, B.A., Michael, L.H., Overbeek, P.A., and Schneider, M.D. 1997. Gene recombination in postmitotic cells. Targeted expression of Cre recombinase provokes cardiac-restricted, site-specific rearrangement in adult ventricular muscle in vivo. *J Clin Invest* **100**(1): 169-179.

Ajiro, K. 2000. Histone H2B phosphorylation in mammalian apoptotic cells. An association with DNA fragmentation. *J Biol Chem* **275**(1): 439-443.

Antos, C.L., McKinsey, T.A., Dreitz, M., Hollingsworth, L.M., Zhang, C.L., Schreiber, K., Rindt, H., Gorczynski, R.J., and Olson, E.N. 2003. Dose-dependent blockade to cardiomyocyte hypertrophy by histone deacetylase inhibitors. *J Biol Chem* **278**(31): 28930-28937.

Backs, J. and Olson, E.N. 2006. Control of cardiac growth by histone acetylation/deacetylation. *Circ Res* **98**(1): 15-24.

Backs, J., Song, K., Bezprozvannaya, S., Chang, S., and Olson, E.N. 2006. CaM kinase II selectively signals to histone deacetylase 4 during cardiomyocyte hypertrophy. *J Clin Invest* **116**(7): 1853-1864.

Bhaumik, S.R., Smith, E., and Shilatifard, A. 2007. Covalent modifications of histones during development and disease pathogenesis. *Nat Struct Mol Biol* **14**(11): 1008-1016.

Bodor, G.S., Oakeley, A.E., Allen, P.D., Crimmins, D.L., Ladenson, J.H., and Anderson, P.A. 1997. Troponin I phosphorylation in the normal and failing adult human heart. *Circulation* **96**(5): 1495-1500.

Bolden, J.E., Peart, M.J., and Johnstone, R.W. 2006. Anticancer activities of histone deacetylase inhibitors. *Nat Rev Drug Discov* **5**(9): 769-784.

Boudina, S. and Abel, E.D. 2006. Mitochondrial uncoupling: a key contributor to reduced cardiac efficiency in diabetes. *Physiology (Bethesda)* **21**: 250-258.

-. 2007. Diabetic cardiomyopathy revisited. *Circulation* **115**(25): 3213-3223.

Cai, R., Kwon, P., Yan-Neale, Y., Sambuccetti, L., Fischer, D., and Cohen, D. 2001. Mammalian histone deacetylase 1 protein is posttranslationally modified by phosphorylation. *Biochem Biophys Res Commun* **283**(2): 445-453.

Camelo, S., Iglesias, A.H., Hwang, D., Due, B., Ryu, H., Smith, K., Gray, S.G., Imitola, J., Duran, G., Assaf, B., Langley, B., Khoury, S.J., Stephanopoulos, G., De Girolami, U., Ratan, R.R., Ferrante, R.J., and Dangond, F. 2005. Transcriptional therapy with the histone deacetylase inhibitor trichostatin A ameliorates experimental autoimmune encephalomyelitis. *J Neuroimmunol* **164**(1-2): 10-21.

Chang, S., McKinsey, T.A., Zhang, C.L., Richardson, J.A., Hill, J.A., and Olson, E.N. 2004. Histone deacetylases 5 and 9 govern responsiveness of the heart to a subset of stress signals and play redundant roles in heart development. *Mol Cell Biol* **24**(19): 8467-8476.

Chang, S., Young, B.D., Li, S., Qi, X., Richardson, J.A., and Olson, E.N. 2006. Histone deacetylase 7 maintains vascular integrity by repressing matrix metalloproteinase 10. *Cell* **126**(2): 321-334.

Cheng, L., Ding, G., Qin, Q., Huang, Y., Lewis, W., He, N., Evans, R.M., Schneider, M.D., Brako, F.A., Xiao, Y., Chen, Y.E., and Yang, Q. 2004. Cardiomyocyte-restricted

peroxisome proliferator-activated receptor-delta deletion perturbs myocardial fatty acid oxidation and leads to cardiomyopathy. *Nat Med* **10**(11): 1245-1250.

Chien, K.R. 1999. Stress pathways and heart failure. *Cell* **98**(5): 555-558.

Chizhikov, V. and Millen, K.J. 2003. Development and malformations of the cerebellum in mice. *Mol Genet Metab* **80**(1-2): 54-65.

Choi, J.H., Kwon, H.J., Yoon, B.I., Kim, J.H., Han, S.U., Joo, H.J., and Kim, D.Y. 2001. Expression profile of histone deacetylase 1 in gastric cancer tissues. *Jpn J Cancer Res* **92**(12): 1300-1304.

Choi, J.H., Oh, S.W., Kang, M.S., Kwon, H.J., Oh, G.T., and Kim, D.Y. 2005. Trichostatin A attenuates airway inflammation in mouse asthma model. *Clin Exp Allergy* **35**(1): 89-96.

Cocco, T., Di Paola, M., Papa, S., and Lorusso, M. 1999. Arachidonic acid interaction with the mitochondrial electron transport chain promotes reactive oxygen species generation. *Free Radic Biol Med* **27**(1-2): 51-59.

Cress, W.D. and Seto, E. 2000. Histone deacetylases, transcriptional control, and cancer. *J Cell Physiol* **184**(1): 1-16.

Cunliffe, V.T. 2004. Histone deacetylase 1 is required to repress Notch target gene expression during zebrafish neurogenesis and to maintain the production of motoneurones in response to hedgehog signalling. *Development* **131**(12): 2983-2995.

Cunliffe, V.T. and Casaccia-Bonnefil, P. 2006. Histone deacetylase 1 is essential for oligodendrocyte specification in the zebrafish CNS. *Mech Dev* **123**(1): 24-30.

D'Arcangelo, G., Miao, G.G., Chen, S.C., Soares, H.D., Morgan, J.I., and Curran, T. 1995. A protein related to extracellular matrix proteins deleted in the mouse mutant reeler. *Nature* **374**(6524): 719-723.

Davis, C.A., Haberland, M., Arnold, M.A., Sutherland, L.B., McDonald, O.G., Richardson, J.A., Childs, G., Harris, S., Owens, G.K., and Olson, E.N. 2006. PRISM/PRDM6, a transcriptional repressor that promotes the proliferative gene program in smooth muscle cells. *Mol Cell Biol* **26**(7): 2626-2636.

de Ruijter, A.J., van Gennip, A.H., Caron, H.N., Kemp, S., and van Kuilenburg, A.B. 2003. Histone deacetylases (HDACs): characterization of the classical HDAC family. *Biochem J* **370**(Pt 3): 737-749.

Dokmanovic, M., Clarke, C., and Marks, P.A. 2007. Histone deacetylase inhibitors: overview and perspectives. *Mol Cancer Res* **5**(10): 981-989.

Dora, E.G., Rudin, N., Martell, J.R., Esposito, M.S., and Ramirez, R.M. 1999. RPD3 (REC3) mutations affect mitotic recombination in Saccharomyces cerevisiae. *Curr Genet* **35**(2): 68-76.

Dover, J., Schneider, J., Tawiah-Boateng, M.A., Wood, A., Dean, K., Johnston, M., and Shilatifard, A. 2002. Methylation of histone H3 by COMPASS requires ubiquitination of histone H2B by Rad6. *J Biol Chem* **277**(32): 28368-28371.

Downs, J.A., Lowndes, N.F., and Jackson, S.P. 2000. A role for Saccharomyces cerevisiae histone H2A in DNA repair. *Nature* **408**(6815): 1001-1004.

Fajas, L., Egler, V., Reiter, R., Hansen, J., Kristiansen, K., Debril, M.B., Miard, S., and Auwerx, J. 2002. The retinoblastoma-histone deacetylase 3 complex inhibits PPARgamma and adipocyte differentiation. *Dev Cell* **3**(6): 903-910.

Finck, B.N., Lehman, J.J., Leone, T.C., Welch, M.J., Bennett, M.J., Kovacs, A., Han, X., Gross, R.W., Kozak, R., Lopaschuk, G.D., and Kelly, D.P. 2002. The cardiac

phenotype induced by PPARalpha overexpression mimics that caused by diabetes mellitus. *J Clin Invest* **109**(1): 121-130.

Finnin, M.S., Donigian, J.R., Cohen, A., Richon, V.M., Rifkind, R.A., Marks, P.A., Breslow, R., and Pavletich, N.P. 1999. Structures of a histone deacetylase homologue bound to the TSA and SAHA inhibitors. *Nature* **401**(6749): 188-193.

Fischle, W., Dequiedt, F., Hendzel, M.J., Guenther, M.G., Lazar, M.A., Voelter, W., and Verdin, E. 2002. Enzymatic activity associated with class II HDACs is dependent on a multiprotein complex containing HDAC3 and SMRT/N-CoR. *Mol Cell* **9**(1): 45-57.

Frey, N. and Olson, E.N. 2003. Cardiac hypertrophy: the good, the bad, and the ugly. *Annu Rev Physiol* **65**: 45-79.

Gao, L., Cueto, M.A., Asselbergs, F., and Atadja, P. 2002. Cloning and functional characterization of HDAC11, a novel member of the human histone deacetylase family. *J Biol Chem* **277**(28): 25748-25755.

Glyn-Jones, S., Song, S., Black, M.A., Phillips, A.R., Choong, S.Y., and Cooper, G.J. 2007. Transcriptomic analysis of the cardiac left ventricle in a rodent model of diabetic cardiomyopathy: molecular snapshot of a severe myocardial disease. *Physiol Genomics* **28**(3): 284-293.

Gregoretti, I.V., Lee, Y.M., and Goodson, H.V. 2004. Molecular evolution of the histone deacetylase family: functional implications of phylogenetic analysis. *J Mol Biol* **338**(1): 17-31.

Groszer, M., Erickson, R., Scripture-Adams, D.D., Lesche, R., Trumpp, A., Zack, J.A., Kornblum, H.I., Liu, X., and Wu, H. 2001. Negative regulation of neural stem/progenitor cell proliferation by the Pten tumor suppressor gene in vivo. *Science* **294**(5549): 2186-2189.

Grozinger, C.M., Hassig, C.A., and Schreiber, S.L. 1999. Three proteins define a class of human histone deacetylases related to yeast Hda1p. *Proc Natl Acad Sci U S A* **96**(9): 4868-4873.

Grozinger, C.M. and Schreiber, S.L. 2000. Regulation of histone deacetylase 4 and 5 and transcriptional activity by 14-3-3-dependent cellular localization. *Proc Natl Acad Sci U S A* **97**(14): 7835-7840.

-. 2002. Deacetylase enzymes: biological functions and the use of small-molecule inhibitors. *Chem Biol* **9**(1): 3-16.

Guan, H.P., Ishizuka, T., Chui, P.C., Lehrke, M., and Lazar, M.A. 2005. Corepressors selectively control the transcriptional activity of PPARgamma in adipocytes. *Genes Dev* **19**(4): 453-461.

Guenther, M.G., Barak, O., and Lazar, M.A. 2001. The SMRT and N-CoR corepressors are activating cofactors for histone deacetylase 3. *Mol Cell Biol* **21**(18): 6091-6101.

Guenther, M.G., Yu, J., Kao, G.D., Yen, T.J., and Lazar, M.A. 2002. Assembly of the SMRT-histone deacetylase 3 repression complex requires the TCP-1 ring complex. *Genes Dev* **16**(24): 3130-3135.

Gui, C.Y., Ngo, L., Xu, W.S., Richon, V.M., and Marks, P.A. 2004. Histone deacetylase (HDAC) inhibitor activation of p21WAF1 involves changes in promoter-associated proteins, including HDAC1. *Proc Natl Acad Sci U S A* **101**(5): 1241-1246.

Haggarty, S.J., Koeller, K.M., Wong, J.C., Grozinger, C.M., and Schreiber, S.L. 2003. Domain-selective small-molecule inhibitor of histone deacetylase 6 (HDAC6)-mediated tubulin deacetylation. *Proc Natl Acad Sci U S A* **100**(8): 4389-4394.

Hasegawa, K., Fujiwara, H., Doyama, K., Miyamae, M., Fujiwara, T., Suga, S., Mukoyama, M., Nakao, K., Imura, H., and Sasayama, S. 1993. Ventricular expression of brain natriuretic peptide in hypertrophic cardiomyopathy. *Circulation* **88**(2): 372-380.

Hassig, C.A., Tong, J.K., Fleischer, T.C., Owa, T., Grable, P.G., Ayer, D.E., and Schreiber, S.L. 1998. A role for histone deacetylase activity in HDAC1-mediated transcriptional repression. *Proc Natl Acad Sci U S A* **95**(7): 3519-3524.

Hatten, M.E. 1999. Central nervous system neuronal migration. *Annu Rev Neurosci* **22**: 511-539.

Hill, J.A., Karimi, M., Kutschke, W., Davisson, R.L., Zimmerman, K., Wang, Z., Kerber, R.E., and Weiss, R.M. 2000. Cardiac hypertrophy is not a required compensatory response to short-term pressure overload. *Circulation* **101**(24): 2863-2869.

Howell, B.W., Hawkes, R., Soriano, P., and Cooper, J.A. 1997. Neuronal position in the developing brain is regulated by mouse disabled-1. *Nature* **389**(6652): 733-737.

Hsieh, J., Aimone, J.B., Kaspar, B.K., Kuwabara, T., Nakashima, K., and Gage, F.H. 2004a. IGF-I instructs multipotent adult neural progenitor cells to become oligodendrocytes. *J Cell Biol* **164**(1): 111-122.

Hsieh, J., Nakashima, K., Kuwabara, T., Mejia, E., and Gage, F.H. 2004b. Histone deacetylase inhibition-mediated neuronal differentiation of multipotent adult neural progenitor cells. *Proc Natl Acad Sci U S A* **101**(47): 16659-16664.

Hu, E., Dul, E., Sung, C.M., Chen, Z., Kirkpatrick, R., Zhang, G.F., Johanson, K., Liu, R., Lago, A., Hofmann, G., Macarron, R., de los Frailes, M., Perez, P., Krawiec, J., Winkler, J., and Jaye, M. 2003. Identification of novel isoform-selective inhibitors within class I histone deacetylases. *J Pharmacol Exp Ther* **307**(2): 720-728.

Hubbert, C., Guardiola, A., Shao, R., Kawaguchi, Y., Ito, A., Nixon, A., Yoshida, M., Wang, X.F., and Yao, T.P. 2002. HDAC6 is a microtubule-associated deacetylase. *Nature* **417**(6887): 455-458.

Huss, J.M. and Kelly, D.P. 2004. Nuclear receptor signaling and cardiac energetics. *Circ Res* **95**(6): 568-578.

Jenuwein, T. and Allis, C.D. 2001. Translating the histone code. *Science* **293**(5532): 1074-1080.

Kee, H.J., Sohn, I.S., Nam, K.I., Park, J.E., Qian, Y.R., Yin, Z., Ahn, Y., Jeong, M.H., Bang, Y.J., Kim, N., Kim, J.K., Kim, K.K., Epstein, J.A., and Kook, H. 2006. Inhibition of histone deacetylation blocks cardiac hypertrophy induced by angiotensin II infusion and aortic banding. *Circulation* **113**(1): 51-59.

Kersten, S., Seydoux, J., Peters, J.M., Gonzalez, F.J., Desvergne, B., and Wahli, W. 1999. Peroxisome proliferator-activated receptor alpha mediates the adaptive response to fasting. *J Clin Invest* **103**(11): 1489-1498.

Khier, H., Bartl, S., Schuettengruber, B., and Seiser, C. 1999. Molecular cloning and characterization of the mouse histone deacetylase 1 gene: integration of a retrovirus in 129SV mice. *Biochim Biophys Acta* **1489**(2-3): 365-373.

Kisanuki, Y.Y., Hammer, R.E., Miyazaki, J., Williams, S.C., Richardson, J.A., and Yanagisawa, M. 2001. Tie2-Cre transgenic mice: a new model for endothelial cell-lineage analysis in vivo. *Dev Biol* **230**(2): 230-242.

Kobayashi, T. and Solaro, R.J. 2005. Calcium, thin filaments, and the integrative biology of cardiac contractility. *Annu Rev Physiol* **67**: 39-67.

Kong, Y., Tannous, P., Lu, G., Berenji, K., Rothermel, B.A., Olson, E.N., and Hill, J.A. 2006. Suppression of class I and II histone deacetylases blunts pressure-overload cardiac hypertrophy. *Circulation* **113**(22): 2579-2588.

Kornberg, R.D. and Lorch, Y. 1999. Twenty-five years of the nucleosome, fundamental particle of the eukaryote chromosome. *Cell* **98**(3): 285-294.

Koshland, D. and Strunnikov, A. 1996. Mitotic chromosome condensation. *Annu Rev Cell Dev Biol* **12**: 305-333.

Kouzarides, T. 2007. Chromatin modifications and their function. *Cell* **128**(4): 693-705.

Kramer, O.H., Zhu, P., Ostendorff, H.P., Golebiewski, M., Tiefenbach, J., Peters, M.A., Brill, B., Groner, B., Bach, I., Heinzel, T., and Gottlicher, M. 2003. The histone deacetylase inhibitor valproic acid selectively induces proteasomal degradation of HDAC2. *Embo J* **22**(13): 3411-3420.

Krishnamoorthy, T., Chen, X., Govin, J., Cheung, W.L., Dorsey, J., Schindler, K., Winter, E., Allis, C.D., Guacci, V., Khochbin, S., Fuller, M.T., and Berger, S.L. 2006. Phosphorylation of histone H4 Ser1 regulates sporulation in yeast and is conserved in fly and mouse spermatogenesis. *Genes Dev* **20**(18): 2580-2592.

Kurabayashi, M., Shibasaki, Y., Komuro, I., Tsuchimochi, H., and Yazaki, Y. 1990. The myosin gene switching in human cardiac hypertrophy. *Jpn Circ J* **54**(9): 1192-1205.

Kuwahara, K., Saito, Y., Takano, M., Arai, Y., Yasuno, S., Nakagawa, Y., Takahashi, N., Adachi, Y., Takemura, G., Horie, M., Miyamoto, Y., Morisaki, T., Kuratomi, S., Noma, A., Fujiwara, H., Yoshimasa, Y., Kinoshita, H., Kawakami, R., Kishimoto, I., Nakanishi, M., Usami, S., Saito, Y., Harada, M., and Nakao, K. 2003. NRSF regulates the fetal cardiac gene program and maintains normal cardiac structure and function. *Embo J* **22**(23): 6310-6321.

Lagger, G., O'Carroll, D., Rembold, M., Khier, H., Tischler, J., Weitzer, G., Schuettengruber, B., Hauser, C., Brunmeir, R., Jenuwein, T., and Seiser, C. 2002. Essential function of histone deacetylase 1 in proliferation control and CDK inhibitor repression. *Embo J* **21**(11): 2672-2681.

Lee, H.B., Noh, H., Seo, J.Y., Yu, M.R., and Ha, H. 2007. Histone deacetylase inhibitors: a novel class of therapeutic agents in diabetic nephropathy. *Kidney Int Suppl*(106): S61-66.

Lin, H., Yutzey, K.E., and Konieczny, S.F. 1991. Muscle-specific expression of the troponin I gene requires interactions between helix-loop-helix muscle regulatory factors and ubiquitous transcription factors. *Mol Cell Biol* **11**(1): 267-280.

Lin, R.J., Sternsdorf, T., Tini, M., and Evans, R.M. 2001. Transcriptional regulation in acute promyelocytic leukemia. *Oncogene* **20**(49): 7204-7215.

Loskovich, M.V., Grivennikova, V.G., Cecchini, G., and Vinogradov, A.D. 2005. Inhibitory effect of palmitate on the mitochondrial NADH:ubiquinone oxidoreductase (complex I) as related to the active-de-active enzyme transition. *Biochem J* **387**(Pt 3): 677-683.

Lu, J., McKinsey, T.A., Zhang, C.L., and Olson, E.N. 2000. Regulation of skeletal myogenesis by association of the MEF2 transcription factor with class II histone deacetylases. *Mol Cell* **6**(2): 233-244.

Luger, K., Mader, A.W., Richmond, R.K., Sargent, D.F., and Richmond, T.J. 1997. Crystal structure of the nucleosome core particle at 2.8 A resolution. *Nature* **389**(6648): 251-260.

Maglott, D., Ostell, J., Pruitt, K.D., and Tatusova, T. 2007. Entrez Gene: gene-centered information at NCBI. *Nucleic Acids Res* **35**(Database issue): D26-31.

Mahadevan, L.C., Willis, A.C., and Barratt, M.J. 1991. Rapid histone H3 phosphorylation in response to growth factors, phorbol esters, okadaic acid, and protein synthesis inhibitors. *Cell* **65**(5): 775-783.

Mannervik, M. and Levine, M. 1999. The Rpd3 histone deacetylase is required for segmentation of the Drosophila embryo. *Proc Natl Acad Sci U S A* **96**(12): 6797-6801.

Marks, P., Rifkind, R.A., Richon, V.M., Breslow, R., Miller, T., and Kelly, W.K. 2001a. Histone deacetylases and cancer: causes and therapies. *Nat Rev Cancer* **1**(3): 194-202.

Marks, P.A. and Breslow, R. 2007. Dimethyl sulfoxide to vorinostat: development of this histone deacetylase inhibitor as an anticancer drug. *Nat Biotechnol* **25**(1): 84-90.

Marks, P.A., Richon, V.M., Breslow, R., and Rifkind, R.A. 2001b. Histone deacetylase inhibitors as new cancer drugs. *Curr Opin Oncol* **13**(6): 477-483.

Marmorstein, R. and Roth, S.Y. 2001. Histone acetyltransferases: function, structure, and catalysis. *Curr Opin Genet Dev* **11**(2): 155-161.

Matsui, H., MacLennan, D.H., Alpert, N.R., and Periasamy, M. 1995. Sarcoplasmic reticulum gene expression in pressure overload-induced cardiac hypertrophy in rabbit. *Am J Physiol* **268**(1 Pt 1): C252-258.

Matsuoka, S., Ballif, B.A., Smogorzewska, A., McDonald, E.R., 3rd, Hurov, K.E., Luo, J., Bakalarski, C.E., Zhao, Z., Solimini, N., Lerenthal, Y., Shiloh, Y., Gygi, S.P., and Elledge, S.J. 2007. ATM and ATR substrate analysis reveals extensive protein networks responsive to DNA damage. *Science* **316**(5828): 1160-1166.

McKinsey, T.A. and Olson, E.N. 2004. Cardiac histone acetylation--therapeutic opportunities abound. *Trends Genet* **20**(4): 206-213.

-. 2005. Toward transcriptional therapies for the failing heart: chemical screens to modulate genes. *J Clin Invest* **115**(3): 538-546.

McKinsey, T.A., Zhang, C.L., Lu, J., and Olson, E.N. 2000a. Signal-dependent nuclear export of a histone deacetylase regulates muscle differentiation. *Nature* **408**(6808): 106-111.

McKinsey, T.A., Zhang, C.L., and Olson, E.N. 2000b. Activation of the myocyte enhancer factor-2 transcription factor by calcium/calmodulin-dependent protein kinase-stimulated binding of 14-3-3 to histone deacetylase 5. *Proc Natl Acad Sci U S A* **97**(26): 14400-14405.

-. 2001. Identification of a signal-responsive nuclear export sequence in class II histone deacetylases. *Mol Cell Biol* **21**(18): 6312-6321.

-. 2002. Signaling chromatin to make muscle. *Curr Opin Cell Biol* **14**(6): 763-772.

Minetti, G.C., Colussi, C., Adami, R., Serra, C., Mozzetta, C., Parente, V., Fortuni, S., Straino, S., Sampaolesi, M., Di Padova, M., Illi, B., Gallinari, P., Steinkuhler, C., Capogrossi, M.C., Sartorelli, V., Bottinelli, R., Gaetano, C., and Puri, P.L. 2006. Functional and morphological recovery of dystrophic muscles in mice treated with deacetylase inhibitors. *Nat Med* **12**(10): 1147-1150.

Minucci, S. and Pelicci, P.G. 2006. Histone deacetylase inhibitors and the promise of epigenetic (and more) treatments for cancer. *Nat Rev Cancer* **6**(1): 38-51.

Montgomery, R.L., Davis, C.A., Potthoff, M.J., Haberland, M., Fielitz, J., Qi, X., Hill, J.A., Richardson, J.A., and Olson, E.N. 2007. Histone deacetylases 1 and 2 redundantly regulate cardiac morphogenesis, growth, and contractility. *Genes Dev* **21**(14): 1790-1802.

Moses, K.A., DeMayo, F., Braun, R.M., Reecy, J.L., and Schwartz, R.J. 2001. Embryonic expression of an Nkx2-5/Cre gene using ROSA26 reporter mice. *Genesis* **31**(4): 176-180.

Mottus, R., Sobel, R.E., and Grigliatti, T.A. 2000. Mutational analysis of a histone deacetylase in Drosophila melanogaster: missense mutations suppress gene silencing associated with position effect variegation. *Genetics* **154**(2): 657-668.

Murthy, V.K. and Shipp, J.C. 1977. Accumulation of myocardial triglycerides ketotic diabetes; evidence for increased biosynthesis. *Diabetes* **26**(3): 222-229.

Nakajima, H., Kim, Y.B., Terano, H., Yoshida, M., and Horinouchi, S. 1998. FR901228, a potent antitumor antibiotic, is a novel histone deacetylase inhibitor. *Exp Cell Res* **241**(1): 126-133.

Nambiar, R.M., Ignatius, M.S., and Henion, P.D. 2007. Zebrafish colgate/hdac1 functions in the non-canonical Wnt pathway during axial extension and in Wnt-independent branchiomotor neuron migration. *Mech Dev* **124**(9-10): 682-698.

Nelson, J.D., Denisenko, O., Sova, P., and Bomsztyk, K. 2006. Fast chromatin immunoprecipitation assay. *Nucleic Acids Res* **34**(1): e2.

Ng, W.A., Grupp, I.L., Subramaniam, A., and Robbins, J. 1991. Cardiac myosin heavy chain mRNA expression and myocardial function in the mouse heart. *Circ Res* **68**(6): 1742-1750.

Nowak, S.J. and Corces, V.G. 2004. Phosphorylation of histone H3: a balancing act between chromosome condensation and transcriptional activation. *Trends Genet* **20**(4): 214-220.

Ohshima, T., Ward, J.M., Huh, C.G., Longenecker, G., Veeranna, Pant, H.C., Brady, R.O., Martin, L.J., and Kulkarni, A.B. 1996. Targeted disruption of the cyclin-dependent kinase 5 gene results in abnormal corticogenesis, neuronal pathology and perinatal death. *Proc Natl Acad Sci U S A* **93**(20): 11173-11178.

Park, J.H., Jung, Y., Kim, T.Y., Kim, S.G., Jong, H.S., Lee, J.W., Kim, D.K., Lee, J.S., Kim, N.K., Kim, T.Y., and Bang, Y.J. 2004. Class I histone deacetylase-selective novel synthetic inhibitors potently inhibit human tumor proliferation. *Clin Cancer Res* **10**(15): 5271-5281.

Parmacek, M.S. and Solaro, R.J. 2004. Biology of the troponin complex in cardiac myocytes. *Prog Cardiovasc Dis* **47**(3): 159-176.

Passier, R., Zeng, H., Frey, N., Naya, F.J., Nicol, R.L., McKinsey, T.A., Overbeek, P., Richardson, J.A., Grant, S.R., and Olson, E.N. 2000. CaM kinase signaling induces cardiac hypertrophy and activates the MEF2 transcription factor in vivo. *J Clin Invest* **105**(10): 1395-1406.

Pflum, M.K., Tong, J.K., Lane, W.S., and Schreiber, S.L. 2001. Histone deacetylase 1 phosphorylation promotes enzymatic activity and complex formation. *J Biol Chem* **276**(50): 47733-47741.

Phiel, C.J., Zhang, F., Huang, E.Y., Guenther, M.G., Lazar, M.A., and Klein, P.S. 2001. Histone deacetylase is a direct target of valproic acid, a potent anticonvulsant, mood stabilizer, and teratogen. *J Biol Chem* **276**(39): 36734-36741.

Robzyk, K., Recht, J., and Osley, M.A. 2000. Rad6-dependent ubiquitination of histone H2B in yeast. *Science* **287**(5452): 501-504.

Rodriguez, C.I., Buchholz, F., Galloway, J., Sequerra, R., Kasper, J., Ayala, R., Stewart, A.F., and Dymecki, S.M. 2000. High-efficiency deleter mice show that FLPe is an alternative to Cre-loxP. *Nat Genet* **25**(2): 139-140.

Roopra, A., Sharling, L., Wood, I.C., Briggs, T., Bachfischer, U., Paquette, A.J., and Buckley, N.J. 2000. Transcriptional repression by neuron-restrictive silencer factor is mediated via the Sin3-histone deacetylase complex. *Mol Cell Biol* **20**(6): 2147-2157.

Roth, S.Y., Denu, J.M., and Allis, C.D. 2001. Histone acetyltransferases. *Annu Rev Biochem* **70**: 81-120.

Rundlett, S.E., Carmen, A.A., Kobayashi, R., Bavykin, S., Turner, B.M., and Grunstein, M. 1996. HDA1 and RPD3 are members of distinct yeast histone deacetylase complexes that regulate silencing and transcription. *Proc Natl Acad Sci U S A* **93**(25): 14503-14508.

Saito, A., Yamashita, T., Mariko, Y., Nosaka, Y., Tsuchiya, K., Ando, T., Suzuki, T., Tsuruo, T., and Nakanishi, O. 1999. A synthetic inhibitor of histone deacetylase, MS-27-275, with marked in vivo antitumor activity against human tumors. *Proc Natl Acad Sci U S A* **96**(8): 4592-4597.

Saito, Y., Nakao, K., Arai, H., Nishimura, K., Okumura, K., Obata, K., Takemura, G., Fujiwara, H., Sugawara, A., Yamada, T., and et al. 1989. Augmented expression of atrial natriuretic polypeptide gene in ventricle of human failing heart. *J Clin Invest* **83**(1): 298-305.

Sakai, K. and Miyazaki, J. 1997. A transgenic mouse line that retains Cre recombinase activity in mature oocytes irrespective of the cre transgene transmission. *Biochem Biophys Res Commun* **237**(2): 318-324.

Sasse, S., Brand, N.J., Kyprianou, P., Dhoot, G.K., Wade, R., Arai, M., Periasamy, M., Yacoub, M.H., and Barton, P.J. 1993. Troponin I gene expression during human cardiac development and in end-stage heart failure. *Circ Res* **72**(5): 932-938.

Sato, O., Kuriki, C., Fukui, Y., and Motojima, K. 2002. Dual promoter structure of mouse and human fatty acid translocase/CD36 genes and unique transcriptional activation by peroxisome proliferator-activated receptor alpha and gamma ligands. *J Biol Chem* **277**(18): 15703-15711.

Schonfeld, P. and Reiser, G. 2006. Rotenone-like action of the branched-chain phytanic acid induces oxidative stress in mitochondria. *J Biol Chem* **281**(11): 7136-7142.

Shahbazian, M.D. and Grunstein, M. 2007. Functions of site-specific histone acetylation and deacetylation. *Annu Rev Biochem* **76**: 75-100.

Sheldon, M., Rice, D.S., D'Arcangelo, G., Yoneshima, H., Nakajima, K., Mikoshiba, K., Howell, B.W., Cooper, J.A., Goldowitz, D., and Curran, T. 1997. Scrambler and yotari disrupt the disabled gene and produce a reeler-like phenotype in mice. *Nature* **389**(6652): 730-733.

Shelton, J.M., Lee, M.H., Richardson, J.A., and Patel, S.B. 2000. Microsomal triglyceride transfer protein expression during mouse development. *J Lipid Res* **41**(4): 532-537.

Shi, Y. 2007. Histone lysine demethylases: emerging roles in development, physiology and disease. *Nat Rev Genet* **8**(11): 829-833.

Shi, Y. and Mello, C. 1998. A CBP/p300 homolog specifies multiple differentiation pathways in Caenorhabditis elegans. *Genes Dev* **12**(7): 943-955.

Shilatifard, A. 2006. Chromatin modifications by methylation and ubiquitination: implications in the regulation of gene expression. *Annu Rev Biochem* **75**: 243-269.

Sohal, D.S., Nghiem, M., Crackower, M.A., Witt, S.A., Kimball, T.R., Tymitz, K.M., Penninger, J.M., and Molkentin, J.D. 2001. Temporally regulated and tissue-specific gene manipulations in the adult and embryonic heart using a tamoxifen-inducible Cre protein. *Circ Res* **89**(1): 20-25.

Stadler, J.A., Shkumatava, A., Norton, W.H., Rau, M.J., Geisler, R., Fischer, S., and Neumann, C.J. 2005. Histone deacetylase 1 is required for cell cycle exit and differentiation in the zebrafish retina. *Dev Dyn* **233**(3): 883-889.

Stanley, W.C., Lopaschuk, G.D., and McCormack, J.G. 1997. Regulation of energy substrate metabolism in the diabetic heart. *Cardiovasc Res* **34**(1): 25-33.

Steffan, J.S., Bodai, L., Pallos, J., Poelman, M., McCampbell, A., Apostol, B.L., Kazantsev, A., Schmidt, E., Zhu, Y.Z., Greenwald, M., Kurokawa, R., Housman, D.E., Jackson, G.R., Marsh, J.L., and Thompson, L.M. 2001. Histone deacetylase inhibitors arrest polyglutamine-dependent neurodegeneration in Drosophila. *Nature* **413**(6857): 739-743.

Strahl, B.D. and Allis, C.D. 2000. The language of covalent histone modifications. *Nature* **403**(6765): 41-45.

Sun, Z.W. and Allis, C.D. 2002. Ubiquitination of histone H2B regulates H3 methylation and gene silencing in yeast. *Nature* **418**(6893): 104-108.

Taunton, J., Hassig, C.A., and Schreiber, S.L. 1996. A mammalian histone deacetylase related to the yeast transcriptional regulator Rpd3p. *Science* **272**(5260): 408-411.

Thomas, P.D., Campbell, M.J., Kejariwal, A., Mi, H., Karlak, B., Daverman, R., Diemer, K., Muruganujan, A., and Narechania, A. 2003. PANTHER: a library of protein families and subfamilies indexed by function. *Genome Res* **13**(9): 2129-2141.

Thomas, P.D., Kejariwal, A., Guo, N., Mi, H., Campbell, M.J., Muruganujan, A., and Lazareva-Ulitsky, B. 2006. Applications for protein sequence-function evolution data: mRNA/protein expression analysis and coding SNP scoring tools. *Nucleic Acids Res* **34**(Web Server issue): W645-650.

Thorne, A.W., Sautiere, P., Briand, G., and Crane-Robinson, C. 1987. The structure of ubiquitinated histone H2B. *Embo J* **6**(4): 1005-1010.

Thys, T.M., Blank, J.M., Coughlin, D.J., and Schachat, F. 2001. Longitudinal variation in muscle protein expression and contraction kinetics of largemouth bass axial muscle. *J Exp Biol* **204**(Pt 24): 4249-4257.

Trivedi, C.M., Luo, Y., Yin, Z., Zhang, M., Zhu, W., Wang, T., Floss, T., Goettlicher, M., Noppinger, P.R., Wurst, W., Ferrari, V.A., Abrams, C.S., Gruber, P.J., and Epstein, J.A. 2007a. Hdac2 regulates the cardiac hypertrophic response by modulating Gsk3 beta activity. *Nat Med* **13**(3): 324-331.

-. 2007b. Hdac2 regulates the cardiac hypertrophic response by modulating Gsk3beta activity. *Nat Med*.

Trommsdorff, M., Gotthardt, M., Hiesberger, T., Shelton, J., Stockinger, W., Nimpf, J., Hammer, R.E., Richardson, J.A., and Herz, J. 1999. Reeler/Disabled-like disruption of neuronal migration in knockout mice lacking the VLDL receptor and ApoE receptor 2. *Cell* **97**(6): 689-701.

Tsai, L.K., Tsai, M.S., Lin, T.B., Hwu, W.L., and Li, H. 2006. Establishing a standardized therapeutic testing protocol for spinal muscular atrophy. *Neurobiol Dis* **24**(2): 286-295.

Tsai, S.C. and Seto, E. 2002. Regulation of histone deacetylase 2 by protein kinase CK2. *J Biol Chem* **277**(35): 31826-31833.

Van Lint, C., Emiliani, S., and Verdin, E. 1996. The expression of a small fraction of cellular genes is changed in response to histone hyperacetylation. *Gene Expr* **5**(4-5): 245-253.

Vega, R.B., Harrison, B.C., Meadows, E., Roberts, C.R., Papst, P.J., Olson, E.N., and McKinsey, T.A. 2004a. Protein kinases C and D mediate agonist-dependent cardiac hypertrophy through nuclear export of histone deacetylase 5. *Mol Cell Biol* **24**(19): 8374-8385.

Vega, R.B., Matsuda, K., Oh, J., Barbosa, A.C., Yang, X., Meadows, E., McAnally, J., Pomajzl, C., Shelton, J.M., Richardson, J.A., Karsenty, G., and Olson, E.N. 2004b. Histone deacetylase 4 controls chondrocyte hypertrophy during skeletogenesis. *Cell* **119**(4): 555-566.

Verdin, E., Dequiedt, F., and Kasler, H.G. 2003. Class II histone deacetylases: versatile regulators. *Trends Genet* **19**(5): 286-293.

Vidal, M. and Gaber, R.F. 1991. RPD3 encodes a second factor required to achieve maximum positive and negative transcriptional states in Saccharomyces cerevisiae. *Mol Cell Biol* **11**(12): 6317-6327.

Voss, A.K., Thomas, T., and Gruss, P. 1998. Efficiency assessment of the gene trap approach. *Dev Dyn* **212**(2): 171-180.

Wang, C., Fu, M., Mani, S., Wadler, S., Senderowicz, A.M., and Pestell, R.G. 2001. Histone acetylation and the cell-cycle in cancer. *Front Biosci* **6**: D610-629.

Watanabe, K., Fujii, H., Takahashi, T., Kodama, M., Aizawa, Y., Ohta, Y., Ono, T., Hasegawa, G., Naito, M., Nakajima, T., Kamijo, Y., Gonzalez, F.J., and Aoyama, T. 2000. Constitutive regulation of cardiac fatty acid metabolism through peroxisome proliferator-activated receptor alpha associated with age-dependent cardiac toxicity. *J Biol Chem* **275**(29): 22293-22299.

Wendt, K.D. and Shilatifard, A. 2006. Packing for the germy: the role of histone H4 Ser1 phosphorylation in chromatin compaction and germ cell development. *Genes Dev* **20**(18): 2487-2491.

Whetstine, J.R., Ceron, J., Ladd, B., Dufourcq, P., Reinke, V., and Shi, Y. 2005. Regulation of tissue-specific and extracellular matrix-related genes by a class I histone deacetylase. *Mol Cell* **18**(4): 483-490.

Wilson, A.J., Byun, D.S., Popova, N., Murray, L.B., L'Italien, K., Sowa, Y., Arango, D., Velcich, A., Augenlicht, L.H., and Mariadason, J.M. 2006. Histone deacetylase 3 (HDAC3) and other class I HDACs regulate colon cell maturation and p21 expression and are deregulated in human colon cancer. *J Biol Chem* **281**(19): 13548-13558.

Xin, M., Davis, C.A., Molkentin, J.D., Lien, C.L., Duncan, S.A., Richardson, J.A., and Olson, E.N. 2006. A threshold of GATA4 and GATA6 expression is required for cardiovascular development. *Proc Natl Acad Sci U S A* **103**(30): 11189-11194.

Yamaguchi, M., Tonou-Fujimori, N., Komori, A., Maeda, R., Nojima, Y., Li, H., Okamoto, H., and Masai, I. 2005. Histone deacetylase 1 regulates retinal neurogenesis in zebrafish by suppressing Wnt and Notch signaling pathways. *Development* **132**(13): 3027-3043.

Yang, W.M., Inouye, C., Zeng, Y., Bearss, D., and Seto, E. 1996. Transcriptional repression by YY1 is mediated by interaction with a mammalian homolog of the yeast global regulator RPD3. *Proc Natl Acad Sci U S A* **93**(23): 12845-12850.

Yang, W.M., Yao, Y.L., Sun, J.M., Davie, J.R., and Seto, E. 1997. Isolation and characterization of cDNAs corresponding to an additional member of the human histone deacetylase gene family. *J Biol Chem* **272**(44): 28001-28007.

Yasui, K., Niwa, N., Takemura, H., Opthof, T., Muto, T., Horiba, M., Shimizu, A., Lee, J.K., Honjo, H., Kamiya, K., and Kodama, I. 2005. Pathophysiological significance of T-type Ca2+ channels: expression of T-type Ca2+ channels in fetal and diseased heart. *J Pharmacol Sci* **99**(3): 205-210.

Yoshida, M., Kijima, M., Akita, M., and Beppu, T. 1990. Potent and specific inhibition of mammalian histone deacetylase both in vivo and in vitro by trichostatin A. *J Biol Chem* **265**(28): 17174-17179.

Young, M.E., Patil, S., Ying, J., Depre, C., Ahuja, H.S., Shipley, G.L., Stepkowski, S.M., Davies, P.J., and Taegtmeyer, H. 2001. Uncoupling protein 3 transcription is regulated by peroxisome proliferator-activated receptor (alpha) in the adult rodent heart. *Faseb J* **15**(3): 833-845.

Yu, X., Guo, Z.S., Marcu, M.G., Neckers, L., Nguyen, D.M., Chen, G.A., and Schrump, D.S. 2002. Modulation of p53, ErbB1, ErbB2, and Raf-1 expression in lung cancer cells by depsipeptide FR901228. *J Natl Cancer Inst* **94**(7): 504-513.

Yu, X., Tesiram, Y.A., Towner, R.A., Abbott, A., Patterson, E., Huang, S., Garrett, M.W., Chandrasekaran, S., Matsuzaki, S., Szweda, L.I., Gordon, B.E., and Kem, D.C. 2007. Early myocardial dysfunction in streptozotocin-induced diabetic mice: a study using in vivo magnetic resonance imaging (MRI). *Cardiovasc Diabetol* **6**: 6.

Zhang, C.L., McKinsey, T.A., Chang, S., Antos, C.L., Hill, J.A., and Olson, E.N. 2002. Class II histone deacetylases act as signal-responsive repressors of cardiac hypertrophy. *Cell* **110**(4): 479-488.

Zhang, X., Ozawa, Y., Lee, H., Wen, Y.D., Tan, T.H., Wadzinski, B.E., and Seto, E. 2005. Histone deacetylase 3 (HDAC3) activity is regulated by interaction with protein serine/threonine phosphatase 4. *Genes Dev* **19**(7): 827-839.

Zhang, Y. 2003. Transcriptional regulation by histone ubiquitination and deubiquitination. *Genes Dev* **17**(22): 2733-2740.

Zhang, Y. and Reinberg, D. 2001. Transcription regulation by histone methylation: interplay between different covalent modifications of the core histone tails. *Genes Dev* **15**(18): 2343-2360.

Zhuo, L., Theis, M., Alvarez-Maya, I., Brenner, M., Willecke, K., and Messing, A. 2001. hGFAP-cre transgenic mice for manipulation of glial and neuronal function in vivo. *Genesis* **31**(2): 85-94.

Zinovyeva, A.Y., Graham, S.M., Cloud, V.J., and Forrester, W.C. 2006. The C. elegans histone deacetylase HDA-1 is required for cell migration and axon pathfinding. *Dev Biol* **289**(1): 229-242.

VITAE

Rusty L. Montgomery was born in Dodge City, Kansas on May 25, 1981 to Rex and Sandy Montgomery, and younger brother to Robyn Kitchings and Ryan Montgomery. After graduating valedictorian of Yukon High School in 1999, he attended the University of Oklahoma in Norman, Oklahoma. In 2002, he joined the laboratory of Dr. Muna Naash at the University of Oklahoma Health Sciences Center for his thesis study. The title of his thesis was "The characterization of the C150S mutation of peripherin/*rds* utilizing a transgenic mouse model." In May 2003, he graduated with highest honors, *summa cum laude*, and received a Bachelor of Science in Biochemistry from the University of Oklahoma. In August 2003, he entered the Graduate School of Biomedical Sciences at the University of Texas Southwestern Medical Center at Dallas. He joined the laboratory of Dr. Eric N. Olson in March 2004 where he developed his permanent desire to pursue research. He married Ashley Norton on August 11, 2007 and received his Ph.D. in Genetics and Development in March 2008.